

BUCKLING ANALYSIS OF OFFSHORE PIPELINE WITH VARIOUS BUCKLE ARRESTOR CONFIGURATIONS UNDER STATIC AXIAL LOAD

Thesis

Submitted in partial fulfillment of the requirements for degree of

DOCTOR OF PHILOSOPHY

by

N. RAMACHANDRA RAO
(148054 AM14F05)



**DEPARTMENT OF WATER RESOURCES AND OCEAN ENGINEERING
NATIONAL INSTITUTE OF TECHNOLOGY KARNATAKA
SURATHKAL, MANGALORE - 575 025**

SEPTEMBER – 2020

**BUCKLING ANALYSIS OF OFFSHORE PIPELINE
WITH VARIOUS BUCKLE ARRESTOR
CONFIGURATIONS UNDER STATIC AXIAL LOAD**

Thesis

Submitted in partial fulfillment of the requirements for degree of

DOCTOR OF PHILOSOPHY

by

N. RAMACHANDRA RAO
(148054 AM14F05)

Under the guidance of

Dr. VADIVUCHEZHIAN KALIVEERAN
Assistant Professor



**DEPARTMENT OF WATER RESOURCES AND OCEAN ENGINEERING
NATIONAL INSTITUTE OF TECHNOLOGY KARNATAKA,
SURATHKAL, MANGALORE - 575 025**

SEPTEMBER – 2020

DECLARATION

I hereby *declare* that the Research Thesis entitled **BUCKLING ANALYSIS OF OFFSHORE PIPELINES WITH VARIOUS BUCKLE ARRESTOR CONFIGURATIONS UNDER STATIC AXIAL LOAD** Which is being submitted to the **National Institute of Technology Karnataka, Surathkal**, in partial fulfillment of the requirements for the award of the Degree of **Doctor of Philosophy** in the **Department of Water Resources and Ocean Engineering**, is a *bonafide report of the research work carried out by me*. The material contained in this Research Thesis has not been submitted to any University or Institution for the award of any degree.

148054 AM14F05, N. RAMACHANDRA RAO

Department of Water Resources and Ocean Engineering
National Institute of Technology Karnataka, Surathkal

Place: NITK-Surathkal

Date: 22-09-2020

C E R T I F I C A T E

This is to *certify* that the Research Thesis entitled **BUCKLING ANALYSIS OF OFFSHORE PIPELINES WITH VARIOUS BUCKLE ARRESTOR CONFIGURATIONS UNDER STATIC AXIAL LOAD** submitted by **N. RAMACHANDRA RAO (Register Number: 148054 AM14F05)**, as the record of the research work carried out by him, is *accepted as the Research Thesis submission* in partial fulfilment of the requirements for the award of degree of Doctor of Philosophy.

Research Guide

(Dr. VADIVUCHEZHIAN KALIVEERAN)

Assistant Professor
Department of Water Resources and Ocean Engineering
National Institute of Technology Karnataka, Surathkal

Chairman – DRPC

Department of Water Resources and Ocean Engineering
National Institute of Technology Karnataka, Surathkal

ACKNOWLEDGEMENT

I wish to record my deep sense of gratitude and profound thanks for my research supervisor **Dr. Vadivuchezhian Kaliveeran**, Assistant Professor, Department of Water Resources and Ocean Engineering, for his keen interest, logical and critical suggestions during this work. The interaction and the time spent in discussions are imprinted in my memory permanently. I would like to thank Dr. Vadivuchezhian Kaliveeran for introducing me to latest concepts, and the pioneers who introduced those concepts. Only with his moral support and guidance, this research work could be completed and I could publish my work in many international journals and conferences.

I express my deep sense of gratitude to the **Director of National Institute of Technology Karnataka, Surathkal**, for permitting me to carry out my research work and to make use of institutional infrastructure facilities.

I sincerely acknowledge the help and support of **Prof. Subba Rao**, **Prof. G. S. Dwarakish**, and **Prof. Amai Mahesha** former Heads of the Department and **Prof. Amba Shetty**, present Head of the Department of Water Resources and Ocean Engineering, NITK, Surathkal, for permitting me to use the departmental resources and their continuous support in completing my research work.

I would like to extend my heartfelt gratitude to Research Progress Appraisal Committee members, **Dr. Manu** and **Dr. Gnanasekaran N.**, for their useful suggestions during the progress of the work.

I sincerely acknowledge the help and support of all the **Professors, Associate Professors, Assistant Professors and non-teaching staff** of Department of Water Resources and Ocean Engineering, NITK, Surathkal, in completing the work.

I take immense pleasure in thanking **Dr V. Arumugam**, Associate professor, Madras Institute of Technology, Chennai, for his support to conduct buckling experiments in Madras Institute of Technology.

I express my special thanks to fellow research scholars **I. Srinivasula Reddy, P. Palani Kumar, Raveesh R.M, R. Raja Pandi, Muralidhar N, N. Murugan, Sahana T. S** and students for their valuable support in completing my research work successfully.

I sincerely acknowledge the invariable help rendered by all the research scholars from Department of Water Resources and Ocean Engineering (**Amogh Mudbhatkal, Akshay, Bina Mary John, Suman Kundapura and Suparno Ghosh for sharing their research experiences with me**) and research scholars from other departments (Civil Engineering and Mechanical Engineering) with whom I attended class work.

I express my heartfelt gratitude to the authors of all those research publications which have been referred to during the process of research work. Finally, I wish to express regards and affection to my parents **Sri N. V. Krishna Rao** and **N. Janani Devi**. My guide, mentor and teacher **Sri N.V. Phaneendrudu** and uncles (paternal uncles and maternal uncles) who stressed on the importance of education. You have given me the power to believe in myself and pursue my dreams. Last but not the least, I would like to express thanks to my wife **Smt. N. Parvathi Lakshmi** and her siblings for their support on the domestic front.

N. Ramachandra Rao

ABSTRACT

During the last three decades, offshore oil and gas exploration and production has ventured into deeper seas as many shallow water fields are already exhausted. Today the production has reached ocean depth of approximately 7,000 ft., while exploration for oil resources is conducted at depths of 11,000 ft. With the development of oil and gas fields in different parts of the world, such as Gulf of Mexico (U.S.), North Sea, Southeast Asia, Brazil, Mediterranean Sea, Persian Gulf, Middle East, South China Sea, Australia etc., the economic importance of offshore pipelines can be gauged by the fact that around a third of the oil and gas extracted worldwide comes from offshore resources. Offshore pipelines are major components used by oil and gas industry for drilling, production and transmission. As a result of the greater depth of oil exploration, offshore pipelines are subjected to several forces such as pressure (internal and external), temperature, axial force acting on pipelines due to the difference between the temperature of material carried and ambient temperature and interaction of the pipelines with the surrounding material. The external forces acting on the pipelines result in buckling of offshore pipelines. Free spanning of offshore pipelines subjects them to bending forces. Offshore pipelines are subjected to lateral buckling, upheaval buckling which causes disruption of offshore facilities and interrupts the supply of oil. Therefore, buckling of offshore pipelines should be controlled within permissible limits. Several methods are employed to control buckling and ensure uninterrupted functioning of offshore pipelines. Use of buckle arrestors, advanced materials and latest techniques such as use of sensors to monitor offshore pipelines are the methods adopted to control buckling.

Current research work focuses on the improvement in structural properties of offshore pipelines stiffened with buckle arrestors of different configurations and placed at different locations along the pipeline. Finite element modeling was performed, and experiments were conducted on pipeline models made of stainless steel of grade SS304 which is suitable for offshore applications. Finite element analysis of offshore pipeline models stiffened with buckle arrestors of different configurations was performed to understand significance of varying length and placement of buckle arrestors. The optimum length of buckle arrestors was identified

from finite element analysis, and pipeline models were fabricated for conducting experiments. Comparison of finite element analysis results and experimental outcomes showed that the efficiency of buckle arrestors increased by increasing the dimensions and location of buckle arrestors. Three point bending experiments were conducted on the pipeline models to determine flexural capacity of the pipeline models.

Keywords: Offshore pipelines; buckling; buckle arrestors; bending; finite element analysis.

TABLE OF CONTENTS

ABSTRACT	i
TABLE OF CONTENTS	iii
LIST OF FIGURES	vii
LIST OF TABLES	xiii
CHAPTER 1	
INTRODUCTION AND LITERATURE SURVEY	1
1.1 General	1
1.2 Background and Motivation	3
1.3 Literature review	5
1.3.1 Offshore pipeline analysis	6
1.3.2 Buckle arrestors for offshore pipelines	14
1.3.3 Experimental studies on buckling of pipelines	21
1.4 Problem formulation	30
1.5 Aim and objectives	31
1.6 Structure of the thesis	32
CHAPTER 2	
FINITE ELEMENT ANALYSIS	33
2.1 Pipeline analysis	33
2.1.1 Finite Element Modelling to Identify Buckle Arrestor Configurations	33
2.1.2 1-D Finite Element Analysis of buckle arrestors for offshore pipelines	34
2.1.3 3-D Finite Element Analysis of buckle arrestors for offshore pipelines	36
2.1.4 Preliminary Finite Analysis Results	38
2.1.5 Modeling of inclined buckle arrestor and inclined buckle arrestor with connecting rod	40
2.1.6 Meshing Parameters	42

2.2	Eigen value buckling analysis results	43
2.2.1	Effect of varying angle of inclination and length of inclined stiffeners	43

CHAPTER 3

DETAILS OF BUCKLING EXPERIMENTS 47

3.1	Material	
3.1.1	Fabrication of specimens for conducting buckling experiments with various buckle arrestor configurations (Sinusoidal, Angular and Longitudinal continuous)	47
3.1.2	Calibration of strain gauges and determination of location of Pasting strain gauges to pipeline models for conducting buckling experiments with various buckle arrestor configurations (Sinusoidal, Angular and Longitudinal continuous)	49
3.1.3	Buckling experimental setup with various buckle arrestor configurations (Sinusoidal, Angular and Longitudinal continuous)	52
3.1.4	Fabrication of specimens for conducting buckling experiments with rectangular pin buckle arrestor configurations welded at different locations	57
3.1.5	Strain gauge pasting for conducting buckling experiments with rectangular pin buckle arrestor configurations welded at different locations	58
3.1.6	Buckling experimental setup with rectangular pin buckle arrestor configurations welded at different locations	60

CHAPTER 4

BUCKLING ANALYSIS OF PIPELINES WITH DIFFERENT BUCKLE ARRESTOR CONFIGURATIONS AND THIER LOCATION 65

4.1	Finite Element Modeling of pipeline various buckle arrestor configurations	65
4.1.1	Pipeline Material and Properties	65

4.1.2	Pipe geometry	66
4.1.3	Finite Element Models	67
4.1.4	Meshing Parameter, Boundary Conditions and Loading	69
4.1.5	Finite Element Analysis Results	71
4.2	Finite Element Modeling of pipeline stiffened with rectangular pin buckle arrestors with different spacing and locations	75
4.2.1	Pipeline Material and Properties	75
4.2.2	Pipe geometry	77
4.2.3	Meshing Parameter, Boundary Conditions and Loading	79
4.2.4	Finite Element Analysis Results	80
CHAPTER 5		
EXPERIMENTAL RESULTS THEIR VALIDATION AND VERIFICATION		85
5.1	Experimental results for pipeline stiffened with various buckle arrestors configurations	85
5.2	Comparison of the Finite Element analysis Results Using the Experimental Results	87
5.3	Experimental results for pipeline stiffened with various buckle arrestors configurations	88
5.4	Verification of the Finite Element analysis results by conducting Experiment	92
5.5	Three point bending experiments	94
CHAPTER 6		
CONCLUSIONS		99
6.1	Limitations of the study	100
6.2	Scope for future work	100
REFERENCES		101
PUBLICATIONS BASED ON PRESENT RESEARCH WORK		110
CURRICULUM VITAE		111

LIST OF FIGURES

Figure 1.1	Imperfections in offshore pipelines. (Neil Taylor and Vinh Tran, 1996)	7
Figure 1.2	Methods to withstand higher pressures acting on offshore pipelines (D. De Geer and M. Nessim, 2008)	14
Figure 1.3	Shell analysis of pipeline (Power, T. L. and Kyriakides S., 1996)	16
Figure 1.4	Buckle Arrestor Configuration (Kyriakides S. <i>et al.</i> 1998)	17
Figure 1.5	Schematic diagram of hyperbaric chamber (Netto, T. A. and Kyriakides, S., 2000)	18
Figure 1.6	Configurations of ring buckle arrestors (Erlend Olso and Stelios Kyriakides 2003)	20
Figure 1.7	Schematic diagram of a buried pipeline (Maltby T. C. and Calladine C. R., 1995)	21
Figure 1.8	Schematic diagram of Bending test on pipe (Aguirre <i>et al.</i> , 2004)	22
Figure 1.9	Pipe specimen after bending test (Hallai J. F. and Kyriakides S., 2011)	23
Figure 1.10	Experimental set up to apply strike slip fault to buried pipeline (Lin T. J. <i>et al.</i> , 2012)	23
Figure 1.11	Experimental set up to apply reverse fault to buried pipeline (Rofooei F. R. <i>et al.</i> , 2012)	24
Figure 1.12	Experimental set up for Brillouin Optical Time Domain Analysis (BOTDA) (Xin Feng <i>et al.</i> , 2015)	26
Figure 1.13	Pipe specimen with internal stiffeners (A-A) and external stiffeners (B-B) (Card and Jones, 1966)	27
Figure 1.14	Axisymmetric and Non-axisymmetric folding of steel tubes. (Bardi F. C. and Kyriakides S., 2006)	28
Figure 2.1	Schematic diagram of different configurations of Buckle Arrestors considered	34
Figure 2.2	Schematic diagram of the simple pipeline with axial load and end conditions	35

Figure 2.3	(a) Convergence study of Simple pipeline (b) Configuration 3 buckling load capacity using <i>MATLAB</i>	36
Figure 2.4	Finite element mesh models of the all nine stiffener configurations of pipeline	37
Figure 2.5	The deflection shapes of the all nine stiffener configurations of pipeline	37
Figure 2.6	Dimensions of a simple pipeline model considered for study	40
Figure 2.7	Cross-sections of a pipe models with inclined stiffener configurations (a) & (c) and inclined stiffener configurations with connecting rods (b) & (d).	41
Figure 2.8	(a) Finite element models without stiffener (b) pipeline with inclined stiffener (c) pipeline with inclined stiffener and connecting rod (d) pipeline with large inclined stiffener.	41
Figure 2.9	(a) Solid element mesh of a plain pipeline model (b) Element Model SOLID187 using <i>ANSYS</i> .	42
Figure 3.1	Specimens fabricated for conducting buckling experiments (a) pipeline without buckle arrestors (b) sinusoidal buckle arrestor (c) Angular buckle arrestor (d) longitudinal continuous buckle arrestor	48
Figure 3.2	Schematic representation shows a pipeline with the groove to attach longitudinal continuous buckler arrestors	49
Figure 3.3	Schematic representation shows a pipeline with the groove to attach sinusoidal and angular buckler arrestors	49
Figure 3.4	Schematic representation of Stainless Steel strip pasted with Strain gauges during calibration.	50
Figure 3.5	Schematic representation of simple pipeline pasted with Strain gauges to conduct the buckling experiment.	51
Figure 3.6	Schematic representation of longitudinal continuous stiffeners pipeline pasted with Strain gauges to conduct the buckling experiment	51
Figure 3.7	Schematic representation of sinusoidal stiffeners pipeline pasted	52

with Strain gauges to conduct the buckling experiment

Figure 3.8	Schematic representation of angular stiffeners pipeline pasted with strain gauges	52
Figure 3.9	Photograph of buckling experimental setup	53
Figure 3.10	Buckling experimental setup to test .(a) plain pipeline, (b) pipeline with longitudinal continuous stiffener, (c) sinusoidal stiffener and (d) angular stiffener respectively	54
Figure 3.11	Upper end and lower end blocks used to apply axial compressive load to the pipe during the buckling experiment	55
Figure 3.12	Strain gauges pasted to the pipeline (a) without Buckle arrestors (b) with longitudinal continuous Buckle arrestors (c) with sinusoidal Buckle arrestors (d) with angular Buckle arrestors to conduct the buckling experiment	56
Figure 3.13	Computerized Data Acquisition System (DAS) connected to the data logger to collect experimental data while conducting experiment on pipeline model	57
Figure 3.14	Schematic representation shows a pipeline with the groove	58
Figure 3.15	Schematic diagram of a Pipeline model without buckle arrestors pasted with strain gauges in longitudinal direction	59
Figure 3.16	Schematic diagram of a Pipeline model stiffened with centrally located buckle arrestors pasted with strain gauges	59
Figure 3.17	Schematic diagram of a Pipeline model with central Stiffeners and two stiffeners at the ends pasted with strain gauges	59
Figure 3.18	Schematic diagram of a Pipeline model stiffened with Longitudinal Continuous Rectangular Stiffeners pasted with strain gauges	60
Figure 3.19	Photograph of buckling experimental setup	61
Figure 3.20	Pipeline models fabricated for conducting buckling experiments- (a) pipeline model without buckle arrestors (b) pipeline model with centrally located buckle arrestors (c) pipeline model with	61

	discontinuous buckle arrestors at center and edges (d) pipeline model with continuous buckle arrestors	
Figure 3.21	Buckling experiments on different pipeline configurations (a) pipeline model without buckle arrestors (b) pipeline model with centrally located buckle arrestors (c) pipeline model with discontinuous buckle arrestors at center and edges (d) pipeline model with continuous buckle arrestors to observe direction of buckling using dial gauges	63
Figure 4.1	Cross-section of longitudinal continuous stiffener model	66
Figure 4.2	Cross-section of sinusoidal stiffener model	66
Figure 4.3	Cross-section of angular stiffener model	66
Figure 4.4	Finite element models of (a) pipeline without buckle arrestors, (b) pipeline stiffened with longitudinal continuous stiffeners, (c) pipeline stiffened with sinusoidal stiffener and (d) pipeline stiffened with angular stiffener	68
Figure 4.5	Solid element mesh of the (a) plain pipeline, (b) pipeline stiffened with longitudinal continuous stiffeners, (c) pipeline stiffened with sinusoidal stiffener and (d) pipeline stiffened with angular stiffener	70
Figure 4.6	Boundary conditions of proposed models ($P_{cr} > P$)	70
Figure 4.7	Buckling of Pipe Model 1 without Buckle arrestors	72
Figure 4.8	Buckling of Pipe Model 2 without Longitudinal Continuous Buckle arrestors	73
Figure 4.9	Buckling of Pipe Model 3 without Sinusoidal Buckle arrestors	73
Figure 4.10	Buckling of Pipe Model 4 without Angular Buckle arrestors	73
Figure 4.11	Variation of critical buckling load of pipeline model stiffened with different types of buckle arrestors	74
Figure 4.12	Schematic diagram of pipeline model without stiffeners	75
Figure 4.13	Schematic diagram of pipeline model stiffened with centrally placed stiffeners	76
Figure 4.14	Schematic diagram of pipeline model stiffened with centrally	76

	placed stiffener and two stiffeners at ends	
Figure 4.15	Schematic diagram of pipeline model stiffened with longitudinal continuous stiffeners	76
Figure 4.16	Finite element model of pipeline without stiffener	77
Figure 4.17	Finite element model of pipeline with centrally placed stiffener of length 150 mm	78
Figure 4.18	Finite element model of pipeline with centrally placed stiffener of length 150 mm and two stiffener of length 135 mm each placed at ends	78
Figure 4.19	Finite element model of pipeline with longitudinal continuous stiffener of length 670 mm	78
Figure 4.20	Convergence study of finite element mesh (plain pipeline model)	79
Figure 4.21	Solid element mesh of the plain pipeline	80
Figure 4.22	Boundary conditions of proposed models ($P_{cr} > P$)	80
Figure 4.23	Buckling of Pipe Model without stiffener	82
Figure 4.24	Buckling of Pipe model with stiffener of 150 mm length	82
Figure 4.25	Buckling of Pipe model with 150 mm long centrally located stiffener and 135 mm long stiffeners at both ends	82
Figure 4.26	Buckling of Pipe model with stiffener of 670 mm length	83
Figure 4.27	Variation of critical buckling load of pipeline model stiffened with and without buckle arrestors of varying length and location	83
Figure 5.1	Graph shows experimentally determined critical buckling load of (a) pipeline model without stiffeners, (b) with longitudinal continuous stiffeners, (c) sinusoidal stiffeners and (d) angular stiffeners	86
Figure 5.2	Variation of experimentally determined critical buckling load	87
Figure 5.3	Finite element analysis vs experimental results for a pipeline without stiffener and pipeline with different stiffener	88
Figure 5.4	Load (Independent variable) versus lateral deflection (dependent variable) at mid length of pipeline without buckle arrestor	90
Figure 5.5	Load (Independent variable) versus lateral deflection (dependent	90

	variable) at mid length of pipeline stiffened with buckle arrestors 150 mm at middle of the length.	
Figure 5.6	Load (Independent variable) versus lateral deflection (dependent variable) at mid length of pipeline stiffened with buckle arrestors 150 mm at middle of the length and two buckle arrestors 135 mm at the ends	91
Figure 5.7	Load (Independent variable) versus lateral deflection (dependent variable) at mid length of pipeline stiffened with 670 mm longitudinal continuous buckle arrestors	91
Figure 5.8	Pipeline with different stiffener configurations before and after buckling. (a-b) pipeline without stiffener, (c-d) pipeline with central stiffeners, (e-f) pipeline with central stiffeners and two stiffeners at the ends and (g-h) pipeline with longitudinal continuous stiffeners	93
Figure 5.9	Load-deflection curves of pipeline with different stiffeners, 1- pipeline without Stiffeners, 2-pipeline with central stiffener, 3- pipeline with central Stiffeners and two stiffeners at the ends and 4- pipeline with longitudinal continuous stiffeners	94
Figure 5.10	Stress in stiffeners from strain gauges pasted on stiffeners of, (a) pipeline with central stiffener, (b) pipeline with central stiffeners and two stiffeners at the ends and (c) pipeline with longitudinal continuous stiffeners (d) Failure of weld connection between pipe and stiffener in pipe with longitudinal continuous stiffeners.	96
Figure 5.11	Three point bending specimens before and after testing (a-b) pipeline without stiffener, (c-d) pipeline with central stiffener, (e-f) pipeline with central stiffeners and two stiffeners at the ends and (g-h) pipeline with longitudinal continuous stiffener	97
Figure 5.12	Strain gauge pasted locations and support conditions of pipeline without stiffeners	97
Figure 5.13	Comparison of theoretical and experimental strain at (a) bottom and (b) top strain gauge pasted locations	98

LIST OF TABLES

Table ##	Description of Table	##
Table 2.1	Buckling load capacity of all nine configurations obtained from 1D linear element (<i>MATLAB</i> code) and <i>ANSYS</i>	38
Table 2.2	Geometrical details of buckle arrestors	40
Table 2.3	Values of buckling load for different pipe configurations with different angle of buckle arrestors	43
Table 3.1	Summary of results obtained during calibration of strain gauges	50
Table 4.1	Geometric parameters and engineering properties of pipe model	65
Table 4.2	Geometrical details of buckle arrestors	67
Table 4.3	Summary of buckling analysis results	74
Table 4.4	Geometric parameters and engineering properties of pipe model	75
Table 4.5	Geometrical details of rectangular pin buckle arrestors	77
Table 4.6	Summary of buckling analysis results	81
Table 5.1	Summary of buckling Experimental results of buckle arrestors with three different configurations	85
Table 5.2	Summary of finite element analysis and experimental results	87
Table 5.3	Summary of buckling Experiment results with rectangular pin buckle arrestors placed at different locations	89
Table 5.4	Summary of Finite Element (FE) analysis and Experimental results	92
Table 5.5	Flexural elastic load limit of different pipeline configurations	95
Table 5.6	The ultimate flexural capacity of different pipeline configurations	96

CHAPTER 1

INTRODUCTION AND LITERATURE SURVEY

1.1 General

India is ranked fourth in the global list of energy consumers after China, USA and Russia, as per data from US energy information administration. Petroleum and Natural Gas contribute 50 percent of the energy requirements of our country. Half of the hydrocarbons produced in our country are from offshore resources. Exploration of oil and natural gas from offshore fields requires a network of pipelines for connecting oil wells and for transportation of oil and natural gas to onshore refineries and storage facilities. Western Offshore fields consisting of north field (Narmada and Tapti) and south field (Bombay High) have a total pipe line length of 3000 km for connecting drilling platforms with onshore refineries. The development of Krishna-Godavari basin and Cauvery basin in Bay of Bengal underlines the importance of offshore pipelines in transporting hydrocarbons. Offshore pipelines become inevitable due to increase in both the depth of offshore exploration and the distance from shore.

Owing to their location and the nature of forces acting on them offshore pipelines require highest safety standards in their design, execution, operation and maintenance. The analysis and design of offshore pipelines is of utmost importance as they are fabricated from steel sections and tubular sections and subjected to severe marine environments and wave forces. Any short comings in their operation leads to serious accidents like the fire in Bombay High in 2005 and Deep Water Horizon incident in Gulf of Mexico 2010.

U. S. Chemical Safety Board (CSB), which conducted an inquiry into the Deepwater Horizon incident, concluded that the blowout preventer (BOP) failed to seal the well as the drill pipes in BOP buckled for largely unknown reasons. According to the investigation report, pipe buckling occurred during the first minutes of the blowout, as crews desperately sought to regain control of oil and gas surging up from the well in Gulf of Mexico. The following factors are main causes of failure in offshore

pipelines: metal loss, cracking, external interference, geotechnical failures, defects in metal manufacturing and ineffective construction methods. They may fail due to any one of the above reasons or a combination of two or more reasons occurring simultaneously. Failure of offshore pipelines leads to disruption of offshore facilities, economic losses, loss of human life and damage to the environment by virtue of oil spills. Though many reasons are cited for failure of pipelines, elastic instability due to buckling is found to be a major cause of failure (Kyriakides, 2007). Buckling affects not only subsea pipelines but also affects slender members like columns and beam-columns which are a part of many offshore structures, mechanical structures and shell structures which are commonly used in aerospace structures (Megson, T. H. G.1972).

The following types of elastic instabilities act on marine structures:

- Classical Buckling – Bifurcation of equilibrium (Bushnell, 1985)
- Snap Through Buckling – Limit equilibrium instability (Wiebe, 2011)
- Dynamic and Flutter Instabilities (Megson, 1972)
- Propagation Buckling (Khalilpasha et al., 2013)

Pipeline buckling analysis is a complex process involving many forces acting on the offshore pipelines such as temperature, axial compression, flexure, pressure (internal pressure and external pressure), ground features, geological features, pipe soil interaction and earthquake forces. Many researchers have studied the phenomenon of buckling through various approaches like analytical (classical mechanics, bending theories, shell theories), numerical (computational analysis and finite element analysis) and experimental methods. They have investigated causes of buckling such as temperature, axial compression, flexure, internal pressure, external pressure, earth pressure, earth quake pressure and fluid flow characteristics; methods of prevention of buckling such as structural methods, buckle arrestors, by using functionally graded materials and pressure sheaths. Even today, efforts are made by several researchers and organizations to improve understanding of buckling process and to add to the repertory of knowledge.

1.2 Background and Motivation

Pipelines are the main means of transporting oil and gas from offshore zones all over the world. Pipelines are buried to avoid interference with other marine activities, like fishing activity and anchors. Pipeline operating at high temperature and pressure are subjected to global buckling due to the combination of forces introduced by depth of sea, axial soil friction, lateral soil friction and other subsea factors such as earth movement along faults. While lateral or horizontal buckling occurs for exposed pipelines, upheaval or vertical buckling occurs for buried or trenched pipelines.

Palmer and Baldry published first paper on pipeline buckling in 1974. It is demonstrated that the constraint of expansion of a pipeline on account of raised internal pressure and temperature could induce buckling through a small-scale test. In 1981 and 1984, Hobbs R.E. summarized basic models of buckling of pipeline caused due to change in temperature and compressive loads induced in pipelines. Major interest was to study buckling of offshore pipelines induced by thermal loads as upheaval buckling incidents occurred in the oil extraction zones in North Sea. Several incidents of upheaval buckling occurred around 1990. The failure of pipeline caused significant loss due to loss of production. Thermal induced buckling became a vital problem for oil and gas industry and a substantial study was conducted on upheaval buckling.

Offshore pipelines under external pressure may also reach their load carrying capacity due to a second failure mode: the localized collapse; in this case the pipe structure collapses with its sections losing its initial round shape. The local buckle failure mechanism is most common during pipeline installation due to excessive bending at the sag bend part of pipeline which is in the process of installation [Kyriakides S. and Netto T.A.2000].

Buckling, which is a result of various forces acting simultaneously on the pipeline, causes failure of the offshore pipelines and marine structures resulting in oil spills and failure of offshore platforms leading to loss to the offshore production systems and environmental damages. Therefore, buckling has to be limited within permissible limits to ensure functioning of offshore facilities. Improvements in computational

facilities and advances in technology shifted the focus from internal stiffeners, external stiffeners and ring stiffeners to spiral arrestors and stringers to keep buckling within permissible limits [S. Kyriakides and C D Babcock.1982].

Offshore pipelines are provided with buckle arrestors at regular intervals to locally increase the strength of the pipeline and therefore they provide an obstacle in the path of the propagating buckle to limit the affect of propagation buckling. Numbers of studies have been conducted for understanding the buckling phenomena of offshore pipelines [Gong et al., 2012]. Analytical and experimental studies have been conducted to understand the effect of geometry and placement of buckle arrestors in improving buckling strength of offshore pipelines [Toscano et al., 2008, Lee L. et al., 2004, Peroti et al., 2013]. Uses of ring stiffeners, pipe-in-pipe transportation systems, internal stiffeners and external stiffeners have been studied by researchers.

Finite element modeling of the upheaval buckling response of buried pipelines has gained significance with advances in programming languages (*ABAQUS*, *ANSYS* and *MATLAB*) and availability of computational software. The knowledge gained by analyzing rail road buckling is further applied to pipeline buckling modes (lateral buckling and upheaval buckling). Extensive use of offshore pipelines for transportation of oil and natural gas from offshore fields and the consequent problems in ensuring structural stability of these pipelines in the face of marine environment and the forces involved brought into focus offshore pipelines with initial imperfections, offshore pipelines with protective coatings, material with non-linear behavior and pipeline with large displacements. Number of studies have been conducted by researchers to understand effect of imperfections on offshore pipelines. The basic models presented by Hobbs have been modified and refined by considering the pipeline imperfections, different ground conditions and the elastic-plastic behavior of offshore pipelines in the past decades. Latest trends in the offshore pipelines include use of Remotely Operated Vehicles (ROVs), cathodic protection methods and use of sensors to ensure smooth and effective functioning of offshore pipelines.

The difficulties in assessing forces acting on offshore pipelines and the importance of offshore pipelines for transporting oil from offshore oil fields are motivating factors

for undertaking the present research work. This research work is based on finite element analysis to identify effective buckle arrestor configurations and experimental validation of pipeline models stiffened with the identified buckle arrestor configurations (triangular, sinusoidal and longitudinal continuous buckle arrestors) by conducting buckling experiments and bending experiments. Buckle arrestor location (central arrestors, continuous arrestors and discontinuous arrestors) were identified based on finite element analysis. The pipeline models with and without different buckle arrestor configurations have been fabricated using stainless steel seamless pipes of grade SS304. Pipeline models considered have lengths of 1 m and 0.8 m, external diameter of 0.016 m (16 mm), internal diameter of 0.00118 m (11.8 mm) and 0.0013 m (13 mm) and thickness of 2.1 mm and 1.5 mm respectively. The accuracy of the pipeline models is validated by comparing the results of the finite element analysis and experimental results.

1.3 Literature review

Oil exploration entered offshore regions in 1894 when piers were constructed to drill wells in California beach. Piers were abandoned and a fleet of tug boats, barges and floating pile drivers were used to drill wells on Grand Lake St. Marys in Ohio (1891) and on Caddo Lake Louisiana (1911). In 1944 offshore pipelines gained significance when “Pluto” 75 mm diameter subsea pipeline was constructed under the English Channel to provide logistic support from Britain to Allied forces in France. As the demand for oil and natural gas increased various oil fields were explored across oil exploration zones in North Sea, Gulf of Mexico and Middle East.

Many investigations were conducted on lateral buckling, upheaval buckling and global buckling of pipelines considering various types of loadings, such as temperature, axial force, bending and pressure are available in the literature to examine the buckling phenomenon and to suggest ways and means to restrict buckling to acceptable limits. A brief review of available literature on buckling of offshore pipelines is presented under the following headings: Offshore Pipeline Analysis; Buckle Arrestors; Experimental Studies.

1.3.1 Offshore pipeline analysis

Roger E. Hobbs (1984) conducted preliminary investigations into analysis of pipeline buckling and studied the influence of axial loads and temperature on pipeline buckling. He extended the work of Kerr, A. D. (1974), who studied lateral buckling of railway tracks due to temperature, stability of railway tracks in vertical plane and thermal buckling of railway tracks. Hobbs analyzed API X65 grade steel tubes of diameter 650 mm and thickness 15 mm to investigate five modes of lateral buckling and vertical buckling. Assumption of ideal pipelines with perfect elasticity was incorporated for his analysis and friction coefficient of 0.5 between pipe and seabed was considered to calculate bending, axial and total stresses for all the buckling modes. It was found that the stresses in mode 3 lateral buckling are closer to yield stress of steel.

Neil Taylor and Vinh Tran (1996) conducted analysis and experiments to study the influence of imperfections on the buckling of subsea pipelines. Three types of imperfections (Figure 1.1) were analyzed: pipeline remains in continuous contact with some distinct vertical undulation, isolated prop and in-filled prop. Series of experiments were conducted, by varying temperature between 20 °C to 30 °C and without change in temperature, on pipes of diameter 9.53 mm and thickness 1.6 mm with the vertical height of the prop varying from 10 mm to 30 mm. The in-filled prop imperfection is found to be a complex case when compared to isolated prop imperfection.

James G. A. Croll (1997) conducted studies to formulate a simplified model of thermal buckling of subsea pipelines by correlating buckling of railway lines with buckling of clamped columns. Imperfections in pipelines were studied by considering a simple support and continuous support and safe lower bound pressure at which uplift occurs was derived by considering the pipeline as a fixed beam.

Inge Lotsberg (2008) derived analytical expressions for stress concentration factors in pipes subjected to internal pressure and axial force. The stress concentration factors calculated were compared with those calculated using classical mechanics approach and theory of elasticity approach.

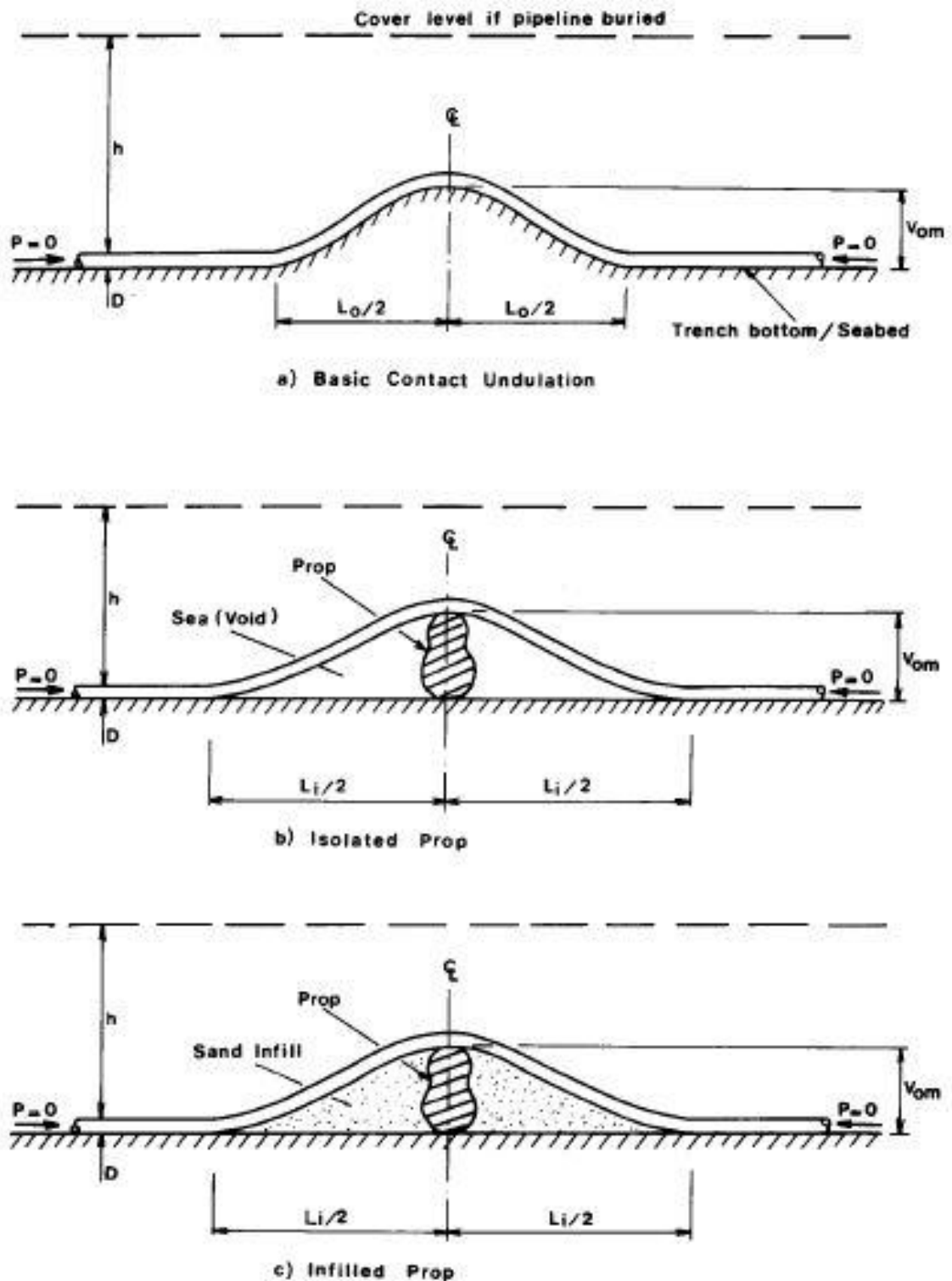


Figure 1.1 Imperfections in offshore pipelines (Neil Taylor and Vinh Tran, 1996).

Nourpanah, N. and Taheri, F. (2012) presented finite element analysis to model strain concentration in the field joints of concrete coated offshore pipelines. Three

dimensional FE modelling was developed using *ABAQUS* software, half circumference of the pipelines was modelled using sixteen rows of elements. Pipeline was modelled with 12160 iso-parametric eight node elements (C3D8R), with reduced integration and hour glass control. Strain Based Design (SBD) was applied to the concrete coated steel pipeline of three regimes of the pipeline were considered for FE analysis: the pipe is loaded within elastic limit in the first regime, the steel pipe enters the inelastic zone without damaging the concrete layer during the second regime and during the third regime the concrete coating deteriorates as the pipe stresses increase in the inelastic region. FE model was utilized to investigate the influence of various parameters pertaining to the geometry of the pipeline, material properties and loading rate on the strain concentration factor (SCF). The pipeline was subjected to two combined loading conditions bending plus internal pressure and bending plus axial force to study their influence on SCF.

Heedo Yun and Stelios Kyriakides (1985) applied beam mode buckling analysis to offshore pipelines. Upheaval buckling of steel pipelines of diameters 16 inches, 8.63 inches and 4.5 inches and with diameters to thickness (D/t) ratios of 42.7, 31.1 and 19 were investigated, through large deflections, for their capacity to withstand axial compression and vertical displacement. Heedo Yun and Stelios Kyriakides (1990) also conducted a comparative study of the beam theory and shell theory as applied to offshore pipelines. They have concluded that the beam behavior causes the pipeline to exert force on the ground and buckle in the vertical plane, whereas the shell type behaviour of the pipeline results in a localized failure, typical to shells. They also investigated influence of imperfections on critical load and strains in analyzing instability of offshore pipelines through both the beam and shell modes.

Ju, G. T. and Kyriakides, S. (1988) investigated thermal buckling of offshore pipelines by modelling offshore pipeline as a heavy beam resting on rigid foundation. Soil resistance to the buried pipeline was modelled as coulomb's friction. Pipelines of X42 grade steel were investigated to study the influence of temperature rise required to cause first uplift (ΔT_u), limit temperature rise beyond which the pipeline is unstable (ΔT_c) and locally minimum temperature rise which occurs after limit temperature rise (ΔT_m) on two types of imperfections in the pipeline, which are fully contacting imperfection and point imperfection. The pipeline becomes unstable after first uplift

in case of point uplift, as ΔT_u coincides with ΔT_u . The pipe friction problem was also extended to inelastic – plastic regime by considering Ramberg – Osgood formulation for stress strain behaviour of the material.

Burak Can Cerik (2015) studied the influence of slenderness ratio on ultimate strength of locally damaged cylinders with different types of stiffeners. Ring-stiffened cylinder specimens dented at the mid-bay, ring-stiffened cylinder specimens dented at the ring-stiffener and orthogonally stiffened cylinder specimens were analysed as part of the study. S4R elements in *ABAQUS* software were used to perform finite element analysis of these cases.

Fu, Y.B. and Lin, Y.P. (2002) adopted Wentzel, Kramers and Brillouin (WKB) method to analyze the buckling behavior of hyper elastic material (Everted Neo-Hookean) used as cylindrical Tube. The Eigen value problem has recently been solved numerically by Haughton and Orr for three different materials. They found that a critical value of A/B does indeed exist for all the three materials they considered, namely the Varga, neo-Hookean and Ogden materials. The thicker the tube is, the more “stressed” it will be after eversion. Thus, the tube may not stay circular cylindrical after eversion if the wall is thick enough. The WKB method is used to derive an asymptotic expression for the critical ratio of the inner radius to the outer radius. The major difference between an everted Varga tube and an everted neo-Hookean tube is that a turning point structure exists in the latter problem and this structure accounts for the difficulty experienced in the numerical integrations.

Jianbei Zhu *et al.* (2015) presented a solution to thermal buckling of a straight pipeline by applying Reissner’s one dimensional finite-strain beam theory and non-linear behaviour of pipeline was considered with hyper elastic constitutive modelling. PIPE288 element was adopted to model the pipelines and interaction between pipeline and soil was simulated using CONTA175 and TARGE170 of ANSYS. The outcomes of numerical modelling was compared to the results obtained using Hobbs analysis.

Jian-xing Yu *et al.* (2014) investigated buckle propagation of offshore pipelines with the help of Ring–Truss theory. A simplified three-dimensional model, known as a ring-truss model is used to predict the propagating pressure with the considerations of both the material hardening effect and axial deformation. A three-dimensional Finite Element model was built using *ABAQUS* to simulate the quasi-static buckle

propagation. The 8-node hexahedron element (C3D8I) was chosen to simulate the pipeline made of stainless steel grades SS304, SS400 and API X65. Kyriakides S and Netto T.A (2000) conducted experiments in hyperbaric chamber to investigate the phenomena of buckle propagation. Both aluminum and stainless steel samples were used with diameter to thickness ratio from 10 to 100 in the experiments. An equation to predict the buckle propagation pressure was proposed by empirically fitting experimental values. Besides using hyperbaric chamber, some researchers performed ring squash test to measure the lower limit of the buckle propagation pressure (Khalilpasha and Albermani, 2013).

Hassan Karampour and Faris Albermani (2013) investigated buckle interaction in deep sea pipelines by conducting experiments on steel pipe and applying the results to finite element analysis of aluminium pipelines. ANSYS thin shell 181 elements were used to model pipeline and COMBIN39 nonlinear spring elements for modelling stiffness of seabed. Aluminium pipe of length 3m and diameter to thickness (D/t) ratio 25 was tested in a hyperbaric chamber, to observe the pressure at which the buckle initiates. Buckle initiation pressure and buckle propagation pressure were graphically represented for different distortion ratios ($\Delta D/D$) of the pipes of different diameter to thickness (D/t) ratios 28.57 and 42.86.

Martins, J.P. *et al.* (2013) investigated Eigen value analysis of cylindrically curved panels to extend European code (EN 1993-1-5) for computing critical stresses of flat panels and shells of revolution to curved panels. Finite element analysis was conducted using ABAQUS software to examine buckling response of shells of different curvatures to twenty one load cases ranging from pure compression to pure bending. Nine node thin shell elements S9R5 were used in numerical modelling of the shells to study the influence of aspect ratio of the shell and loading conditions on the elastic critical stress. The study also included understanding the influence of curvature and aspect ratio on the buckling pattern of the shells. The pipeline is predominantly subjected to bending forces in both lateral buckling and upheaval buckling. Propagation buckling and bending experiments have been conducted on two aluminium pipes of different diameter to thickness ratios by Hassan Karampour and Faris Albermani (2014). Two meter long pipe was subjected to bending test and the mid span deflection was measured using two camera Digital Image Correlation (DIC)

system. Bi-Linear material model using Von-Mises plasticity with isotropic hardening is used for Finite Element analysis. Half length, Half-circumference model suggested by Hassan Karampour and Farris Albermani (2013) was used for numerical modelling. The initiation pressure (P_1) values obtained from propagation buckling tests conducted in hyperbaric chamber were compared to the Det Norske Veritas (DNV) standards.

Shuaijun Li *et al.* (2015) presented a review of Fluid Structure Interaction (FSI) in pipeline systems. They reviewed literature in terms of fluid parameters, pipeline parameters, different types of couplings (friction, junction, Bourdon and Poisson couplings) and different boundary conditions. Galerkin's method was applied along with generalized beam theory, which extends Vlasov's classical beam theory, to obtain buckling results of Circular Hollow Sections (CHS). N. Silvestre (2007) made a comparative study of critical buckling stresses obtained from finite element analysis using S4R elements of *ABAQUS* and that obtained using GBT by applying circular hollow sections to compression, bending, combined bending-compression and torsion. Kalliontzis, C. *et al.* (1997) applied finite difference method of numerical analysis to analyse offshore pipeline for empty, water-filled, gas-filled and pressurized loading conditions. The seabed is modelled for both rigid and elastic spring conditions. Von Mises equivalent stress formula is used for testing stability of pipeline as suggested by British Standard (BS8010) and Det Norske Veritas (DNV). The influence of internal pressure and external pressure on the buckling behaviour of offshore pipelines was explored using PIPE16 and SHELL93 elements of *ANSYS* by Ahmed Elshafey *et al.* (2010). The numerical modelling results showed that internal pressure increases the critical buckling load whereas the external pressure decreases the same.

Peroti, S. *et al.* (2013) studied the influence of stiffeners of different shapes (rectangular, T-shaped and L-shaped) on the buckling strength of the pipeline. The pipeline was modelled with S4R elements of *ABAQUS* software to study the effect of ring stiffeners on the pipeline subjected to hydrostatic pressure. It was observed that the rectangular stiffeners with stood higher pressures and the T-shaped stiffeners buckled at lower pressures.

Run Liu *et al.* (2014) conducted finite element analysis of subsea pipeline, which is subjected to temperature change, using 2D explicit, 2D implicit, 3D explicit and 3D

implicit models. PIPE32H beam elements of *ABAQUS* were used for 2D modelling and C3D8R elements were used for 3D modeling. Modified Riks method (Hibbitt, 2000), Explicit dynamic method were used for finite element analysis. Initial imperfections were introduced in the pipeline and the computational results obtained were compared with analytical results of Taylor and Gan (1986). The pipeline buckling amplitude, internal pipeline stress and initial buckling axial force computed using implicit Riks method are different from those obtained using explicit dynamic method. Two different techniques of finite element analysis, for evaluating stiffness properties and equilibrium forces, were applied for modelling pipeline problems as soil beam interaction problems by Zhillong Zhu and David W. Murray (1996). Reduced Modulus Direct Integration (RMDI) technique is valid for local buckling of Elastic Plastic Softening (EPS) material. Integration of Section Property Deformation Relations (ISPDR) can be applied for both Elastic Plastic Softening (EPS) and Elastic Plastic Hardening (EPH) materials. Both the models showed results similar to those from simulations using PIPLIN-III software.

Schupp, J. *et al.* (2014) investigated pipeline unburling behaviour in loose sand to study upheaval buckling using Particle Image Velocimetry (PIV) analysis in both loose dry sand and also in fully saturated soil samples of two grades. Pipeline behaviour was studied for four conditions namely: initial compression above pipeline, flow around pipeline, vertical slip failure along with slip and flow near surface. The definition of suitable probability density function for the soil properties is a complex problem. Reliability functions of buried pipelines subjected to upheaval buckling under High Pressure High Temperature (HPHT) conditions were investigated by Celestino Valle-Molina *et al.* (2014). A three dimensional finite element model of the soil-pipe system was developed using SOLID45 eight node brick and prism elements. It was concluded that lognormal distribution is suitable to represent both intact and distributed samples of clay in Campeche bay located in the North Sea.

Fuzzy inference system proposed by Mamdani and Assilian was applied to evaluate overall and local buckling behaviour of cylindrical tubes by Nazary Moghadam, S. *et al.* (2012). Eight-node degenerated shell element is used to represent nonlinear behaviour of cylindrical elements. The proposed fuzzy inference system considers three input parameters (diameter to thickness (D/t) ratio, slenderness ratio and

normalized axial shortening) and one output parameter normalized axial reaction force. The dimensions of the member are 4.504 in. (11.44 cm) in outer diameter, 0.92 in. (0.23 cm) in thickness and 225 in. (571.5 cm) in length.

Kyriakides, S. *et al.* (2012) conducted experiments on SAF2507 steel with diameter to thickness ratio (D/t) values ranging from 23 to 52. Wrinkling of circular tubes under axial compression effects of anisotropy. They considered the effect of anisotropy variables S_r and S_θ on critical strain and wrinkle wave length of the specimen. The wrinkling of cylindrical tubes under different test conditions (pure compression combined internal pressure and compression) have been predicted with accurately using an anisotropic deformation theory based on Hill's anisotropic yield function. Investigations were made to study the effect of yield anisotropy on buckling of circular tubes under bending by E. Corona *et al.* (2006). Experiments were conducted on aluminium specimen with diameter to thickness (D/t) ratio of 36 and length equal to $20D$. Effect of anisotropy on bending critical states is considered in a parametric study in which nine combinations of anisotropy variables (S_r and S_θ) are varied between values of 0.85 and 1.15. *ABAQUS* software was used for Finite element analysis of the post buckling response of the specimen. C3D27 elements, 27 node brick elements with full integration, were used for modelling the pipe specimen.

The review of literature of the offshore pipeline analysis reveals that the beam analysis and shell analysis of pipelines was extensively considered and *ABAQUS* and *ANSYS* softwares were used for Finite element modeling. The current technologies like Plasticity analysis, Plastic analysis and, WKB analysis and Eigen-value analysis have also been applied for the analysis of offshore pipelines. However, there have not been comprehensive studies on the use of FINS, Stress-frozen plates and Shot-peened pipelines as offshore pipelines.

1.3.2 Buckle arrestors for offshore pipelines

Increasing depth of the oil exploration and distance from shore not only increases the forces acting on offshore pipelines but also increases the transport temperature and pressure required for productively extracting oil from offshore fields. Methods adopted to withstand the higher forces acting on the pipelines include increasing the wall thickness of the pipeline, pipe-in-pipe (PIP) systems, high density polyethylene (HDPE) casing for pipelines and providing protective cover for offshore pipelines (Figure 1.2).

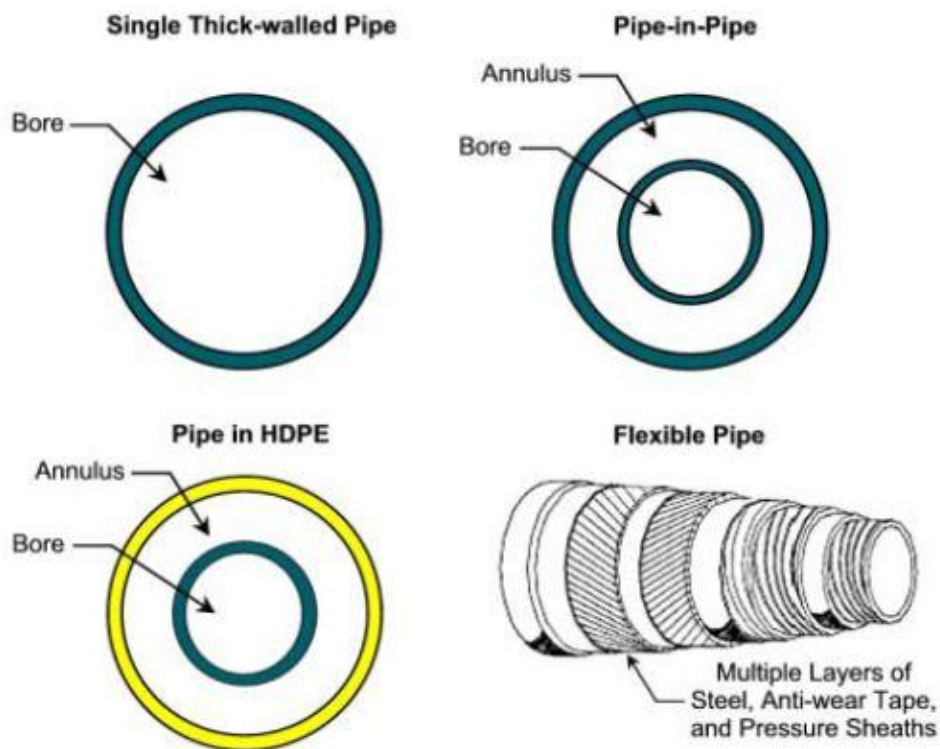


Figure 1.2 Methods to withstand higher pressures acting on offshore pipelines

(D. De Geer and M. Nessim, 2008).

As the understanding of the buckling process increased researchers investigated different types of buckle arrestors to prevent and to restrict the effect of buckling. Netto, T. A. and Estefan, S. F.(1995) investigated efficiency of buckle arrestors for deep water pipelines. They conducted experiments with ring and cylindrical type of buckle arrestors on steel pipes of diameter to thickness (D/t) ratio equal to 16 and 23,

in a 5 m long 0.38 m internal diameter hyperbaric chamber with 50 N/mm² working pressure. Spacing between buckle arrestors was kept at 15-20 pipe diameters to avoid interference between them. Continuous and homogenous transitions between the arrestors and the pipe were obtained through tungsten inert gas (TIG) welding process. All experimental data collated and the ratio of cross-over pressure to propagating pressure was plotted as a function of the parameters of buckle arrestors to obtain the following expression by fitting a straight line to the experimental data through minimum square error approach:

$$\frac{P_{co}}{P_p} = 11.46 * \left[\left(\frac{\sigma'_0}{\sigma} \right) \left(\frac{h_{ba}}{D} \right) \left(\frac{L_{ba}}{t} \right)^{0.4} \right]$$

Where,

- P_{co} is collapse pressure of the pipeline
- P_p is propagating pressure of the pipeline
- σ'_0 is pipe material yield stress
- σ is arrestor material yield stress
- D is outside diameter of the pipeline
- t is pipe wall thickness
- h_{ba} is buckle arrestor height
- L_{ba} is buckle arrestor length

Power, T. L. and Kyriakides S., (1996) studied the penetration of propagating collapse front through a circumferential stiffener as buckle arrestors in long panels (Figure 1.3). The nonlinear shell kinematics (Sanders, 1963) used in the analysis to determine the length of stiffener (L_s) and thickness of the stiffener (h). Normalized values of propagation pressure (P_p) and displaced volume ($\Delta\bar{u}$) given by the following equations are used for plotting results:

$$P_p = \frac{P}{\left(\frac{E}{12(1-\nu^2)}\right)\left(\frac{\pi}{\alpha}\right)^2\left(\frac{L}{R}\right)^3} \quad \text{And} \quad (\Delta\bar{u}) = \frac{1}{\alpha^3} \frac{\Delta u}{R^2} \frac{1}{L}$$

Where,

- P_p is propagating pressure of the pipeline
- P is pressure in the pipeline
- E is Young's modulus of pipe material
- ν is Poisson's ratio of pipe material
- α is arch span angle
- t is pipe wall thickness
- R is outer radius of the pipeline
- L is length of pipeline considered

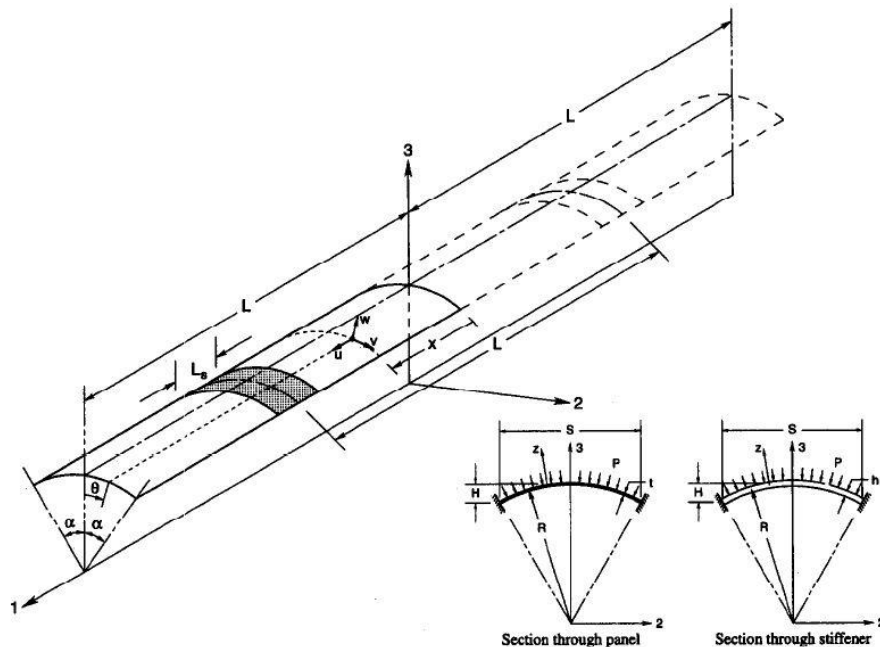


Figure 1.3: Shell analysis of pipeline (Power, T. L. and Kyriakides S., 1996).

Stelios Kyriakides. *et al.* (1998) conducted investigations into several design parameters of integral buckle arrestors for offshore pipelines. Pipes of nominal grade steel X-52 were used with 4.5 in inner diameter and 5.5 in outer diameter ($D/t = 4.5/0.5 = 9$). Arrestors were investigated for seven lengths with the length of arrestor to diameter of pipe (L_a/D) ratios of 2.5, 2.0, 1.5, 1.0, 0.75, 0.50 and 0.25. The experiments were conducted inside a 4 m long pressure vessel with a pressure capacity of 9000 psi (620 bar). This allowed testing an assembly consisting of three pipe sections and two arrestors. Arrestor efficiency vs. pipe parameters graph was

plotted for D/t ratios of 17, 22.5 and 34. Finite element model was developed using ABAQUS which can simulate numerically the crossing of an integral arrestor by a buckle propagating quasi-statically. The hardness of girth welds was made to be the same as that of pipe and the arrestor. The triple pass slow welding used reduced the width of the heat affected regions in the pipe. These characteristics are necessary in order to avoid cracking of the welds when they are deformed by a propagating buckle (Figure 1.4).

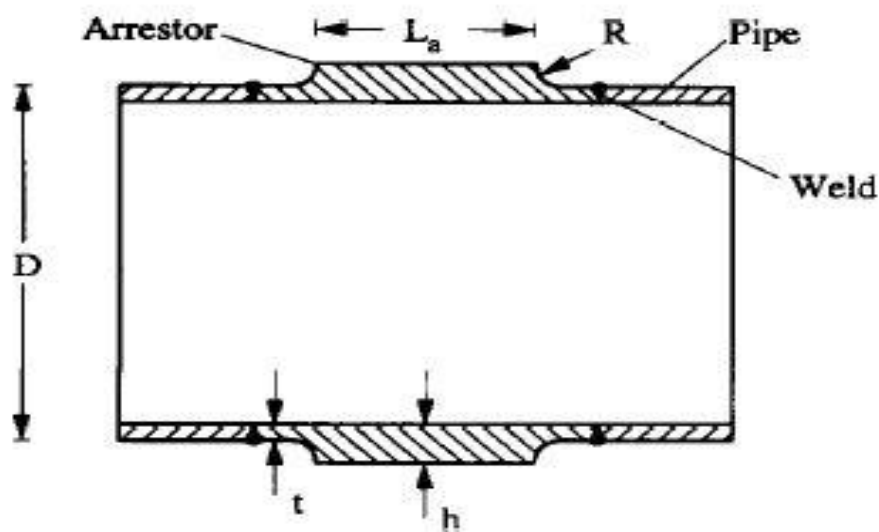


Figure 1.4 Buckle Arrestor Configuration (Kyriakides S. *et al.* 1998).

Netto, T. A. and Kyriakides, S. (2000) investigated the dynamic performance of integral buckle arrestors for offshore pipelines. The experiments were conducted inside hyperbaric chamber consisting of a 4 m long pressure vessel with a pressure capacity of 9000 psi (620 bar) (Figure 1.5). For dynamic experiments, the pressure vessel is filled with water leaving an air pocket which is pressurized using two air boosters working in series. The pressure is monitored by an electrical pressure transducer as well as by analog pressure gauges. The pressure transducer signal, that of the load cell, the LVDT and the ones from the three strain gages suitably conditioned are monitored via a computer based data acquisition system operating in the Lab VIEW environment. Several dynamic experiments similar to the ones reported here were conducted by Johns *et al.* in their study of welded ring buckle arrestors. The tubes and buckle arrestors of the above experiments were discretized

with three-dimensional, 27-node, quadratic brick elements (C3D27R) with reduced integration. Eighteen-node, quadratic, triangular prisms (C3D15V) were used for the transition regions between the arrestor and the tubes. SS304 pipes with Diameter to thickness ratio (D/t) ratio of 27.9 Length of the stiffener to diameter of pipe ratio (L_s/D) of 0.5 were tested. In the quasi-static model, the tube and arrestor materials are modeled as J_2 flow theory solids with isotropic hardening. In the dynamic model, the rate dependence of SS-304 is assumed to exhibit an overstress power law dependence.

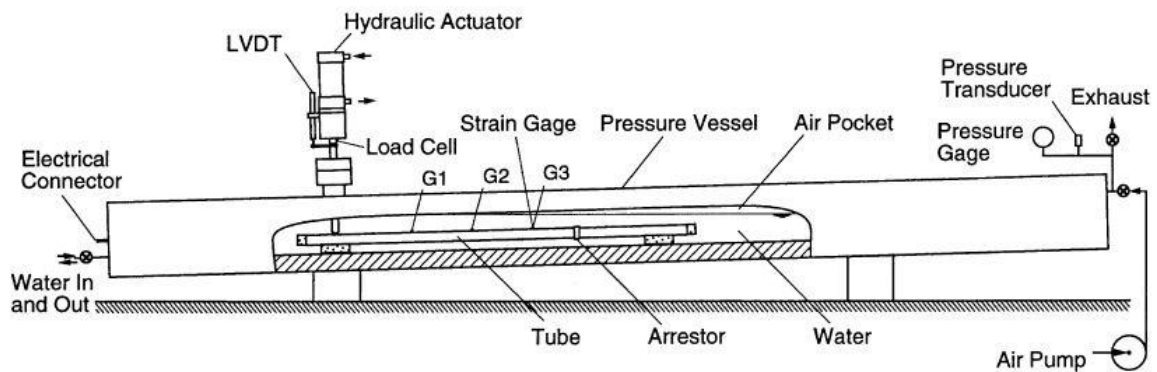


Figure 1.5 Schematic diagram of hyperbaric chamber (Netto, T. A. and Kyriakides, S., 2000).

L. H. Lee, S. Kyriakides and T. A. Netto (2008) conducted experiments to investigate the efficiency of Integral buckle arrestors for offshore pipelines. The tests were performed on 2-inch stainless steel (SS) 304 seamless tubes with diameter to thickness (D/t) ratio of approximately 24 and 21. The arrestors were machined out of SS-304 solid stock and welded between sections. Arrestor efficiency was calculated by conducting eighteen experiments, nine experiments for each diameter to thickness (D/t) ratio, in twelve cases arrestors were crossed by flattening mode and by flipping mode in the other six cases. The study of PK involved X65 pipes with diameter to thickness ratio (D/t) of 17, 22.5, and 34 and arrestors were fabricated from the same material.

The pipes analyzed had a diameter to thickness (D/t) ratio of 22.5, the arrestor length was kept at L equal to $0.5D$, while the yield stresses of the pipe and arrestors were varied independently. In the new calculations, the hardening characteristics of the stress-strain responses used were kept the same as those of the X65 grade steel.

Ramberg–Osgood hardening exponent (n) of 10.7 was considered up to a strain of 8%; the elastic limit was however varied to achieve various values of yield stress (σ_o and σ_{oa}).

Before experiments, efficiency of buckle arrestor (η) is a function of material properties and buckle dimensions, i.e.,

$$\eta = f \left[\left(\frac{E}{\sigma_o} \right)^{0.5}, \left(\frac{\sigma_{oa}}{E} \right)^{0.5}, \left(\frac{D}{t} \right)^{1.25}, \left(\frac{L}{t} \right)^{0.8}, \left(\frac{h}{t} \right)^{2.5} \right]$$

After experiments, the data obtained could be fitted to find the efficiency of buckle arrestor (η) as a function of the following buckle dimensions, i.e.,

$$\eta = f \left[\left(\frac{E}{\sigma_o} \right)^{0.65}, \left(\frac{\sigma_{oa}}{E} \right)^{0.95}, \left(\frac{D}{t} \right)^{1.25}, \left(\frac{L}{t} \right)^{0.8}, \left(\frac{h}{t} \right)^{2.5} \right]$$

where ,

- η is efficiency of the pipeline
- E is Young's modulus of pipe material
- σ_o is pipe material yield stress
- σ_{oa} is arrestor material yield stress
- D is outside diameter of the pipeline
- t is pipe wall thickness
- L is length of pipeline considered
- h is height of the arrestor

Erlend Olso and Stelios Kyriakides (2003) conducted experiments on internal ring buckle arrestors for pipe-in-pipe systems (Figure 1.6). Three configurations of pipe-in-pipe systems were considered with the outer carrier tubes of diameter 2 in (51 mm) and diameter to thickness (D/t) ratios of 24.1, 21.1 and 16.7. The inner tubes had nominal diameters of 1.375 and 1.25 in (35 and 32 mm). The first configuration of the buckle arrestor investigated is a single ring of length L and thickness h which does not contact the inner pipe. The second configuration, has the same length and thickness but is split into N sections of length $L=N$ (here $N =3$). This concept is axially more flexible which can be an important advantage if the pipe is spooled over a small radius reel. In the third configuration, the ring is narrower but is in close contact with both pipes.

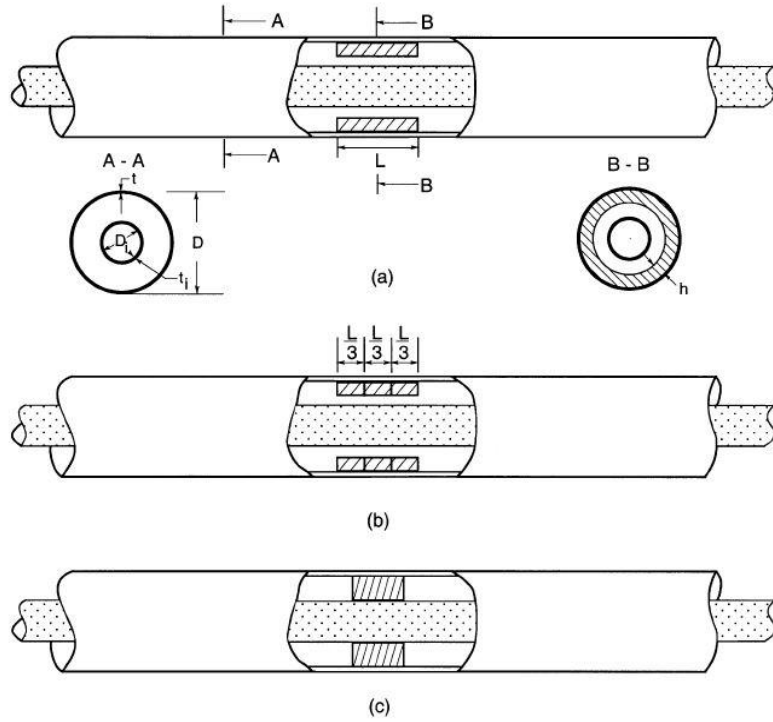


Figure 1.6 Configurations of ring buckle arrestors (Erlend Olso and Stelios Kyriakides 2003).

Lee L. H. and S. Kyriakides (2004) conducted experiments to investigate the arresting efficiency of slip-on buckle arrestors for offshore pipelines. The experiments were conducted on small-scale seamless, SS-304 tubes with diameter to thickness ratios (D/t) of approximately 35.7, 25.5 and 19.1. The tubes and the arrestors were discretized by three-dimensional, 27-node quadratic brick elements with reduced integration (C3D27R). Experiments were conducted to determine α_i , Before experiments, efficiency of buckle arrestor

$$\eta = f \left[\left(\frac{E}{\sigma} \right)^{\alpha_1}, \left(\frac{\sigma}{E} \right)^{\alpha_2}, \left(\frac{D}{t} \right)^{\alpha_3}, \left(\frac{L}{t} \right)^{\alpha_4}, \left(\frac{h}{t} \right)^{\alpha_5} \right]$$

The values displaying best correlation with the experimental data are as follows:

$$\eta = \frac{A1 * \left[\left(\frac{\sigma_0}{\sigma_{oa}} \right)^{0.8} \left(\frac{t}{D} \right)^{0.75} \left(\frac{L}{t} \right)^{0.98} \left(\frac{h}{t} \right)^{2.1} \right]}{[(P_{CO}/P_p) - 1]}$$

1.3.3 Experimental studies on buckling of pipelines

Maltby T. C. and Calladine C. R. (1995) studied upheaval buckling of steel pipes buried in a bed of artificial soil made up of polycarbonate particles. They conducted several experiments by burying a pipe of length 5 m and diameter 6 mm under a soil cover of varying depths 6 mm, 12 mm and 18 mm. The buried pipe was subjected to axial load, transverse load and pressure cycles (Figure 1.7). Axial load was applied in increasing increments of 20 N by means of a screw at one end and the load in the pipe was measured by means of a strain gauges. They plotted curves of vertical force exerted on the pipe against the vertical displacement of the pipe and approximated an exponential relationship for the vertical force per unit length of bar. The researchers identified three constraints while conducting the experiments:

- Sensitivity to the presence of initial imperfections.
- The ends of the pipes are fixed to the end blocks so it is not possible to model growth of isolated buckle.
- Modeling of soil particles by means of polycarbonate particles

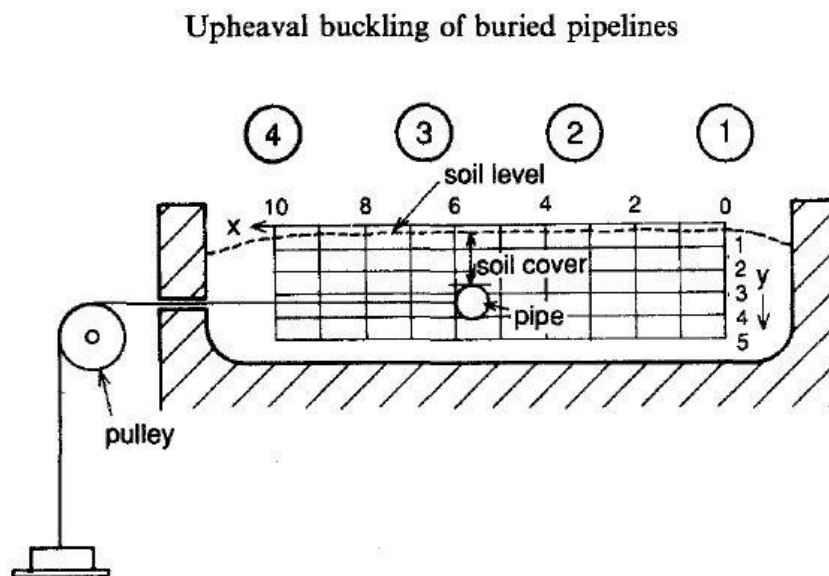


Figure 1.7 Schematic diagram of a buried pipeline (Maltby T. C. and Calladine C. R., 1995).

Aguirre *et al.* (2004) studied plastic bending of steel tubes which exhibit Lüders bands. They applied a layer of stress coat to visualize evolution of localized deformation induced by bending. The brittle ceramic coating (ST -75F) shatters displaying the Lüders bands pattern. They conducted experiments on pipe specimens having a diameter to thickness (D/t) ratio of 27.2 and length equal to 20 times of diameter. Bending tests were conducted on pipe specimens (Figure 1.8) to study Lüders' deformation. C3D8I elements of ABAQUS were best suited for Finite element modeling and it was found that the calculated mass-curvature responses reproduced measured results.

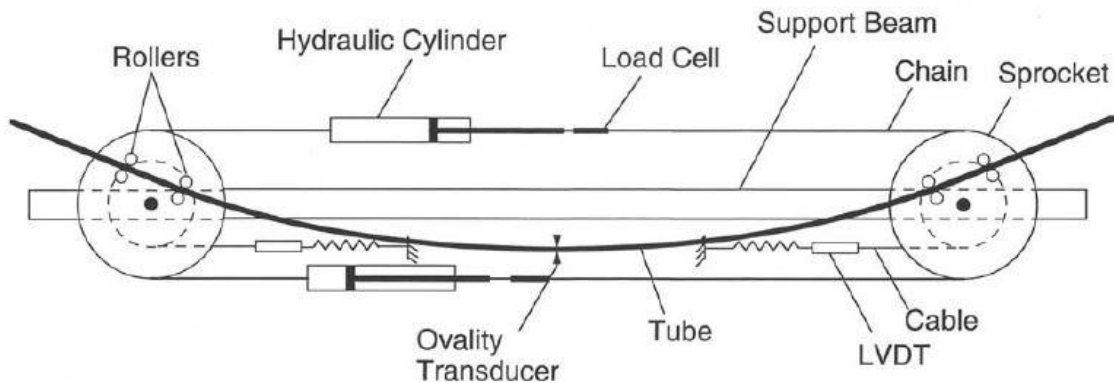


Figure 1.8 Schematic diagram of Bending test on pipe (Aguirre *et al.*, 2004).

Hallai J. F. and Kyriakides S. (2011) studied the impact of Lüders bands on the bending of steel tubes. They conducted experiments on carbon steel 1020 pipes with diameter to thickness (D/t) ratio of 14.7, 18.7, 24.2, 26.7 and 33.2. They considered two pipes of 32 mm and 35 mm diameter and the diameter was measured at 100 mm intervals along the length of the pipe to observe imperfections and ovality of the pipe. After bending test was conducted, it was observed that a pipe length five diameters long on the LHS experienced excessive deformation (Figure 1.9). Material properties of tubes which collapsed before reaching homogenous deformation and those which survived inhomogeneous deformation were compared to arrive at the conclusion that Lüders banding induces inhomogeneous bending which in turn induces inhomogeneous ovality in the pipe.



Figure 1.9 Pipe specimen after bending test (Hallai J. F. and Kyriakides S., 2011).

Lin T. J. *et al.* (2012) investigated the influence of large fault movements on buried pipelines by conducting small scale experiments and by using *ABAQUS* numerical models. SR4 four-node reduced integration shell elements were used for modeling pipes and C3D8R eight-node reduced integration brick elements were used for modeling soil particles. Strike slip fault movements are applied to aluminum pipes of thickness 1 mm and diameter 38 mm, 28 mm and 18 mm. The pipe length of 1.2 m was placed across two shear boxes of size 60 cm × 23 cm × 32 cm so that pipe is subjected to strike slip movement of 14 cm (Figure 1.10). They conducted the experiments using loose sand and dense sand for different depths of burial 75 mm, 125 mm and 175 mm. Five strain gauges were used to measure the axial strain in the pipe subjected to fault displacement. They also conducted numerical simulation of the response of buried pipelines to lateral movement caused by strike slip fault to understand three dimensional behavior of the pipelines.



Figure 1.10 Experimental set up to apply strike slip fault to buried pipeline (Lin T. J. *et al.*, 2012).

Rofooei F. R. *et al.* (2012) conducted full scale testing of buried pipelines subjected to reverse faulting. The test was conducted on full length HDPE pipes of outside diameter 114.3 mm and thickness 4.4 mm (D/t ratio of 26) in a chamber of dimensions $8.1 \times 1.7 \times 2.1$ m (length \times width \times depth) with a dip angle of 61° (Figure 1.11). The pipe is buried at 1 m depth in well graded sand and subjected to 600 mm ground displacement. The response of the pipeline to the vertical moment along the fault is measured by using 50 strain gauges and 6 Linear Variable Differential Transformers (LVDT) sensors. SR4 four-node reduced integration shell elements were used for modeling pipes and C3D8R eight-node reduced integration brick elements were used for modeling soil particles.

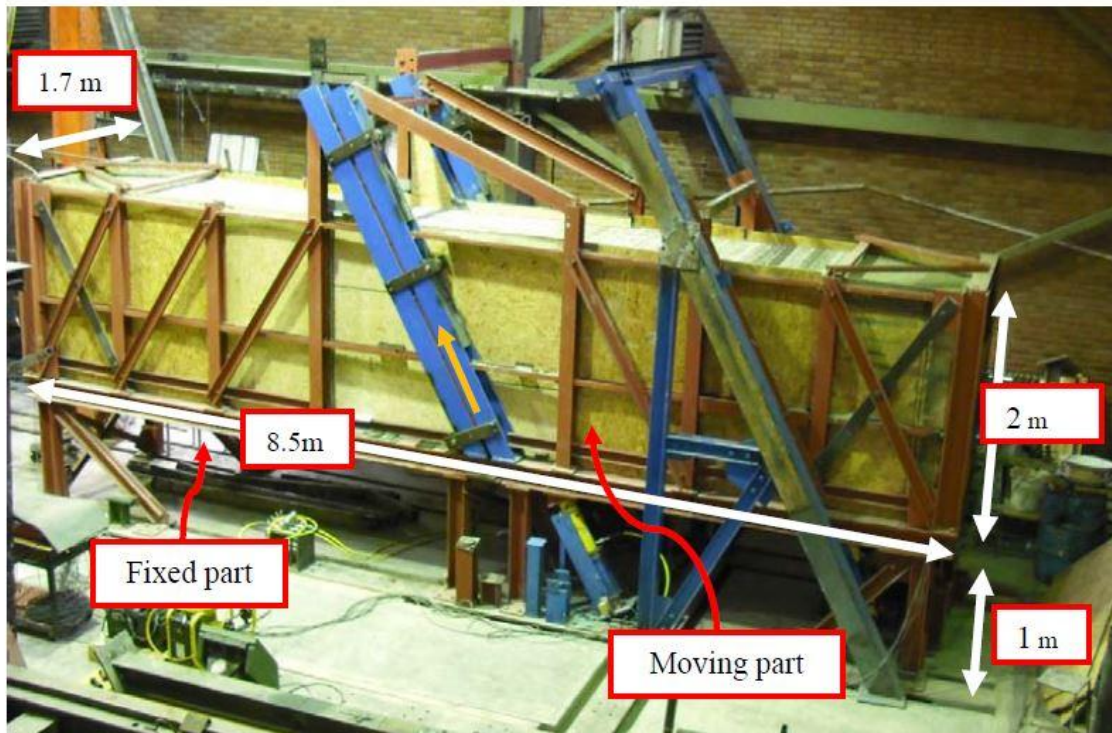


Figure 1.11 Experimental set up to apply reverse fault to buried pipeline (Rofooei F. R. *et al.*, 2012).

Run Liu *et al.* (2015) conducted experiments to study thermal buckling of pipes buried in bohai soft clay. They constructed an experimental set up measuring $3 \text{ m} \times 1 \text{ m} \times 1 \text{ m}$. Three pipes of 30 mm, 50 mm and 80 mm diameter (D) were buried at depths (H) ranging from H/D ratio ranging from 1 to 8. The embedded pipe lengths

were subjected to axial pullout and vertical uplift by means of pulleys and a vertical uplift bracket. Displacement transducers, pressure sensors and dynamic data processor connected to computer were used to collect the test parameters used in two-dimensional finite element analysis. Based on the uplift tests and *ABAQUS* simulation of pipe behavior a non-linear model was proposed to simulate the soil resistance acting on the pipe during vertical movement of the pipe through clay.

Ming Cai Xu and Guedes Soares C. (2013) conducted experiments on wide stiffened panel with four stiffeners to understand the influence of initial imperfections on the buckling behavior of plates. Five different specimen were tested with constant spacing (0.3 m) of horizontal stiffener, comprising of I- section 30 mm × 8 mm, and different spacing (0.2 m, 0.3 m, 0.4m, 0.45 m and 0.5m) of longitudinal stiffeners, comprising of L-section 60 mm × 40 mm × 6 mm. Different end conditions such as simply supported, periodical symmetric and restrained boundary condition were considered. Numerical analysis was done by *ANSYS* to assess the ultimate strength of the panels. Shell 181 element with four nodes and six degrees of freedom was used for Finite Element modeling. The FE analysis and tests conducted on stiffened panels showed similar results for average stiffness during loading phase but the results are different for unloading phase.

Distributed fiber optic sensors are used extensively for monitoring the subsea pipelines. Xin Feng *et al.* (2015) conducted experiments to measure lateral buckling of subsea pipelines by using fiber optic sensors. They conducted experiments on PVC pipe 5.47 m long, 160 mm outer diameter and of wall thickness 5 mm. Brillouin Optical Time Domain Analysis (BOTDA), which has higher spatial resolution and measurement accuracy was used in the experimental set up for distributed measurement of strain and for detecting lateral buckling of the pipe (Figure 1.12). Corning SMF-28, single mode optical fiber, was adopted as the distributed sensor. It was placed on both sides of the pipe along its length at $\theta = \pi/2$ and $\theta = 3\pi/2$. A load cell was used to measure the axial compressive load applied by the hydraulic jack. Axial and lateral displacements, along the neutral axis of the pipe, were measured by using a laser total station. Six cases of axial load were considered from 5.5 kN to 42.3

kN and sensors placed at 0.9 m spacing along the length of the pipe were monitored to obtain axial strains and bending strains. (figure of sensor placement) Longitudinal strains measured by the distributed sensors reveal bending behavior of the pipe but they cannot be used to detect the onset and evolution of lateral buckling in subsea pipelines.

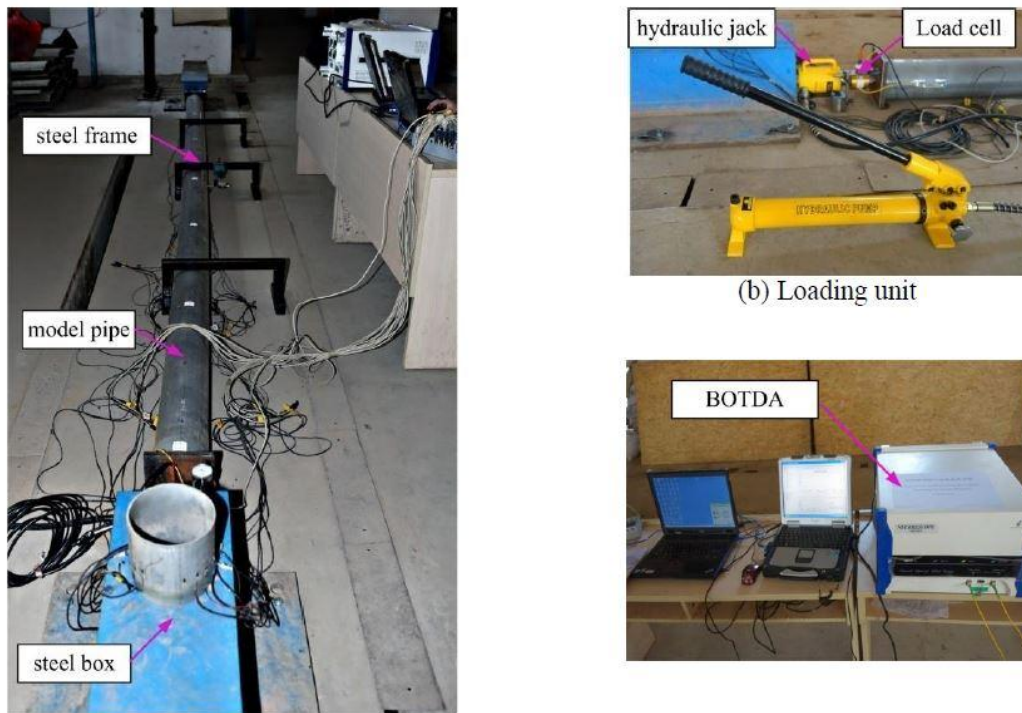


Figure 1.12 Experimental set up for Brillouin Optical Time Domain Analysis (BOTDA) (Xin Feng *et al.*, 2015).

C. Farhat et al (2013) conducted experiments on the dynamic implosion of cylindrical shells under water. The dynamic pressure associated with an implosion event is monitored with PCB piezotronics 138A06 underwater ICP blast dynamic sensors placed at one diameter away from the pipe and the implosion event is monitored with high speed digital cameras. Six pressure sensors were placed around the pipe at the mid section and two sensors were placed along the length. Experiments were conducted on Al6061-T6 shells with diameter to thickness ratio of 53.6 for different Length to diameter ratios of 2.0 and 8.0. The first specimen with Length to diameter ratio of 2.0 showed 4 mode collapse at a pressure of 676 psi. The second specimen with Length to

diameter ratio of 8.0 resulted in a flattened pipe at a pressure of 197 psi corresponding to elastic bifurcation buckling.

Card and Jones (1966) conducted experiments to study the buckling of eccentrically stiffened cylinders by considering internal stiffeners, external stiffeners, integral stiffeners and “Z- stiffeners”. They studied the behavior of cylinders with internal rectangular stiffeners manufactured from 3/8 inch aluminum alloy sheets (Figure 1.13). The researchers used Aluminum 2024-T351 for integral stiffeners and Aluminum 7075 T 6 for “Z-stiffeners”, which were riveted to the external surface of the pipe. Twelve resistance-wire strain gauges were mounted on the cylindrical specimens and on the stringers to know about stress distribution and to detect buckling. The externally stiffened cylinders buckled with a loud sound and appearance of several diamond-shaped buckles, whereas the externally stiffened cylinders buckled with diamond shaped buckles of smaller amplitude. They concluded that the externally stiffened cylinders carried twice the load when compared to internally stiffened cylinders.

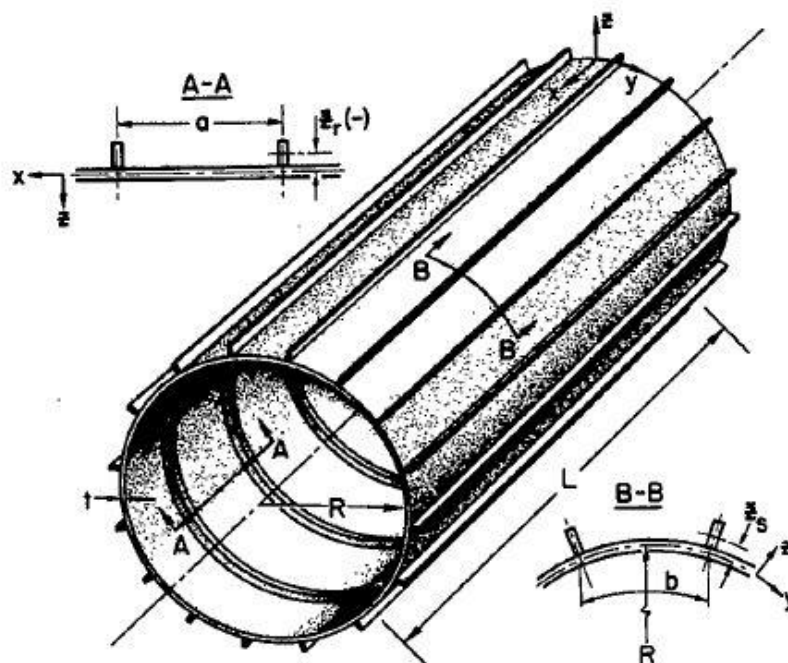


Figure 1.13 Pipe specimen with internal stiffeners (A-A) and external stiffeners (B-B) (Card and Jones, 1966).

Bardi F. C. and Kyriakides S. (2006) conducted experiments to analyze plastic buckling of circular tubes under axial compression. A separate set of experiments were conducted to study crushing behavior of pipes of same material. They conducted experiments on cold finished seamless tubes of stainless steel of grade SAF3, SAF4 and SAF5. The length of pipe specimen considered is 280 mm and diameter and thickness of the pipe are 60.3 mm and 3.91 mm respectively. A custom extensometer was used to measure the shortening of the test section. A scanning device consisting of LVDT displacement transducer was used to scan the surface of the specimen during the test. The tube is first scanned at zero axial strain and then at regular strain intervals as the compression load increased. The local circumferential strains and axial strains were measured using strain gauges. The localized deformation is in the form of one axisymmetric bulge which grows until the pipe's folded walls come into contact. This process is repeated with increase in compression load, resulting in concertina folding. Sometimes, the zone of localization develops into non-axisymmetric mode with two, three or more circumferential waves (Figure 1.14).

The results of the tests were used to validate J2 flow theory, which gives higher values of critical stress and strain and J2 deformation theory which is closer to experimental results but still over predicts critical stress and strain by a factor of two over the entire range of D/t ratio (23 to 52) is taken into account. It was observed that for tubes lower D/t ratio m is calculated as 2 and for higher D/t ratio m is calculated as 3.



(a) Carbon steel tube that developed axisymmetric concertina folding, (b) mode 2 folding and (c) mode 3 folding of stainless steel tubes.

Figure 1.14 Axisymmetric and Non-axisymmetric folding of steel tubes (Bardi F. C. and Kyriakides S., 2006).

R.Shahandeh and H.Showkati (2016) studied influence of ring stiffeners on buckling behavior of pipelines under hydrostatic pressure they used QTS4 element of LUSAS software to conduct finite element analysis of pipelines they observed ovalization on pipeline wall as buckle propagation begins they observed formation of yield lines and hexangular shape on the pipeline wall as yield lines formed. The yield lines change from straight yield lines to V shape yield lines before failure they concluded that introducing ring stiffeners does not contribute in reducing lateral displacement of pipeline models.

Jian-xing Yu et.al, (2017) conducted experiments in hyperbaric chamber to study cross-over mechanisms of integral buckle arrestors provided in offshore pipelines to address buckling problems have also contributed to preventing propagation buckling finite element modeling was performed using ABAQUS to investigate flattening mode and flipping mode of cross over mechanisms they concluded that the initial local ovalization of downstream pipeline effects the cross over mode of integral buckle arrestors.

Federico Guarracino (2018) conducted four point bending test to evaluate effect of stiffeners and buckle arrestors on bending of pipelines, which acts on the pipeline during the installation stage experiments were conducted on pipeline of diameter 152 mm and thickness of 3.8 mm They evaluated methods to prevent ovalization of pipes to derive a simple formula which offers insight into mechanics of ovalization problem.

Shunfeng Gong et al., (2019) conducted experiments using welded ring buckle arrestors and integral buckle arrestors and studied propagation pressure (PP), collapse (PCO), and Crossover pressure they concluded that arresting integral buckle arrestors are better than welded ring buckle arrestors when arresting efficiency required is low. When arresting efficiency required is high welded ring buckle arrestors are better alternative due to their cost efficiency and ease of fabrication.

Yidu Bu et.al, (2020) used stainless steel as corrosion resistant alloy to line the inner surface of a pipeline they performed tensile coupon test, geometric imperfections measurements and axial compression test as axial compression is induced by thermal field by the heat of the material transported when transporting hot hydrocarbons and they proposed a new buckling curve for lined pipelines.

1.4 Problem Formulation

In spite of many theoretical, analytical and experimental studies carried out on the behavior of different materials (steel, aluminum and composite materials), the study of literature showed that no comprehensive study was conducted on the buckling phenomena as applied to offshore pipelines. The present study focuses on finding the critical buckling load and flexural load carrying capacity of different pipe models, stiffened with various buckle arrestor configurations, using finite element analysis and experimental investigations.

The present work attempts to bridge this knowledge gap by investigating the concept of buckling by conducting buckling experiments and bending experiments on stainless steel pipe models of SS304 grade, the finite element software (*ANSYS*) have been used to analyze the experimental results and further extend these results to Static Axial loading conditions. Comparative analysis of experimental results and finite element analysis results had been performed to analyze the effectiveness of different buckle arrestors configurations.

The 1,166 km Langeded gas pipeline connects the Norwegian oil fields in the North Sea to the eastern coast of UK. This pipeline consists of 42 inch diameter northern leg and 44 inch southern leg. The 620 km long Europipe-I subsea gas pipeline running from the Draupner platform in the North Sea to the German coast. The 40 in diameter pipeline, is capable of transporting up to 54 million units of gas per day. The West Natuna gas pipe line runs for 654 km carrying gas from the west Natuna area in south China Sea to Palau Sakra on the coast of Singapore. The gas transportation line comprises of 28 inch, 22 inch, 16 inch and 14 inch diameter pipes. The Yacheng 13-1 subsea pipeline runs 780 km from the Yacheng gas field located 100 km south of Hainan Island, in the South China Sea, to an onshore facility at Black Point near Hong Kong. The 28 inch diameter subsea pipeline supplies natural gas for power generation. After considering dimensions of different offshore pipelines, 44 inch diameter southern leg of Langeded pipeline was considered to calculate dimensions of steel pipe as having length of 15 m, 1190 mm outer diameter, 1120 mm inner diameter and 35 mm thickness were considered for finite element modelling.

The different types of buckle arrestors were considered for analysis are as follows:

1. Pipelines stiffened with 16 mm outer diameter and bars
2. Pipelines stiffened with 20 mm diameter semi-circular bars
3. Pipelines stiffened with concrete coating
4. Pipelines stiffened with concrete coating and 20 mm diameter bars
5. Pipelines stiffened with continuous rectangular stiffener
6. Pipelines stiffened with rectangular pins
7. Pipelines stiffened with varying cross-section (18 degree fins)
8. Pipelines stiffened with sinusoidal curved plates
9. Pipelines stiffened with both longitudinal and ring stiffeners (20 mm diameter rods)

1.5 Aim and objectives

It is essential to understand the forces causing buckling and measures to be adopted to limit buckling to an extent where it does not affect the functioning of offshore pipelines. It is also important to investigate different types of buckle arrestors as effective means of controlling buckling and their contribution to increase in crippling load of the offshore pipeline. The following objectives have to be full filled as part of the proposed study:

The main objectives of this thesis are:

- Perform finite element modeling of different types of arrestors to understand the influence of Static Axial loading conditions.
- Design and fabrication of specimens of stainless steel of grade SS304 to conduct buckling experiments and bending experiments on pipe models stiffened with different types of buckle arrestors to investigate efficiency of buckle arrestors and to understand their contribution to the stability of offshore pipelines.
- Compare the experimental results and modeling outcomes to investigate efficiencies of various types of buckle arrestors and selection of a suitable buckle arrestor model.

1.6 Structure of the thesis

Chapter 1 provides an introduction to the offshore pipelines, Literature review of the evolution of offshore pipeline usage, different analytical method adopted and contribution of finite element analysis to analyze complex forces acting on offshore pipeline, problem formulation and objectives of present research work.

Chapter 2 contains one dimensional finite element analysis using *MATLAB* code to identify suitable buckle arrestor configurations, three dimensional finite element analysis using *ANSYS* for Eigen value buckling analysis of inclined stiffeners and inclined stiffeners with connecting rods and finite elements analysis results.

Chapter 3 gives detail procedure of material selection, fabrication of pipe specimens, strain gauge pasting and buckle arrestors, fabrication of end blocks to ensure end conditions.

Chapter 4 focuses on finite element modeling performed on pipeline models made of stainless steel of SS304 grade. Present research work focuses on the improvement in structural properties of offshore pipelines stiffened with various buckle arrestor configurations (sinusoidal, angular and longitudinal continuous) and rectangular pin buckle arrestors of different lengths and placed at different locations along the pipeline.

Chapter 5 focuses on experiments conducted on pipe model stiffened with 920 mm longitudinal continuous stiffeners, sinusoidal stiffeners (880 mm) and angular stiffeners (900 mm) were compared with that of a pipeline model without stiffeners and rectangular pin buckle arrestors of different lengths and placed at different locations along the pipeline and their validation.

Chapter 6 is devoted to conclusions arising from this research study, limitations of present study and scope of future work, followed by references.

CHAPTER 2

FINITE ELEMENT ANALYSIS

This chapter focuses on improving buckling strength of offshore pipelines by strengthening them with eight different configurations of buckle arrestors, inclined stiffeners and inclined stiffeners with connecting rods, to select suitable buckle arrestor configurations and to fabricate pipeline models strengthened with the same to enable experimental validation of their buckling strength. Eigen value buckling analysis was carried out using Finite Element Methods to find the buckling strength of pipeline models which were considered. Seamless stainless steel pipe models of SS304 grade were considered for finite element analysis. The pipeline models were provided with inclined stiffeners whose angle of inclination varies from 100° - 176° . Connecting rods of different lengths were used to improve buckling capacity of inclined stiffeners. Buckling analysis of pipeline sections with different stiffener configurations were analyzed using *MATLAB* code and *ANSYS*.

2.1 Pipeline analysis

2.1.1 Finite Element Modeling to Identify Buckle Arrestor Configurations

Finite Element software (*ANSYS*) was used to analyze all pipeline configurations with and without stiffeners. The preliminary study of buckle arrestors started with nine different configurations of buckle arrestors (Figure 2.1). A steel pipeline cross-section of outer diameter 1.19 m, thickness of 35 mm and length of 15 m was chosen for buckling analysis. A two node linear element was used for the one dimensional Finite Element Analysis using *MATLAB* program. SOLID186 element was used for 3-D finite element analysis using *ANSYS* software. Buckling analysis was done with pinned boundary condition at one end and roller boundary condition at the other end of the pipeline. Pipeline stiffened with rectangular pins (Configurations 3) has improved the buckling capacity of the pipeline by 43% according to the results obtained from the 3-D finite element analysis using *ANSYS*. The results obtained from the 1-D analysis using *MATLAB* program and 3-D analysis using *ANSYS* package and comparison of results obtained from these methods are analyzed.

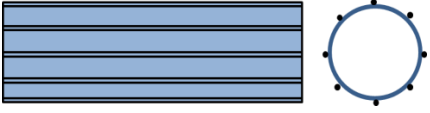

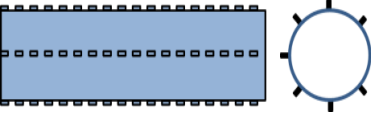
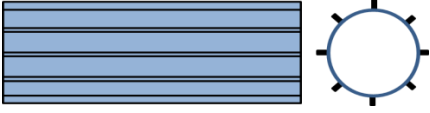
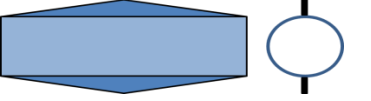


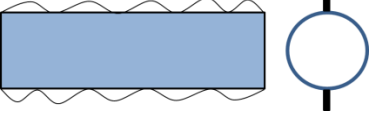
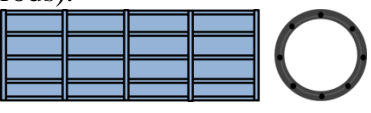
<p>Configuration 1: Pipelines stiffened with 20 mm diameter circular bars along the length.</p> 	<p>Configuration 2: Pipelines stiffened with 20 mm diameter semi-circular bars embedded in concrete layer along the length.</p> 	<p>Configuration 3: Pipelines stiffened with 10 mm x 50 mm x 150 mm cross section rectangular pins.</p> 
<p>Configuration 4: Pipelines stiffened with 10 mm x 50 mm x 15000 mm cross section rectangular bars.</p> 	<p>Configuration 5: Pipelines stiffened with varying cross-section (200 mm height at mid length).</p> 	<p>Configuration 6: Pipelines stiffened with 20 mm diameter semi-circular bars along the length.</p> 
<p>Configuration 7: Pipelines stiffened with 10 mm thick concrete coating along the length.</p> 	<p>Configuration 8: Pipelines stiffened with sinusoidal curved plates.</p> 	<p>Configuration 9: Pipelines stiffened with both longitudinal and ring stiffeners (20 mm diameter rods).</p> 

Figure 2.1 Schematic diagram of different configurations of Buckle Arrestors considered.

2.1.2 1-D Finite Element Analysis of buckle arrestors for offshore pipelines

The preliminary buckling analysis of the all the proposed buckle arrestor configurations was done using *MATLAB* programming. One dimensional finite element analysis of stiffeners was performed using two node 1-D linear element which was developed from the Euler-Bernoulli bending equation. The pipeline section is considered as a horizontal column (Figure 2.2) of length ‘L’ with pinned supports on both the ends of the pipeline. The governing equations and the end conditions used for the 1-D finite element analysis is given in the following equations (2.1), (2.2) and (2.3.)

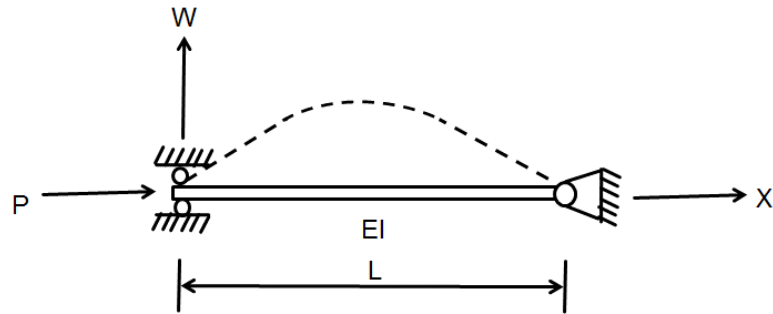


Figure 2.2 Schematic diagram of the simple pipeline with axial load and end conditions.

Governing equation:

$$\frac{d^2}{dx^2} \left(EI \frac{d^2 w}{dx^2} \right) + P \frac{d^2 w}{dx^2} = 0 \quad (0 \leq x \leq L) \dots \dots \dots (2.1)$$

Boundary condition:

$$w(0) = w(L) = 0 \text{ (Essential boundary conditions)}$$

$$\frac{d^2 w(0)}{dx^2} = \frac{d^2 w(L)}{dx^2} = 0 \text{ (Natural boundary conditions)}$$

Where, E = Young's modulus of the material, I = Moment of inertia, w = Vertical deflection and P = Axial load. The eq. 1 can be converted to second order differential equation by replacing the term $\frac{d^2 w}{dx^2}$ with a variable 'y'. The modified governing equation with the boundary conditions is given below:

$$\frac{d^2}{dx^2} (EIy) + P y = 0 \quad \text{(Governing equation)} \dots \dots \dots (2.2)$$

$$y(0) = y(L) = 0 \quad \text{(Essential boundary conditions)}$$

The governing equation is solved by using Galerkin's method to form finite element formulation of two node one dimensional element of length-*l* (eq. 3). The finite element equation (3) is used to find the buckling load capacity of the all proposed pipeline configurations. The general *MATLAB* code was written for 'n' number of elements to analyse the pipeline for varying elements. The convergence study was done by varying number of elements of all the configurations of pipeline stiffeners and results of simple pipe section and configuration 3 have given in Figure 2.3.

$$\left[\frac{1}{l} \begin{bmatrix} 1 & -1 \\ -1 & 1 \end{bmatrix} + \frac{Pl}{EI} \begin{bmatrix} -\frac{1}{3} & -\frac{1}{6} \\ -\frac{1}{6} & -\frac{1}{3} \end{bmatrix} \right] \begin{Bmatrix} y_1 \\ y_2 \end{Bmatrix} = \begin{Bmatrix} 0 \\ 0 \end{Bmatrix} \dots\dots\dots (2.3)$$

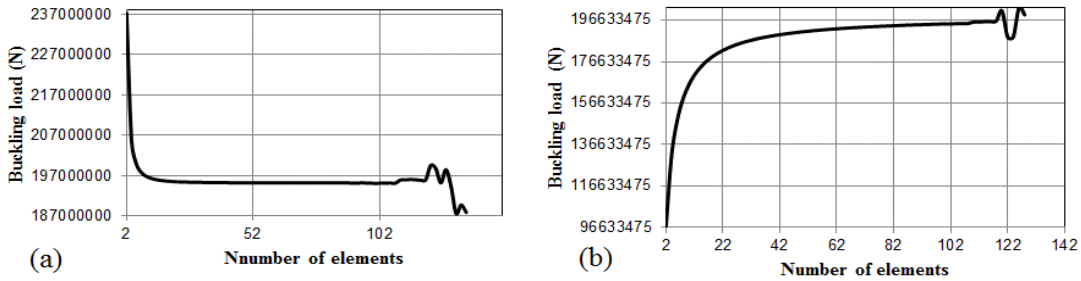


Figure 2.3 (a) Convergence study of Simple pipeline, (b) Configuration 3 buckling load capacity using MATLAB.

2.1.3 3-D Finite Element Analysis of buckle arrestors for offshore pipelines

The preliminary three dimensional finite element analysis of the proposed stiffener configurations was performed using ANSYS workbench. SOLID186 element was considered for the 3-D finite element analysis. SOLID186 is a higher order 3-D 20-node solid element that exhibits the quadratic displacement behaviour with three degrees of freedom per node. The geometries of the proposed pipe configurations with stiffeners were drawn using AUTOCAD software and imported to ANSYS workbench for buckling analysis. The pipeline configurations were analysed for the pinned boundary conditions at both ends of the pipeline. The meshed models and the deflection shapes of the all nine configurations are given in Figure 2.4 and Figure 2.5 respectively. The buckling load capacities of all the configurations are tabulated.

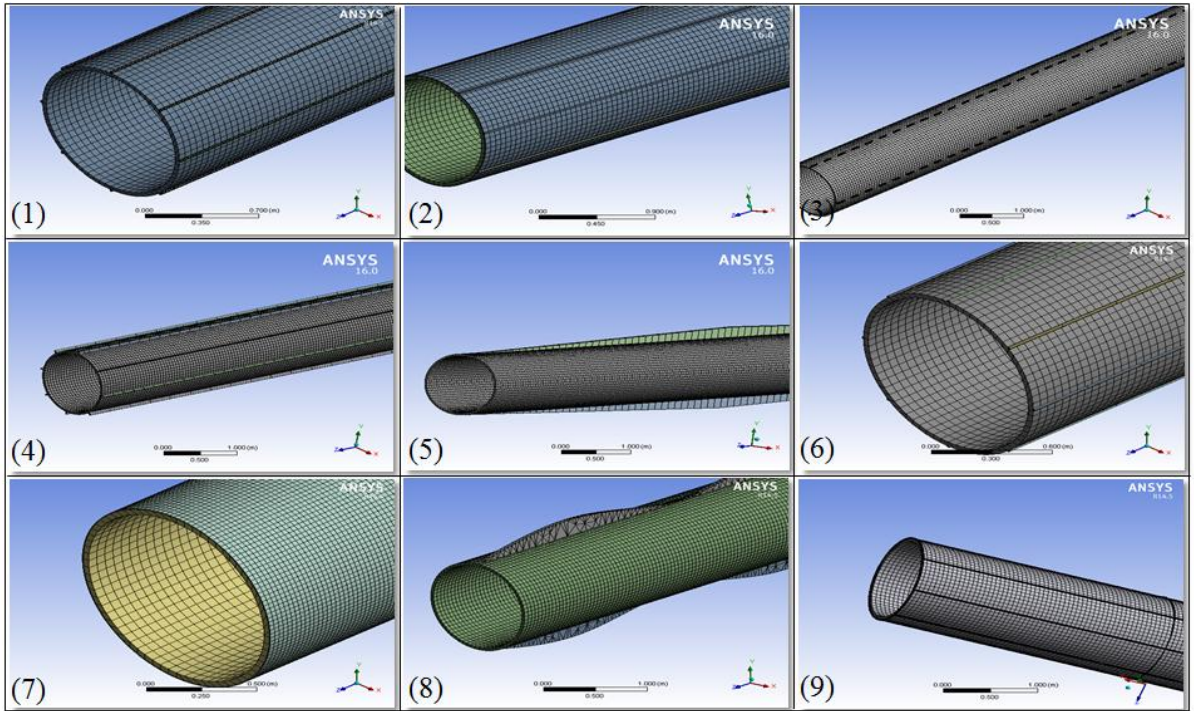


Figure 2.4 Finite element mesh models of the all nine stiffener configurations of pipeline.

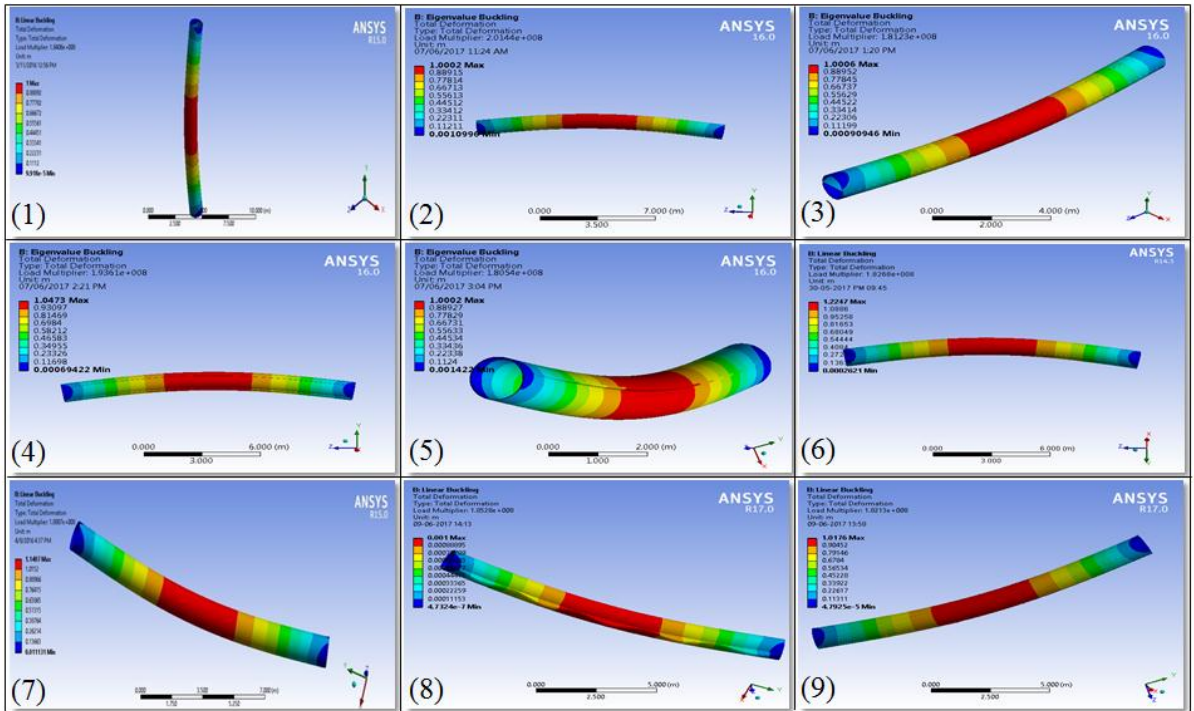


Figure 2.5 The deflection shapes of the all nine stiffener configurations of pipeline.

2.1.4 Preliminary Finite Analysis Results

The theoretical buckling load capacity of the simple pipeline configuration was calculated, using Euler's column elastic buckling theory ($P_{cr} = \pi^2 \frac{EI}{l^2}$), as 1.85×10^8 N. The buckling capacity of the all nine pipeline configurations along with simple pipeline section were analysed using *MATLAB* program and *ANSYS* software. The buckling load capacity obtained with stiffener configurations were compared with simple pipeline configuration and the percentage of increments in buckling load capacity due to stiffener are listed in Table 2.1.

Table 2.1 Buckling load capacity of all nine configurations obtained from 1D linear element (*MATLAB* code) and *ANSYS*.

CONFIGURATIONS	Buckling load ($\times 10^8$ N)		Buckling load increment (Percentage)	
	MATLAB	ANSYS	MATLAB	ANSYS
SIMPLE HOLLOW PIPE	1.8588	1.8021	-	-
CONFIGURATION 1: (pipe section stiffened with 20 mm rods)	1.9969	1.8406	7	2
CONFIGURATION 2: (pipe section with concrete coating and 20 mm rods)	1.9232	2.0144	3	12
CONFIGURATION 3: (pipe section with rectangular pins)	2.1419	2.5680	15	43
CONFIGURATION 4: (pipe section stiffened with rectangular plate (50 mm x 20 mm x 15000 mm))	1.9643	1.9361	6	7
CONFIGURATION 5: (pipe section with rectangular block 200 mm x 50 mm x 15000 mm)	1.9301	1.8045	4	0
CONFIGURATION 6: (pipe section with 20 mm hemispherical rods)	1.8435	1.8268	-1	1

CONFIGURATION 7: (pipe section coated with 10 mm concrete coating)	1.8438	1.8907	-1	5
CONFIGURATION 8: (Pipe sections stiffened with 200 mm curved plate)	1.8660	1.8140	0	1
CONFIGURATION 9: (pipelines stiffened with both horizontal and vertical 20 mm rods)	1.9867	1.8210	7	1

MATLAB considers one dimensional linear elements and facilitates computation of buckling load using Matrix analysis. The buckling load for various buckle arrestor configurations is compared with the buckling load of pipeline model without stiffeners. *ANSYS* considers quadratic elements with 20 nodes therefore it considers the effects at half the thickness ($T/2$) of the pipeline. The buckling load for various buckle arrestor configurations is compared with the buckling load of pipeline model without stiffeners. *MATLAB* results are dependent on analytically calculated moment of inertia values and confirm with analytical results given by Euler's formula. In case of three dimensional analysis performed using *ANSYS* the moment of inertia value is manually fed into the system as input and this could vary from section to section depending on the type of buckle arrestor configuration (Sinusoidal stiffeners and Angular Stiffeners) this explains the variation in buckling loads for the same configurations and there is no conformity between *MATLAB* results and *ANSYS* results. Data in the table 2.1 doesn't compare *MATLAB* results with *ANSYS* results, but presents both one dimensional and three dimensional analysis. Pipe section with rectangular pins (Configuration 3) stiffener has given more buckling strength to pipeline than the other configurations. The buckling load capacity increased up to 43 % than the simple pipe section according to the *ANSYS* results, according to *MATLAB* results it showed an increase of 15 % . . For fabrication of pipeline models rectangular pin buckle arrestors model was considered along with angular stiffeners and sinusoidal stiffeners. The three dimensional finite element analysis performed using *ANSYS* is suitable for analysis of buckling load of pipeline models.

2.1.5 Modeling of inclined buckle arrestor and inclined buckle arrestor with connecting rod

Finite element modeling of seamless stainless steel pipes of dimensions 15 m length, 1.19 m outer diameter, 1.12 m inner diameter and 0.035 m thickness was considered and the material properties as Density of steel 7850 kg/m³, Young's modulus 200 GPa, Poisson's ratio 0.3 was considered for analysis of offshore pipelines and their schematic diagram is as shown in Figure 2.6.

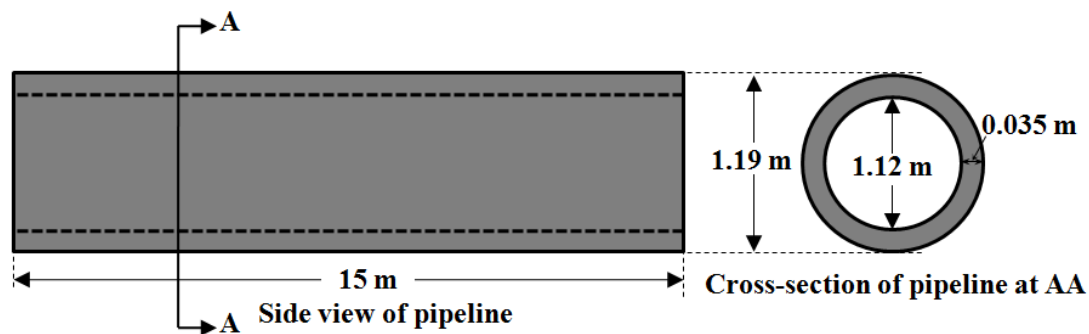


Figure 2.6 Dimensions of a simple pipeline model considered for study.

Schematic diagrams of all the pipe models are drawn using computer-aided design software *AutoCAD*. Dimensions of buckle arrestors and angle between each buckle arrestor for inclined stiffener model are given in Table 2.2. Pipe geometry and configuration of inclined stiffeners models are shown schematically in Figure 2.7(a) (b) (c) and (d). Finite element meshing of pipeline models with inclined stiffeners and inclined stiffeners with connecting rods are shown in Figures 2.8 (a) (b) (c) and (d).

Table 2.2 Geometrical details of buckle arrestors

Pipe models	Dimensions of buckle arrestors (m)			Angle of buckle arrestors	Connecting Rod Diameter (m)	Buckle arrestor spacing (m)
	Length	Width	Thickness			
Pipe with inclined stiffeners	2.25	0.3	0.1	100° - 174°	-	4.5
Pipe with inclined stiffeners and connecting rod	2.25	0.3	0.1	100° - 150°	0.2	4.5
Pipe with large inclined stiffeners	1.5	0.3	0.1	100° - 176°	-	3
Pipe with large inclined stiffeners and connecting rod	1.5	0.3	0.1	120° - 150°	0.2	3

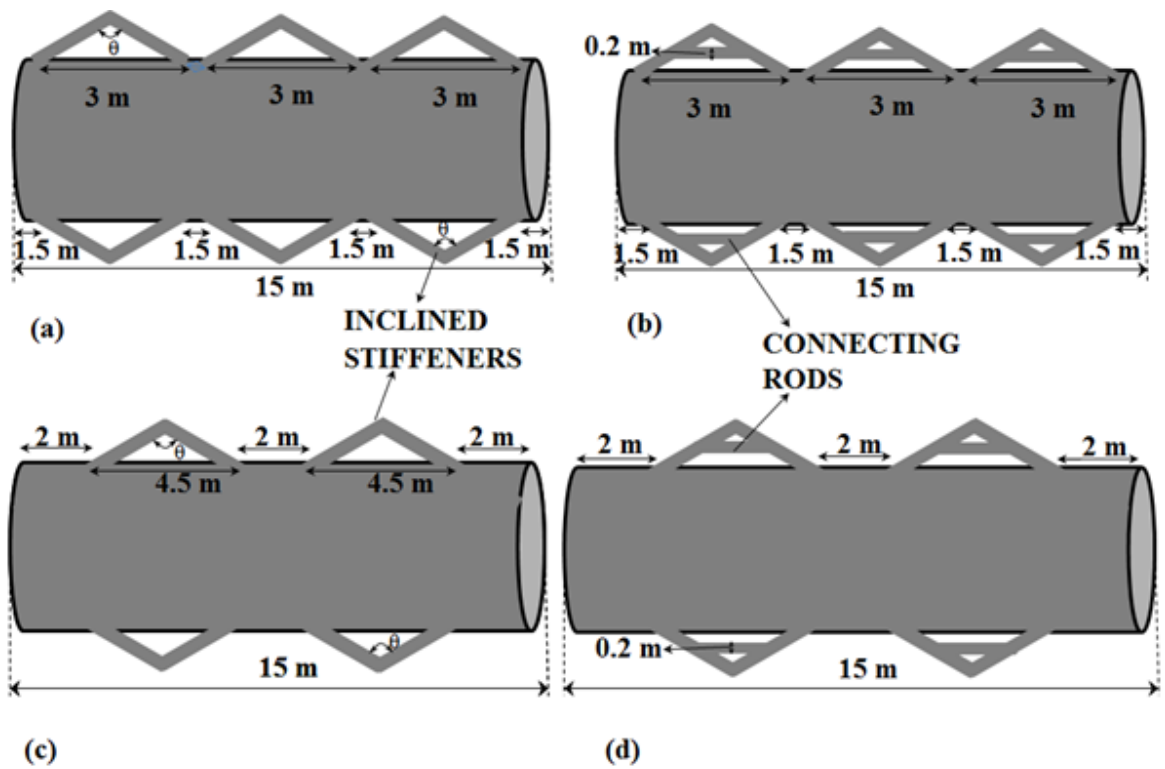


Figure 2.7 Cross-sections of a pipe models with inclined stiffener configurations (a) & (c) and inclined stiffener configurations with connecting rods (b) & (d).

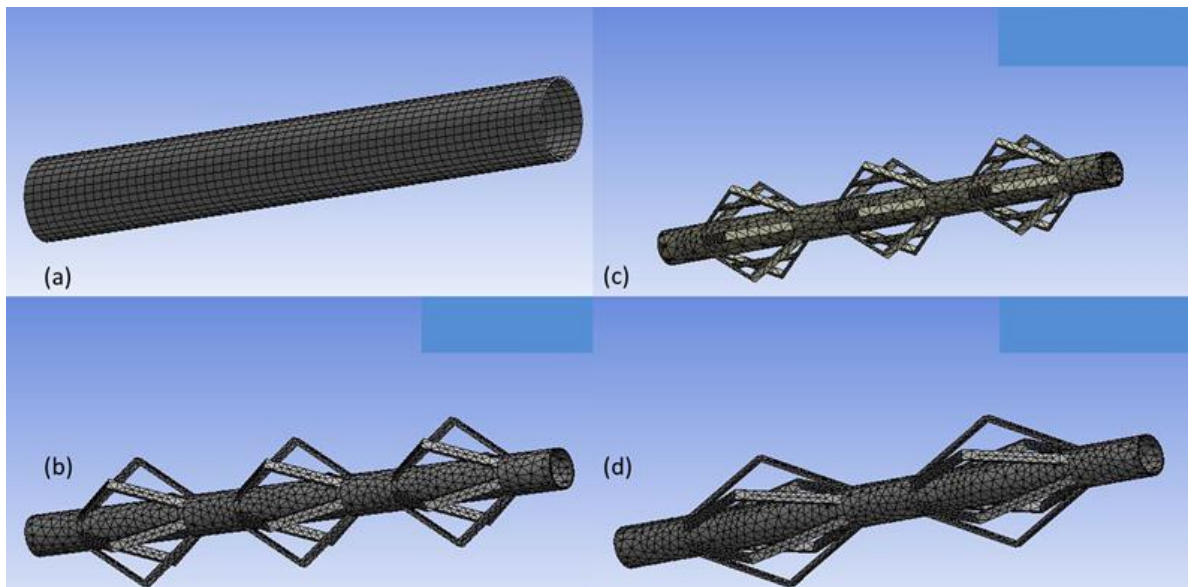


Figure 2.8 (a) Finite element models without stiffener (b) pipeline with inclined stiffener (c) pipeline with inclined stiffener and connecting rod (d) pipeline with large inclined stiffener

2.1.6 Meshing Parameters

Pipeline models were analyzed employing eigenvalue buckling analysis; finite element models were developed using ANSYS software. For modeling and meshing offshore pipelines, SOLID187 elements were considered to study deformation along X, Y and Z axes (u, v and w). SOLID187 is a higher order three dimensional solid element that shows quadratic displacement behaviour and is characterized by 10 nodes having three degrees of freedom per node and translations along the nodal x, y, and z directions. This element comprises 7 nodes on the outer surface and inner surface of the pipe model and 3 nodes in mid-thickness of a pipe. Meshing criterion was set to be fine and program controlled. Shape transition was considered to be medium. Span angle centre and smoothing boundary were considered to be moderate. Element area for pipeline meshing is 5 mm. For both, triangle and rectangle elements, there are higher order formulations such as 6 node triangle and 8 noded rectangle (Q8) which are both more accurate.

An axial compressive load of 1N applied over the entire circumference of a pipeline. An Eigenvalue buckling analysis was performed to find buckling load of pipeline due to the axial compressive load. Fig. 2.9 (a) shows the meshing of a pipeline model in ANSYS used for eigenvalue buckling analysis. In terms of meshing for Figure 2.9 (b), triangle elements can be extremely useful near finished curved geometry as it is a lot simpler to fill out regions with triangles. For finite element analysis of pipe models, total 7584 nodes and 1072 elements was considered.

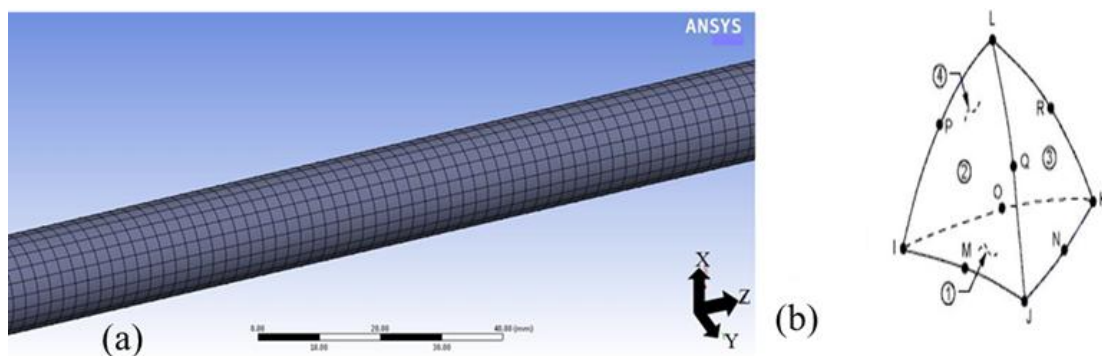


Figure 2.9 (a) Solid element mesh of a plain pipeline model (b) Element Model SOLID187 using ANSYS.

2.2 Eigen value buckling analysis results

Pipe models strengthened with inclined stiffeners, inclined stiffeners with connected rods and pipe model without inclined stiffeners were modeled using ANSYS. The buckling load obtained for each model by performing Eigen value buckling analysis. The results obtained from finite element analysis have been presented in Table 2.3. Further these results have been used for estimating increase in load carrying capacity of the pipe model with and without inclined stiffeners under the effect of axial compressive load.

2.2.1 Effect of varying angle of inclination and length of inclined stiffeners

The pipe models were analyzed with and without inclined stiffeners. The percentage variation of buckling load of pipe configurations with and without inclined stiffeners, with stiffener angle variation is listed below in Table 2.3.

Table 2.3 Values of buckling load for different pipe configurations with different angle of buckle arrestors.

Sl. No.	Configuration	Angle of inclination	Buckling load (kN)	Percentage increase (%)
1	Pipe without stiffener		4.6204×10^4	-
2	Pipe with inclined stiffener	100°	4.8581×10^4	5.14
3		110°	4.8935×10^4	5.91
4		120°	4.9593×10^4	7.33
5		130°	5.0541×10^4	9.38
6		140°	5.1979×10^4	12.49
7		150°	5.4576×10^4	18.11
8		160°	6.0044×10^4	29.95
9		170°	6.5356×10^4	41.45
10		174°	6.1266×10^4	32.59
11		Pipe with inclined stiffener and connecting rod	100°	5.4270×10^4
12	110°		5.2354×10^4	13.31
13	120°		5.4225×10^4	17.35
14	130°		5.6862×10^4	23.06
15	140°		6.0341×10^4	30.59

16		150°	6.4993 x 10 ⁴	40.66
17	Pipe with large inclined stiffener	120°	4.8615 x 10 ⁴	5.21
18		130°	4.9197 x 10 ⁴	6.47
19		140°	5.0083 x 10 ⁴	8.39
20		150°	5.1581 x 10 ⁴	11.63
21		160°	5.5024 x 10 ⁴	19.08
22		170°	6.4309 x 10 ⁴	37.23
23		176°	6.1367 x 10 ⁴	32.81
24	Pipe with large inclined stiffener with connecting rod	120°	5.1422 x 10 ⁴	11.29
25		130°	5.3209 x 10 ⁴	15.16
26		140°	5.5693 x 10 ⁴	20.53
27		150°	5.9912 x 10 ⁴	29.66

From the above table it has been observed that the, buckling load carrying capacity of a pipe models increases with increase in angle of a stiffener. Pipe models with stiffener and with angle variation 100°-174°. Pipe model configuration with angle variation 170° is found to be more effective in carrying buckling load of 6.4993 x 10⁴ kN and shows highest percentage increase (41.45 %). Pipe models with stiffener and rod, with angle variation 100°-150°. Pipe model configuration with angle variation 150° is found to be more effective in carrying buckling load of 6.499 x 10⁴ kN and shows highest percentage increase (40.66 %). Pipe models with large stiffener, with angle variation 100°-176°. Pipe model configuration with angle variation 170° is found to be more effective in carrying buckling load of 6.4993 x 10⁴ kN and shows highest percentage increase (37.23 %). Pipe models with large stiffener and rod, with angle variation 120°-150°. Pipe model configuration with angle variation 150° is found to be more effective in carrying buckling load of 5.9912 x 10⁴ kN and shows highest percentage increase (29.66 %) when compared with pipe model without buckle arrestors. The change in angle of inclined stiffener changes the moment of inertia of the pipeline section. The increase in buckling load capacity of the pipeline with increase in inclined stiffener angle is due to increase in moment of inertia of the pipeline.

Three dimensional finite element modeling was used to understand buckling behaviour of inclined buckle arrestors with angle variation ranges from 100°-174°

welded over a pipeline. Based on finite element analysis results conclusions are drawn as:

- Stiffening of pipelines is an effective method of increasing critical buckling load of offshore pipelines.
- Pipeline with stiffeners like bent plate with internal angle of 170° can increase buckling load by 41.45% for an effective length of 15 m pipeline with 6 stiffeners placed at three positions with spacing of 1.5 m and horizontal coverage of 3 m.
- Pipeline with stiffeners like bent plate with internal angle of 150° along with the cylindrical rod can increase buckling load by 40.66% for an effective length of 15 m pipeline with 6 stiffeners with rod placed at three positions with spacing of 1.5 m and horizontal coverage of 3 m.
- Pipeline with large stiffeners like bent plate with internal angle of 170° can increase buckling load by 37.23% for an effective length of 15 m pipeline with 6 stiffeners placed at two positions with spacing of 2 m and horizontal coverage of 4.5 m.

From the finite element analysis results, longitudinal continuous stiffeners (**Configuration 4**), sinusoidal stiffeners (**Configuration 8**), and angular stiffeners (**Configuration 5**) were selected for specimen fabrication and experimental validation.

CHAPTER 3

DETAILS OF BUCKLING EXPERIMENTS

This chapter gives detail procedure of material selection, fabrication of pipe specimens and buckle arrestors, fabrication of end blocks to ensure end conditions. The methodology adopted for the present research work, which involves finite element modeling and analysis of results, fabrication, of specimens, conducting experiments, validation of experiment results.

3.1 Material

Stainless steel grade SS304 is most widely used stainless steel. The austenitic structure enables it to be deep drawn without intermediate annealing, which has made this grade dominant in the manufacture of seamless pipes. It has excellent forming and welding characteristics, corrosion resistant with usage in a wide range of atmospheric environments on exposure to chemicals. The present study, material considered for pipeline and stiffeners is stainless steel. Seamless stainless steel pipes of SS304 grade with Young's modulus of 197 GPa, Poisson's ratio 0.3 and density of steel 7850 kg/m³.

3.1.1 Fabrication of specimens for conducting buckling experiments with various buckle arrestor configurations (Sinusoidal, Angular and Longitudinal continuous)

Stainless Steel pipelines, made of SS304 grade steel, were used for conducting buckling experiments, considering the material's ease of welding and its suitability for marine applications (Figure 3.1). SS304 grade stainless steel pipes 1100 mm long are cut using Computerized Numerical Control (CNC) Lathe machine to the required length of 1000 mm. The external diameter (D) of the pipe is 16 mm and the internal diameter (d) of the pipe is 11.80 mm. The thickness of the steel pipe is 2.1 mm. On the outer surface of the pipeline, a groove of 1.1 mm (Figure 3.2 & 3.3) was made at regular intervals along the circumference of a pipeline in the longitudinal direction using computerized numerical control machine to attach 8 rectangular pin buckle arrestors of stainless steel (SS304 grade) to the pipeline at an angle of 45°, 2

sinusoidal and angular buckle arrestors of stainless steel (SS304 grade) is welded to the pipeline using plasma arc welding process.

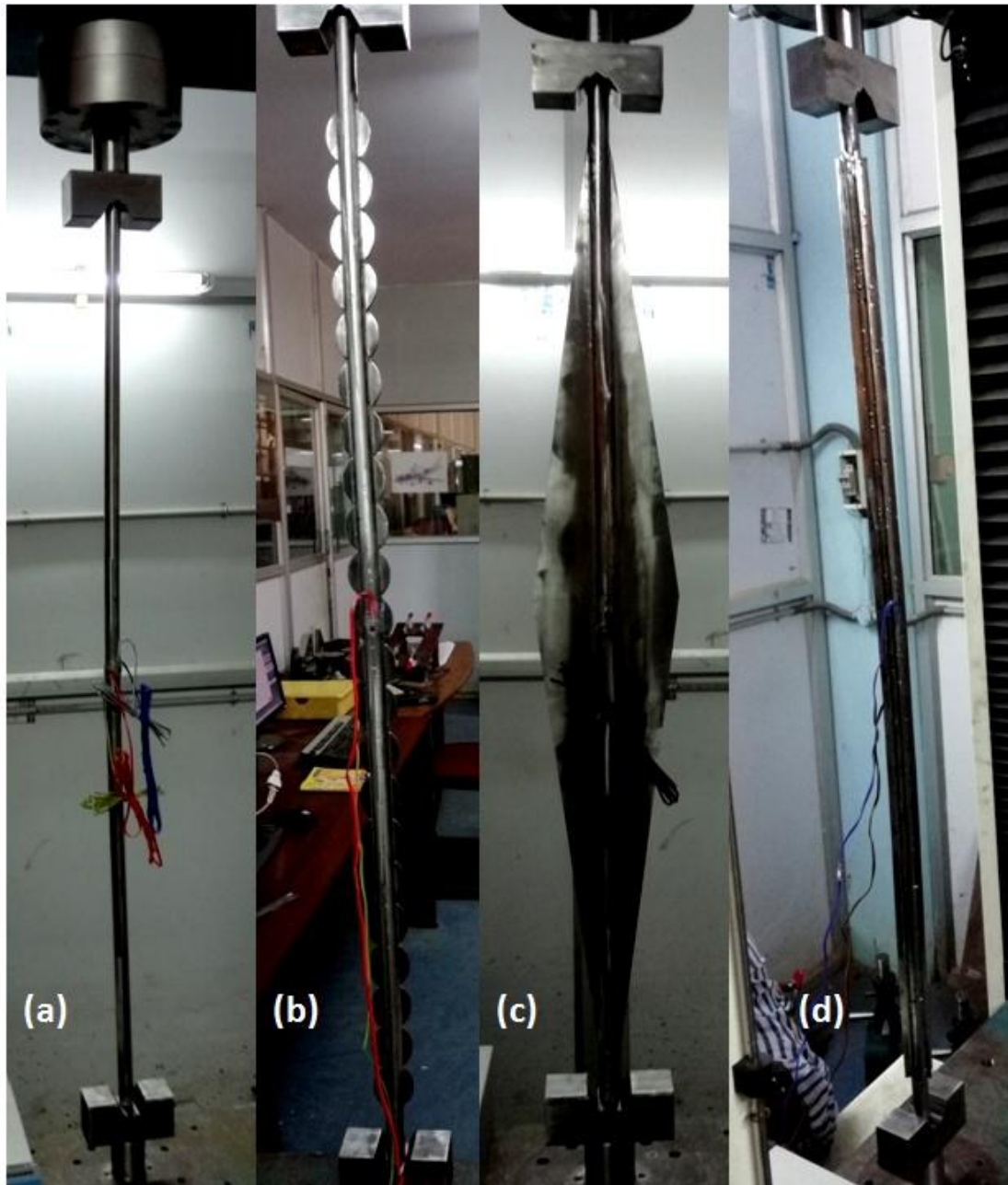


Figure 3.1 Specimens fabricated for conducting buckling experiments (a) pipeline without buckle arrestors (b) sinusoidal buckle arrestor (c) Angular buckle arrestor (d) longitudinal continuous buckle arrestor.

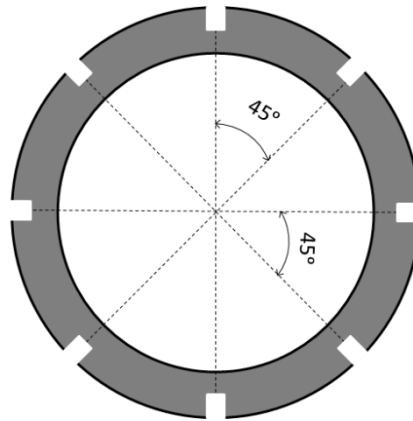


Figure 3.2 Schematic representation shows a pipeline with the groove to attach longitudinal continuous buckler arrestors.

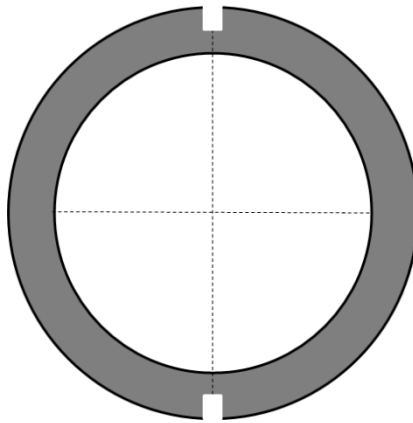


Figure 3.3 Schematic representation shows a pipeline with the groove to attach sinusoidal and angular buckler arrestors.

3.1.2 Calibration of strain gauges and determination of location of pasting strain gauges to pipeline models for conducting buckling experiments with various buckle arrestor configurations (Sinusoidal, Angular and Longitudinal continuous)

The calibration of strain gauges was done by pasting strain gauges to Stainless Steel strip (Figure 3.4) and using the stainless strip as a cantilever beam and completing the cantilever beam testing set up by connecting the strain gauges to data acquisition system connected to laptop. The cantilever beam was then loaded with constant increments of loads and the deflections corresponding to each load increment were measured. Euler's bending theory formula was used to calculate Young's modulus of Stainless Steel by substituting corresponding loads and strain value given in table 3.1 . The Young's modulus thus calculated, which was in the range of 200GPa - 210GPa,

was used to calibrate the strain gauges. Similarly, before conducting the buckling experiments, after fixing the specimen between the Upper end block and Lower end block a trial data set consisting of force, strain and stress was collected, before the onset of buckling, in the Data Acquisition System, before loading the specimen to confirm the effective functioning of the buckling testing equipment.

Table 3.1: Summary of results obtained during calibration of strain gauges

Sl.No	W(gms)	micro strain
1	0	106
2	50	141
3	100	177
4	150	216
5	200	253
6	250	291
7	200	253
8	150	215
9	100	176
10	50	138
11	0	99

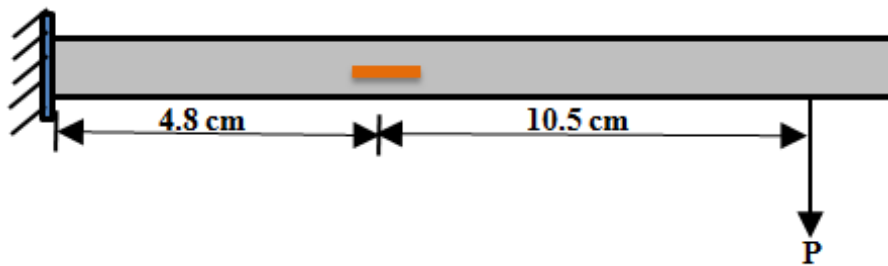


Figure 3.4 Schematic representation of Stainless Steel strip pasted with Strain gauges during calibration.

The external surface of a pipeline cleaned with Acetone (C_3H_6O) solution and strain gauges were bonded to an outer surface using Cyanoacrylate Adhesive (Anabond 202). Quarter-bridge circuit strain gauges of gauge resistance 120Ω having a gauge factor of 2.1 and grid size 5 mm was used to measure Strain. Connecting wire was soldered to strain gauges, which were pasted to the external surface of the pipeline sample. The other end of the connecting wire is connected to the data logger, which is connected to a computerized data acquisition system to observe time, the compressive force applied, stress, strain, and position of the pipeline.

Four strain gauges were pasted to the pipeline without stiffener. Two strain gauges were glued along the longitudinal direction, and two strain gauges were pasted along the lateral direction at the centre of a test specimen. Pipeline specimen stiffened with longitudinal continuous stiffeners was glued with two strain gauges to stiffeners located diametrically opposite to each other, one at the centre of the span and the other at a distance of 530 mm, Pipeline specimen stiffened with sinusoidal stiffeners was glued with two strain gauges to pipe located diametrically opposite to each other, one at the centre of the span and Pipeline specimen stiffened with angular stiffeners was glued with two strain gauges to pipe located diametrically opposite to each other, one at the centre of the span schematic diagram has been shown in Figure 3.5, Figure 3.6, Figure 3.7 and Figure 3.8.

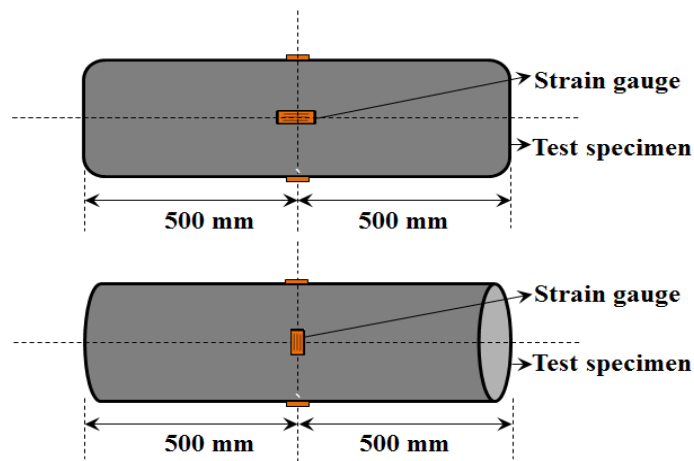


Figure 3.5 Schematic representation of simple pipeline pasted with Strain gauges to conduct the buckling experiment.

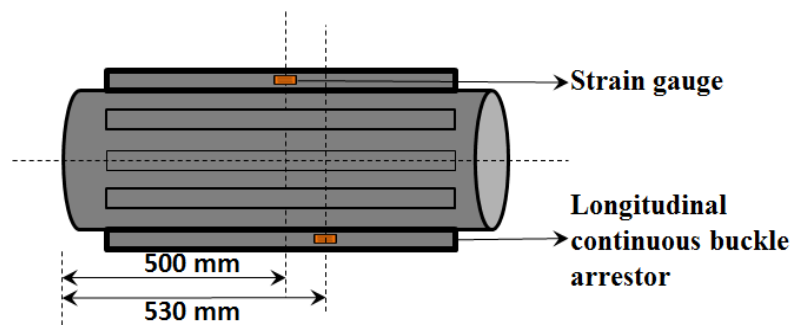


Figure 3.6 Schematic representation of longitudinal continuous stiffeners pipeline pasted with Strain gauges to conduct the buckling experiment.

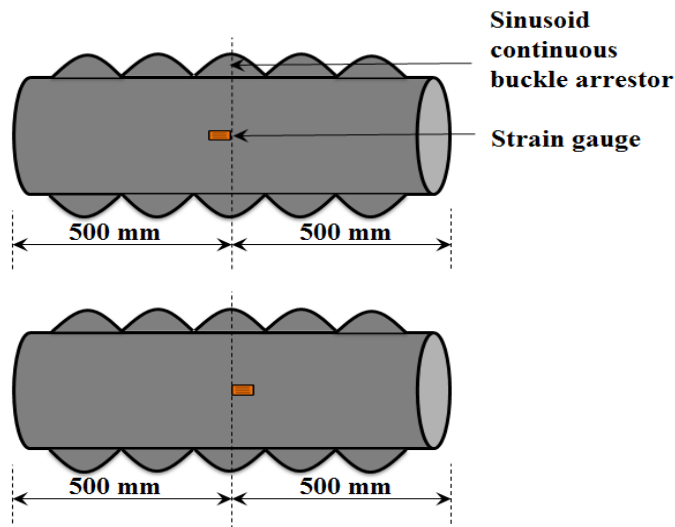


Figure 3.7 Schematic representation of sinusoidal stiffeners pipeline pasted with Strain gauges to conduct the buckling experiment.

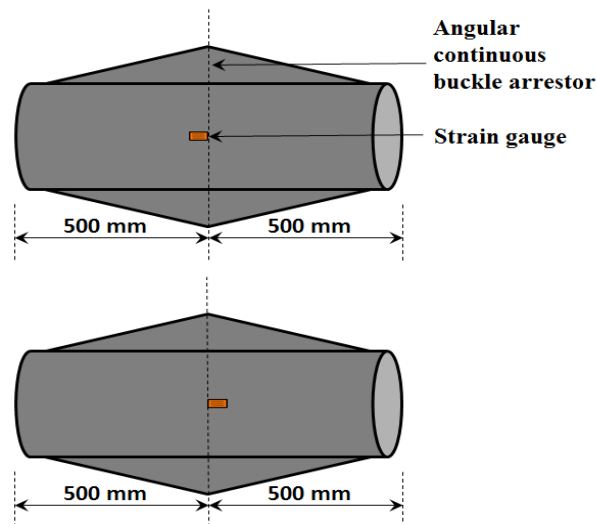


Figure 3.8 Schematic representation of angular stiffeners pipeline pasted with strain gauges.

3.1.3 Buckling experimental setup with various buckle arrestor configurations (Sinusoidal, Angular and Longitudinal continuous)

The buckling experimental setup is supported on an upper bed and lower bed. It consists of two grip holders, one at the top end and other at the bottom end, which is supported by two vertical steel columns. The upper grip is attached to the upper-end holder, and the lower grip is attached to the lower end holder which is connected to the loading system. The load applied by the loading system transfers to the specimen by the piston rod which is connected to the upper grip. The load applied by the system

would be monitored by the load cell attached to the upper grip. The axial compressive load, which has displacement control of 0.1mm/min, would be applied by the operating 100 kN UTM is shown in Figure 3.9. Strains at mid-length of the pipeline were measured by strain gauges pasted to the pipe specimen the load and strain measuring systems were connected to the computerized data acquisition system. The diagram of the buckling experimental set-up with plain pipeline and pipeline stiffened with longitudinal continuous, sinusoidal stiffener and angular stiffener is given in Figure 3.10.

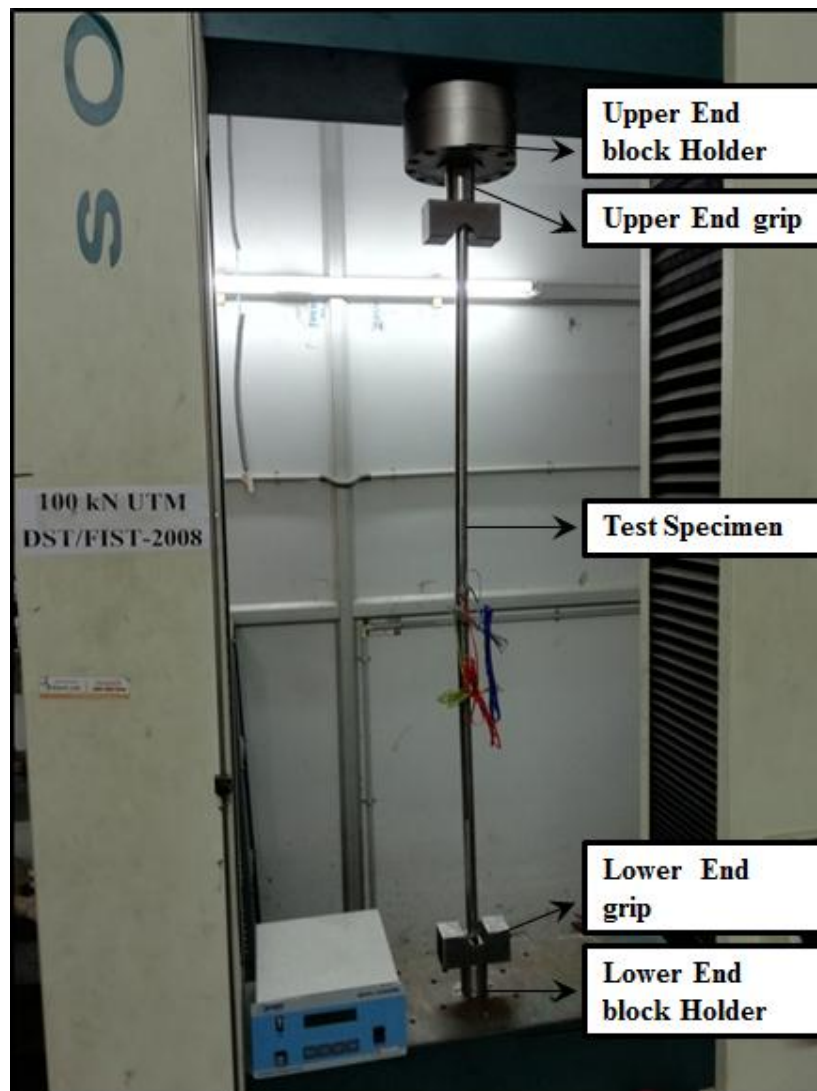


Figure 3.9 Photograph of buckling experimental setup.

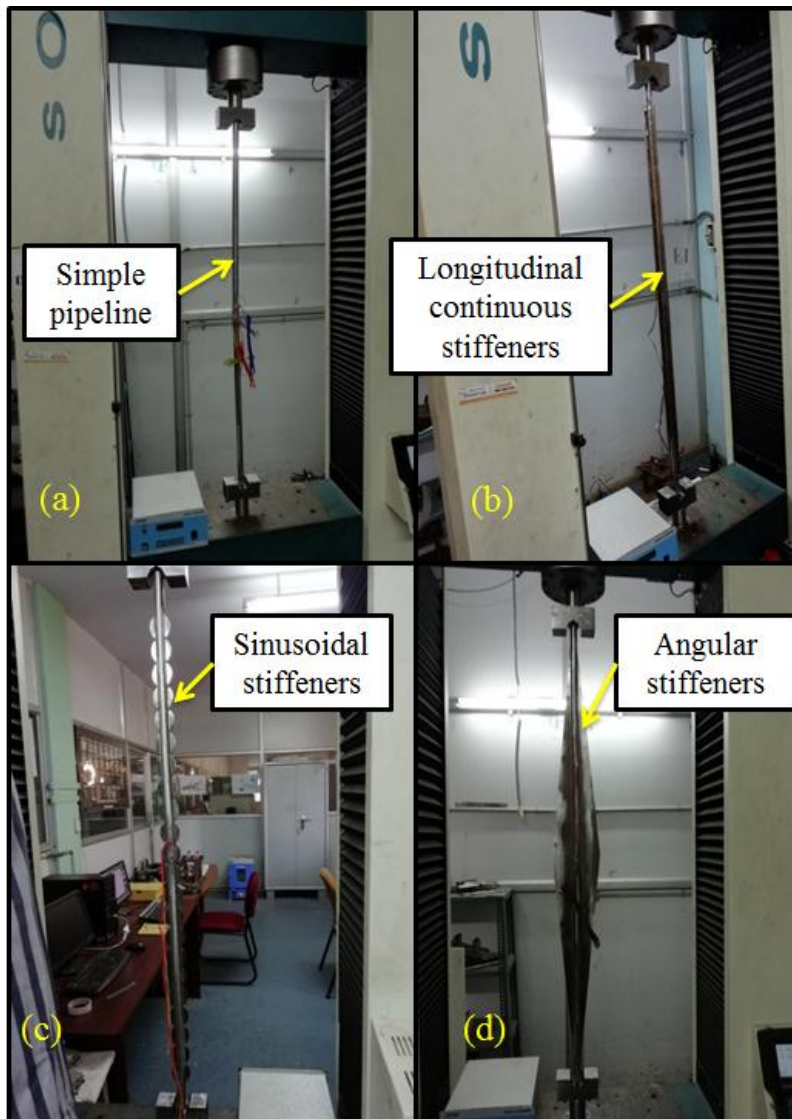


Figure 3.10 Buckling experimental setup to test (a) plain pipeline, (b) pipeline with longitudinal continuous stiffener, (c) sinusoidal stiffener and (d) angular stiffener respectively.

A steel pipeline section of outer diameter 16 mm, thickness 2.1 mm measured using digital vernier callipers and inner diameter of 11.8 mm and length of 1 m was used for conducting buckling experiments. The pipeline diameter was measured at 20 cm interval to ensure uniformity of the pipeline. The experimental set up comprising strain gauges, data logger and Data Acquisition System was used to collect thousand data samples of axial compressive load applied, resulting stress and strain in the pipeline stiffened with different buckle arrestors.

The specimen was supported by both the upper end and lower end blocks (Figure 3.11) to ensure pinned–pinned boundary condition, vertical alignment and application of axial compressive load. The load applied by the loading system transfers to the specimen by the piston rod which is connected to the upper grip. The load applied by the system would be monitored by the load cell attached to the upper grip.



Figure 3.11 Upper end and lower end blocks used to apply axial compressive load to the pipe during the buckling experiment.

Totally, four specimens were fabricated and tested in the laboratory. All buckle arrestors have been fabricated using the same material (SS304) as pipeline specimens and welded to the outer diameter of pipeline model. Quarter bridge strain gauges pasted to the pipeline (a) without Buckle arrestors (b) stiffened with longitudinal continuous Buckle arrestors (c) stiffened with sinusoidal continuous Buckle arrestors (d) stiffened with angular continuous Buckle arrestors to conduct the buckling experiment is as shown in Figure 3.12. The quarter bridge strain gauges pasted to the pipeline were connected to the data logger and the data logger sends buckling experiment data, i.e., axial loads, stresses, strains and axial displacements to computerized Data Acquisition System (DAS). Figure 3.13 shows buckling experiment in progress.

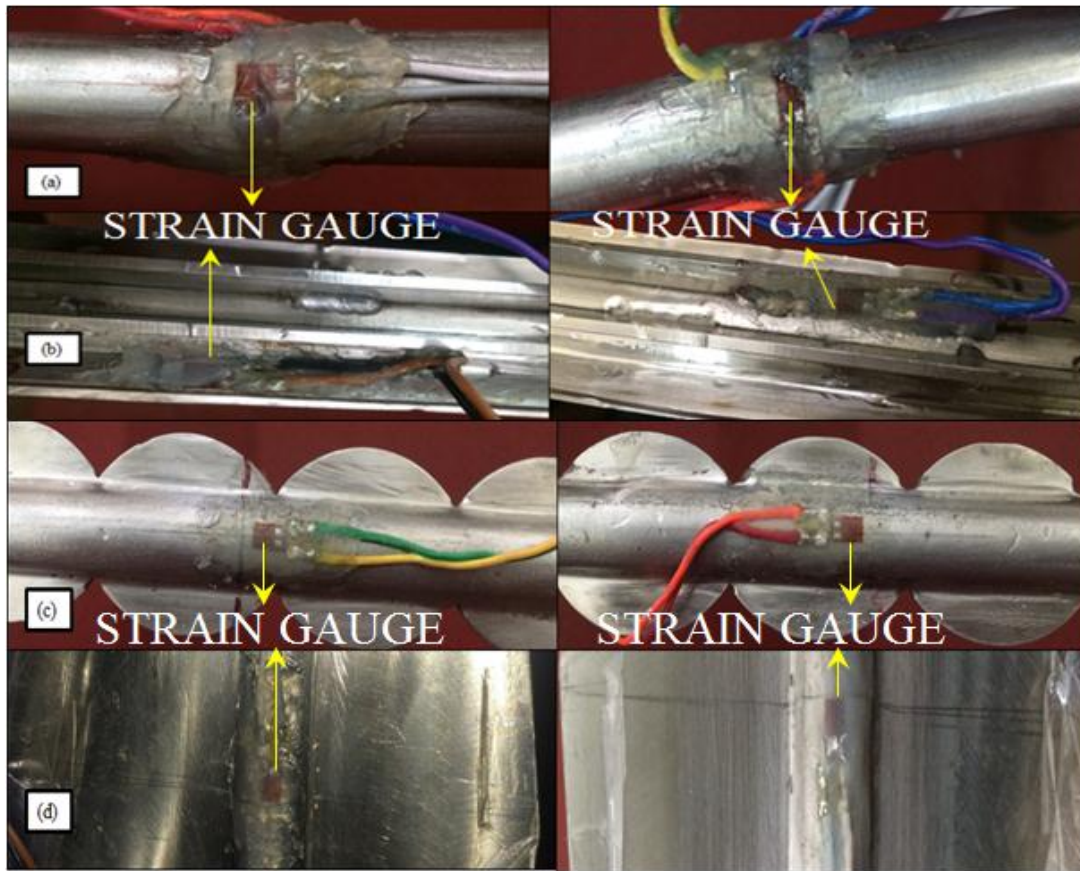


Figure 3.12 Strain gauges pasted to the pipeline (a) without Buckle arrestors (b) with longitudinal continuous Buckle arrestors (c) with sinusoidal Buckle arrestors (d) with angular Buckle arrestors to conduct the buckling experiment.

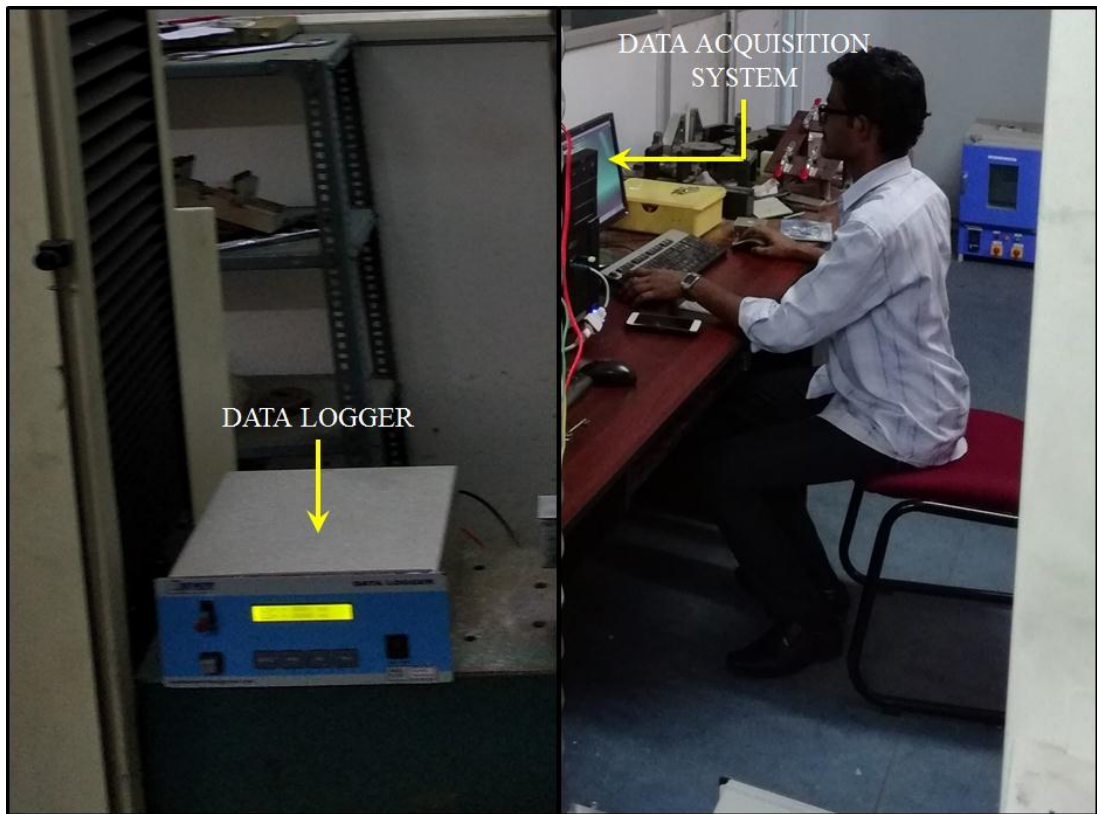


Figure 3.13 Computerized Data Acquisition System (DAS) connected to the data logger to collect experimental data while conducting experiment on pipeline model.

3.1.4 Fabrication of specimens for conducting buckling experiments with rectangular pin buckle arrestor configurations welded at different locations

Stainless Steel pipelines, made of SS304 grade steel, were used for conducting buckling experiments, considering the material's ease of welding and its suitability for marine applications. SS304 grade stainless steel pipes 900 mm long are cut using Computerized Numerical Control (CNC) Lathe machine to the required length of 700 mm. The external diameter (D) of the pipe is 16 mm and the internal diameter (d) of the pipe is 13 mm. The thickness of the steel pipe is 1.5 mm. Depth of cutting of the steel pipe is 0.4 mm per minute. On the outer surface of the pipeline, a groove of 0.2 mm (Figure 3.14) was made at regular intervals along the circumference of a pipeline in the longitudinal direction using computerized numerical control machine to attach 8 rectangular pin buckle arrestors of stainless steel (SS304 grade) to the pipeline at an angle of 45° using Tungsten Inert Gas (TIG) spot welding process. Optimized 70

volts DC power supply is used for spot welding to avoid thermal bending, buckling and related damages to the pipeline. The external surface of a pipeline cleaned with Acetone (C_3H_6O) solution and strain gauges were bonded to an outer surface using Cyanoacrylate Adhesive (Anabond 202). Quarter-bridge circuit strain gauges of gauge resistance 120Ω having a gauge factor of 2.1 and grid size 5 mm was used to measure Strain. Connecting wire was soldered to strain gauges, which were pasted to the external surface of the pipeline sample. The other end of the connecting wire is connected to the data logger, which is connected to a computerized data acquisition system to observe time, the compressive force applied, stress, strain, and position of the pipeline.

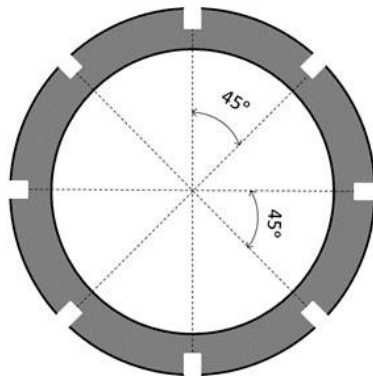


Figure 3.14 Schematic representation shows a pipeline with the groove.

3.1.5 Strain gauge pasting for conducting buckling experiments with rectangular pin buckle arrestor configurations welded at different locations

Two quarter bridge circuit strain gauges were pasted to the pipeline without stiffener. Two quarter bridge circuit strain gauges were pasted along the longitudinal direction one at the top and other at the bottom of a test specimen at a distance of 350 mm (Figure 3.15). Pipeline model stiffened with 150 mm long centrally located buckle arrestors was pasted with two strain gauges at center of pipeline located diametrically opposite to each other at a distance of 350 mm, third strain gauge is pasted to the stiffeners at a distance of 15 mm away from center of the span (Figure 3.16), Pipeline model with central stiffeners and two stiffeners at the ends were pasted with three strain gauges to pipeline one at center of the span, two strain gauges were pasted at left hand side end at a distance of 60 mm and 95 mm and one to the stiffeners at a

distance of 65 mm from left end of the span (Figure 3.17) and Pipeline model stiffened with longitudinal continuous rectangular stiffeners: two strain gauges were pasted one at center of the pipeline and another one on back side of the pipeline 15 mm towards right of the center and third strain gauge were pasted 30 mm towards left of the center on stiffener (Figure 3.18).

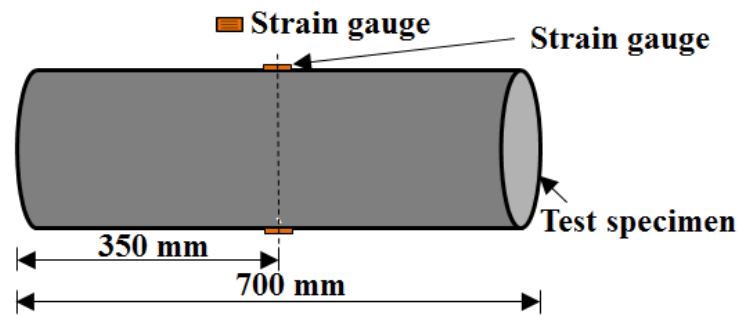


Figure 3.15 Schematic diagram of a Pipeline model without buckle arrestors pasted with strain gauges in longitudinal direction.

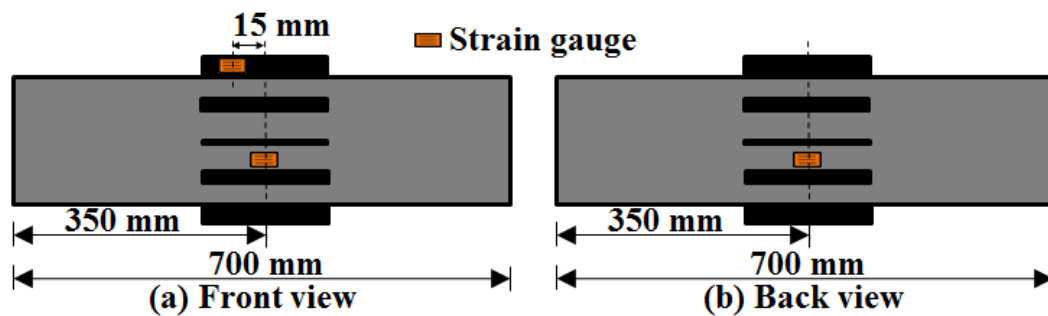


Figure 3.16 Schematic diagram of a Pipeline model stiffened with centrally located buckle arrestors pasted with strain gauges.

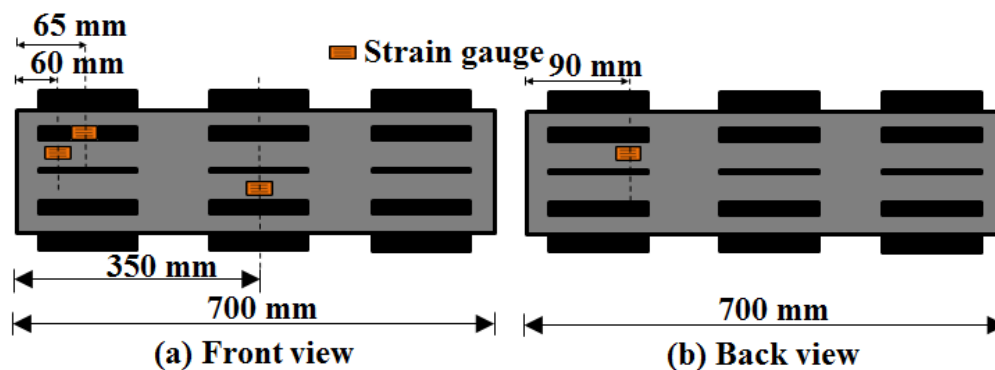


Figure 3.17 Schematic diagram of a Pipeline model with central Stiffeners and two stiffeners at the ends pasted with strain gauges.

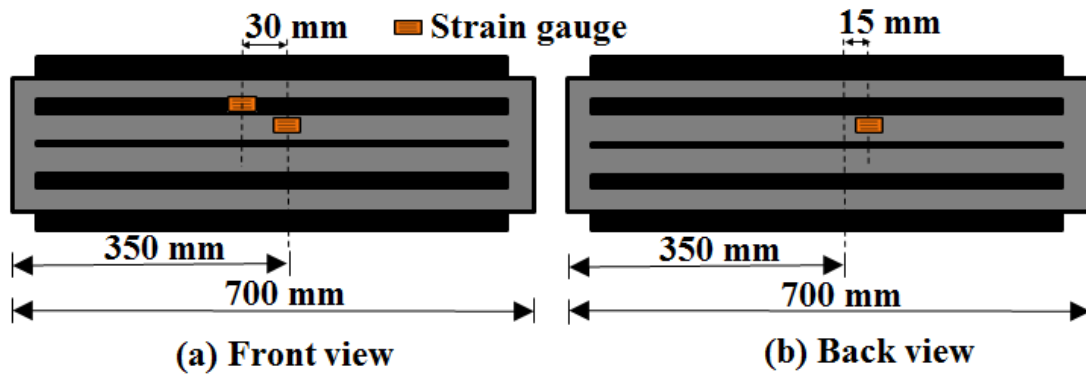


Figure 3.18 Schematic diagram of a Pipeline model stiffened with Longitudinal Continuous Rectangular Stiffeners pasted with strain gauges.

3.1.6 Buckling experimental setup with rectangular pin buckle arrestor configurations welded at different locations

The buckling experimental setup is supported on a lower bed. It consists of two grip holders, one at the top end and other at the bottom end, which is supported by four vertical steel columns. The upper grip is attached to the upper-end holder, and the lower grip is attached to the lower end holder which is connected to the loading system. The load applied by the loading system transfers to the specimen by the piston rod which is connected to the upper grip. Vertical alignment of the pipeline model is maintained and load is applied to the specimen by operating upper grip. The axial compressive load would be applied by the operating 400 kN UTM is shown in Figure 3.19. Pipeline models fabricated for conducting buckling experiments are shown in Figure 3.20.

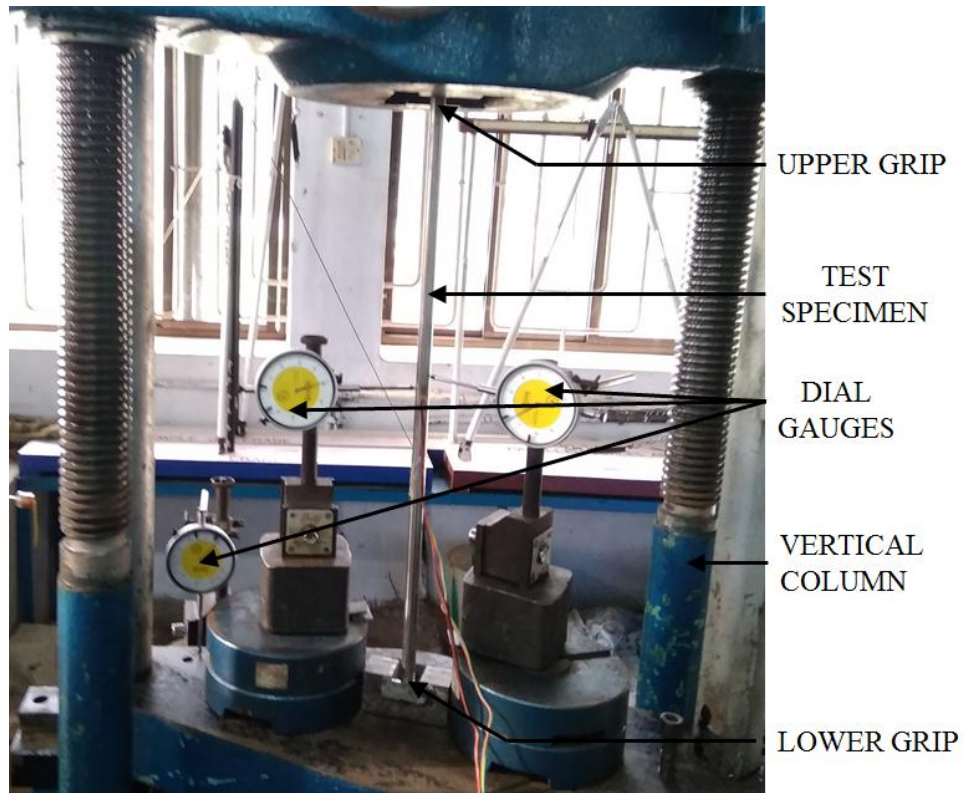


Figure 3.19 Photograph of buckling experimental setup.

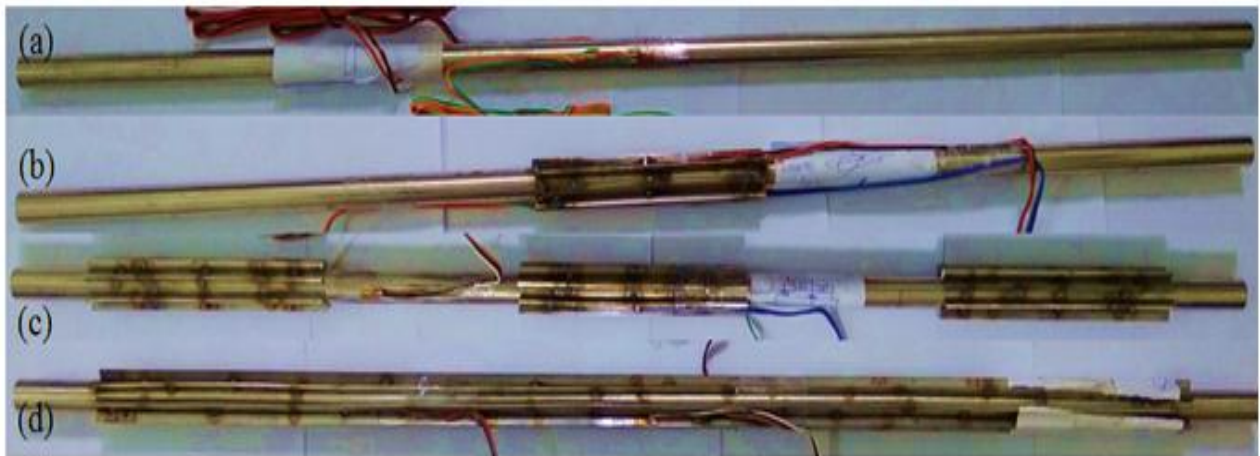


Figure 3.20 Pipeline models fabricated for conducting buckling experiments-(a) pipeline model without buckle arrestors (b) pipeline model with centrally located buckle arrestors (c) pipeline model with discontinuous buckle arrestors at center and edges (d) pipeline model with continuous buckle arrestors.

The pipeline outer diameter was measured at 20 cm interval to ensure uniformity of the pipeline outer diameter of a pipeline was to be 16 mm, measured using digital vernier calipers, which has a least count of 0.01 mm to ensure that the pipeline dimensions are free from imperfections. The thickness of the pipeline was measured at both ends of the pipe at a 90° interval along the circumference, and the average thickness of the pipeline was found to be 1.51 mm. By considering significant digit thickness was taken as 1.5 mm and inner diameter was calculated as 13 mm. A pipeline of length 700 mm was used for conducting buckling experiment. The experimental set up comprising strain gauges, data logger and Data Acquisition System was used to collect thousand data samples of the compressive load applied, resulting in stress and strain in the pipeline models.

The specimen was supported by both the upper end and lower end grips to ensure vertical alignment of the pipe specimen, pinned – pinned boundary condition and application of axial compressive load. The load applied by the loading system transfers to the specimen by means of hydraulic system which is connected to the upper grip.

The quarter bridge circuit strain gauges pasted to the pipeline models were connected to the data logger using connecting wire, with one end soldered to the strain gauge and the other end connected to the data logger. The data logger collects buckling experiment data, i.e., strain on surface of pipeline to computerized Data Acquisition System (DAS). Figure 3.21 shows the buckling experiment in progress.



Figure 3.21 Buckling experiments on different pipeline configurations (a) pipeline model without buckle arrestors (b) pipeline model with centrally located buckle arrestors (c) pipeline model with discontinuous buckle arrestors at center and edges (d) pipeline model with continuous buckle arrestors to observe direction of buckling using dial gauges.

CHAPTER 4

BUCKLING ANALYSIS OF PIPELINES WITH DIFFERENT BUCKLE ARRESTOR CONFIGURATIONS AND THEIR LOCATION

This chapter focuses on finite element modeling performed on pipeline models made of stainless steel of SS304 grade. Present research work focuses on the improvement in structural properties of offshore pipelines stiffened with various buckle arrestor configurations (sinusoidal, angular and longitudinal continuous) and rectangular pin buckle arrestors of different lengths and placed at different locations along the pipeline.

4.1 Finite Element Modeling of pipeline various buckle arrestor configurations

4.1.1 Pipeline Material and Properties

The pipeline material used in this study for both experimental work and finite element analysis is stainless steel of grade SS304 with longitudinal continuous, sinusoidal and angular buckle arrestors as shown in Figure 4.1, Figure 4.2 and Figure 4.3 .Geometric parameters and engineering properties of the stainless steel are given in below Table 4.1.

Table 4.1 Geometric parameters and engineering properties of pipe model.

Description	Value	Unit
External diameter	16	mm
Internal diameter	11.80	mm
Length	1000	mm
Poisson's ratio	0.3	
Young's modulus	210	GPa



Figure 4.1 Cross-section of longitudinal continuous stiffener model.

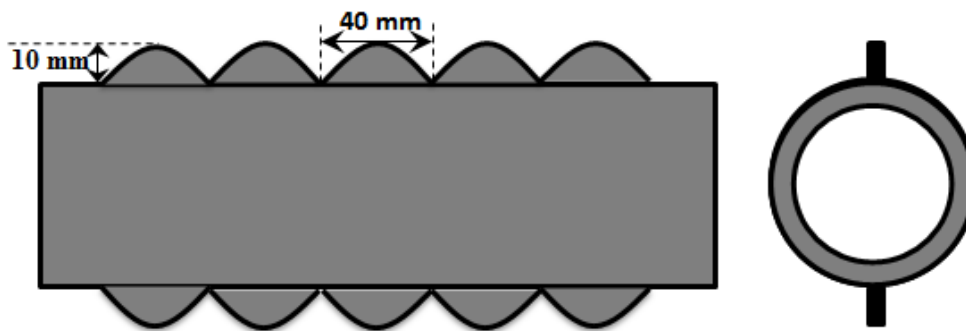


Figure 4.2 Cross-section of sinusoidal stiffener model.

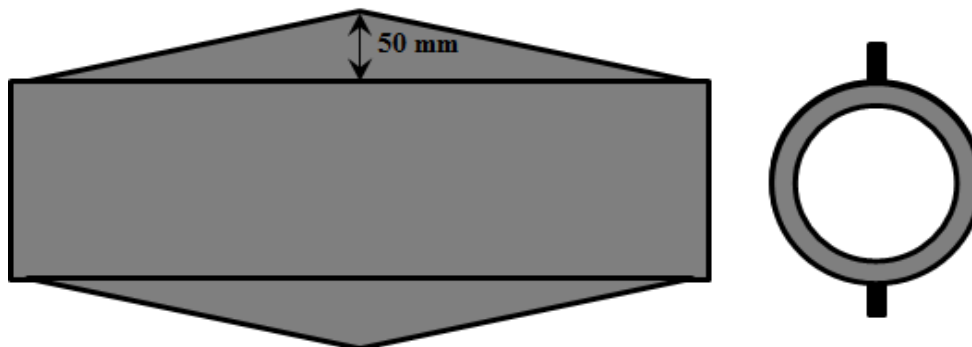


Figure 4.3 Cross-section of angular stiffener model.

4.1.2 Pipe geometry

The pipe models which are considered for finite element modeling consist of seamless stainless steel pipes of 1 m length, 16 mm outer diameter, 11.80 mm inner diameter, 2.1 mm thickness. Geometries of all the pipe models are drawn using computer aided design software AutoCAD. Geometrical details of buckle arrestors; longitudinal continuous stiffener, sinusoidal stiffeners and angular stiffeners along with their variation in length of buckle arrestor for each model are given in Table 4.2.

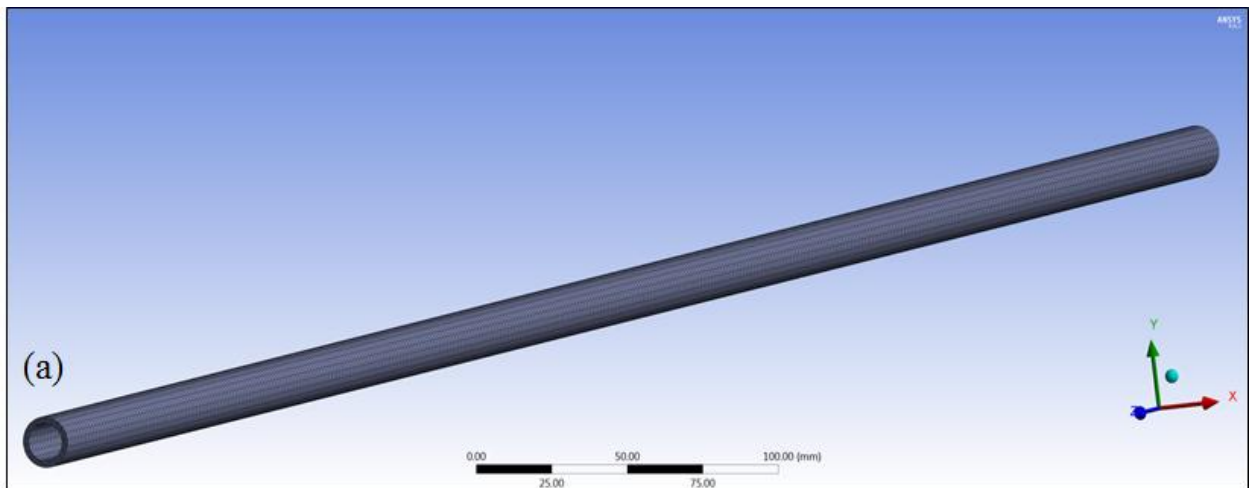
Table 4.2 Geometrical details of buckle arrestors.

Configurations	Dimensions of buckle arrestors (in mm)			Buckle arrestor length (in mm)	No of elements
	Length	Width	Height		
Simple pipeline	Without Stiffeners				9592
Longitudinal continuous stiffener	920	2	6	920	9850
Sinusoidal stiffener	880	2	10	880	17571
Angular stiffener	900	2	50	900	23810

Pipe geometry and configuration of buckle arrestors of all models are showed in Figure 4.4 (a), (b), (c) and (d).

4.1.3 Finite Element Models

In this present study, pipe models with and without buckle arrestors were modelled using ANSYS.



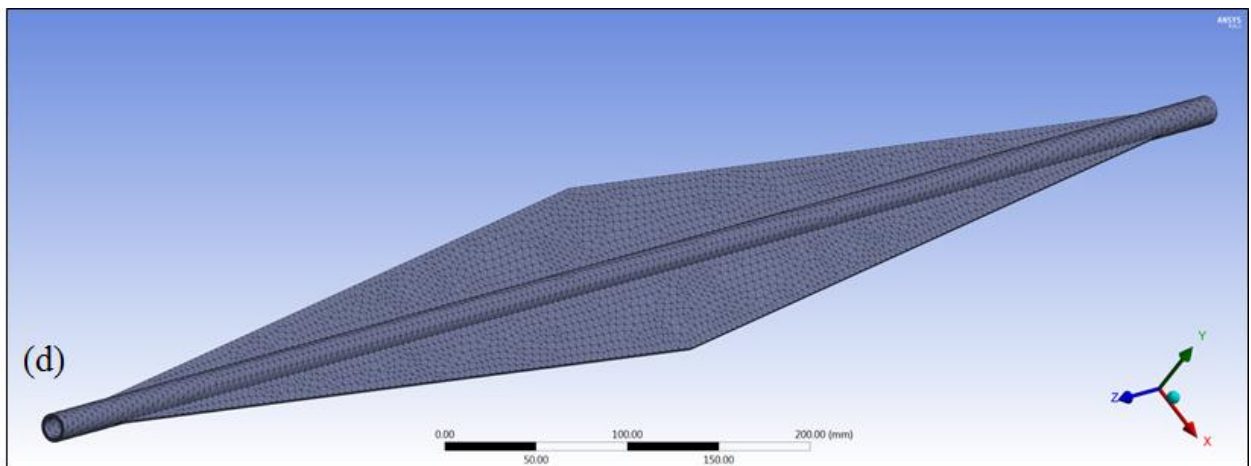
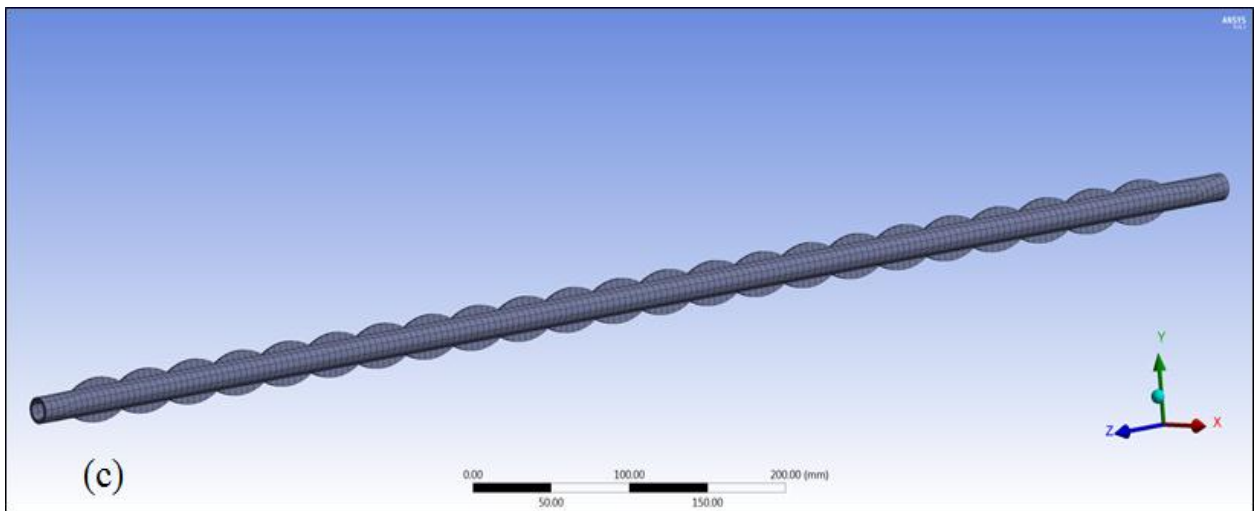
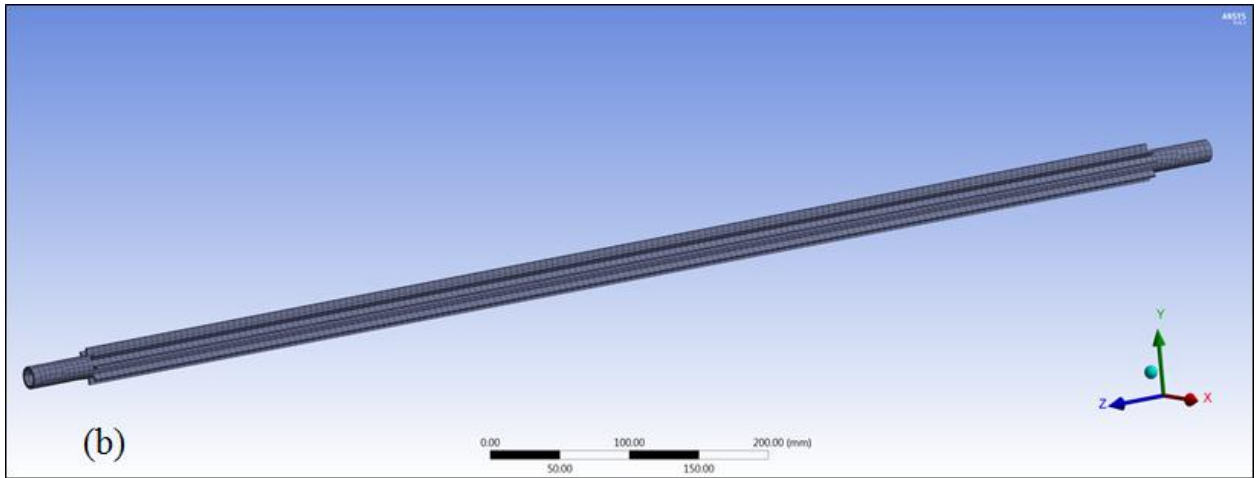


Figure 4.4 Finite element models of (a) pipeline without buckle arrestors, (b) pipeline stiffened with longitudinal continuous stiffeners, (c) pipeline stiffened with sinusoidal stiffener and (d) pipeline stiffened with angular stiffener.

4.1.4 Meshing Parameter, Boundary Conditions and Loading

Pipeline models were analyzed employing eigenvalue buckling analysis; finite element models were developed in ANSYS Workbench. For modeling and meshing offshore pipelines, SOLID186 elements were considered to study deformation along X, Y and Z axes (u, v and w). SOLID186 is a higher order three dimensional solid element that shows quadratic displacement behaviour and is characterized by 20 nodes having three degrees of freedom per node and translations along the x, y, and z directions. This element comprises 8 nodes on the outer surface of the pipe model, 8 nodes on the inner surface of the pipe model and 4 nodes in mid-thickness of a pipe. Meshing criterion was set to be automatic and program controlled. Shape transition was considered to be slow. Span angle centre and smoothing boundary were considered to be moderate. Element area for pipeline meshing is 5 mm. Total no of elements for finite element analysis of each model listed in Table 4.2.

Boundary conditions considered for Finite Element Analysis at the one end are $u=0, v=0, w=0, \theta_x \neq 0, \theta_y \neq 0, \theta_z \neq 0$. The boundary conditions considered for Finite Element Analysis at loading end are $u=0, v=0, w \neq 0, \theta_x \neq 0, \theta_y = 0, \theta_z = 0$. An axial compressive load of 1N applied over the circumference face (loading end) of a pipeline. An Eigenvalue buckling analysis has been carried out to study a mode shape of pipeline due to the axial compressive load. Figure 4.5 shows the various model meshing in ANSYS used for analysis.

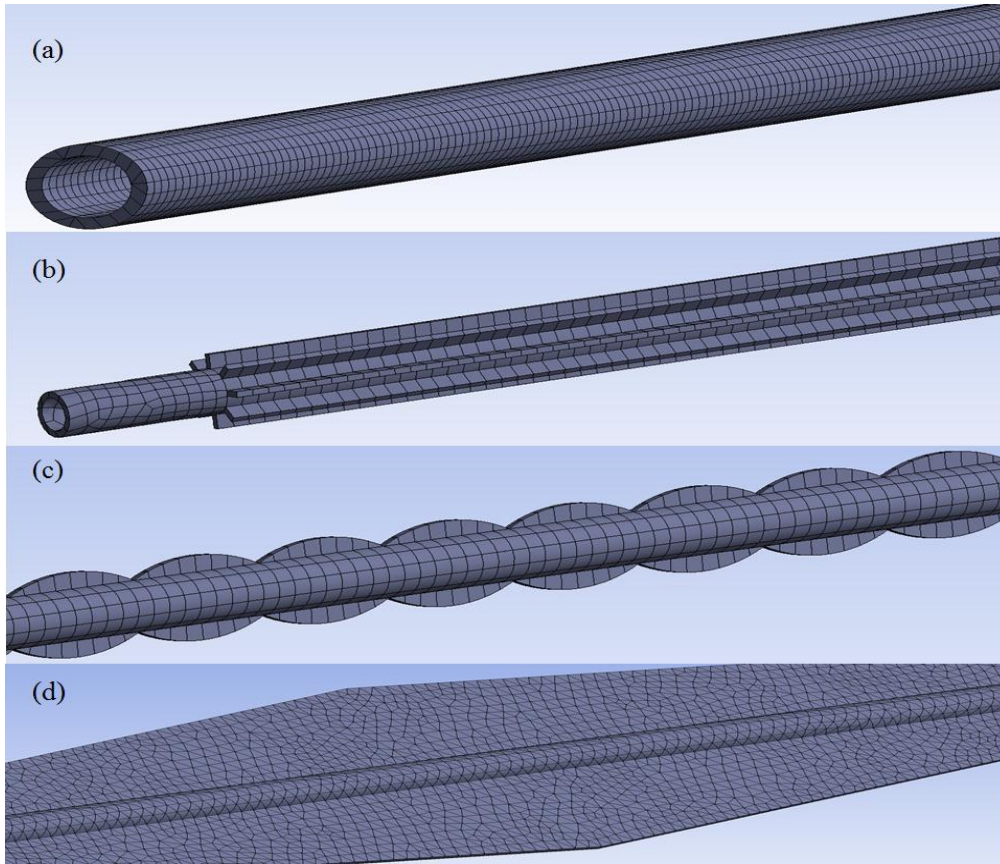


Figure 4.5 Solid element mesh of the (a) plain pipeline, (b) pipeline stiffened with longitudinal continuous stiffeners, (c) pipeline stiffened with sinusoidal stiffener and (d) pipeline stiffened with angular stiffener.

For understanding boundary conditions, the schematic representation of 2-D pipeline model shown in Figure 4.6.

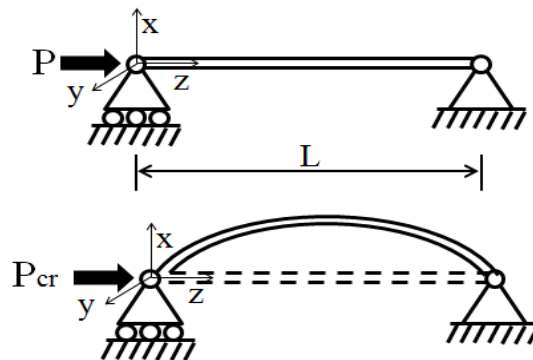


Figure 4.6: Boundary conditions of proposed models ($P_{cr} > P$)

4.1.5 Finite Element Analysis Results

The values of buckling load obtained from eigenvalue buckling analysis of different buckle arrestor configurations are compared with that of pipe model without buckle arrestor, and the outcomes of experiments are compared with finite element modelling results. The value of buckling load for the pipe section without buckle arrestor is 4.69 kN. For the second pipe model with longitudinal continuous buckle arrestor 920 mm long, the value of the critical buckling load is 13.981 kN which gives 198.1% higher buckling load, For the third pipe model with sinusoidal buckle arrestor 880 mm long, the value of the critical buckling load is 6.852 kN which gives 46.1% higher buckling load and for the fourth pipe model with angular buckle arrestor 900 mm long, the value of the critical buckling load is 4.870 kN which gives 3.63% higher buckling load than that of the basic model in spite of large size of Angular arrestor this is because the pipeline model buckles in the direction of least moment of inertia. Hence, it is clear that by providing buckle arrestor, buckling resistance cannot be increased. However, Model 4 kind of buckle arrestor configuration can't be used effectively due to less increment in buckling load.

The values of buckling load and percentage increase for all the models shown in Table 4.3. From Table 4.3, it was observed that reinforcing pipeline with buckle arrestor increases the stiffness of the pipeline and contributes to an increase in buckling load. Buckling of each pipe model is shown from Figure 4.7 to Fig 4.10. From Figure 4.7 to Figure 4.10, longitudinal continuous stiffener provides an increase in buckling load of 66.45 % when compared to the unstiffened pipeline. Variation of buckling load with respect to different types of buckle arrestors shown in Figure 4.11. From Model 1 (Figure 4.7) to Model 4 (Figure 4.10), provided with longitudinal continuous buckle arrestors increase the strength of the pipeline and also increase the buckling load carrying capacity of the pipelines whereas model 3 provided with sinusoidal buckle arrestor shows moderate increase in buckling load carrying capacity of the pipelines, model 4 provided with angular buckle arrestor shows least contribution in carrying buckling load. The critical buckling load value for the model 2, stiffened with longitudinal continuous buckle arrestor is 13.981 kN has given the highest increase (198.1 %) of buckling load among all the models.

Longitudinal continuous stiffeners (2 no's) have not contributed significantly to the buckling load ($I_x < I_y$) as the pipeline buckles along the direction of least moment of inertia. Longitudinal continuous stiffeners (4 no's) have not contributed significantly to the buckling load ($I_x = I_y$) as the pipeline buckles along the direction of least moment of inertia. Longitudinal continuous stiffeners (8 no's) have contributed significantly to the buckling load ($I_x = I_y$) and ($I_{x8} > I_{x4}$) as the pipeline buckles along the direction of least moment of inertia. Based on the finite element analysis pipeline models were fabricated with a specific dimension (Table 4.2) of buckle arrestors for laboratory experiments.

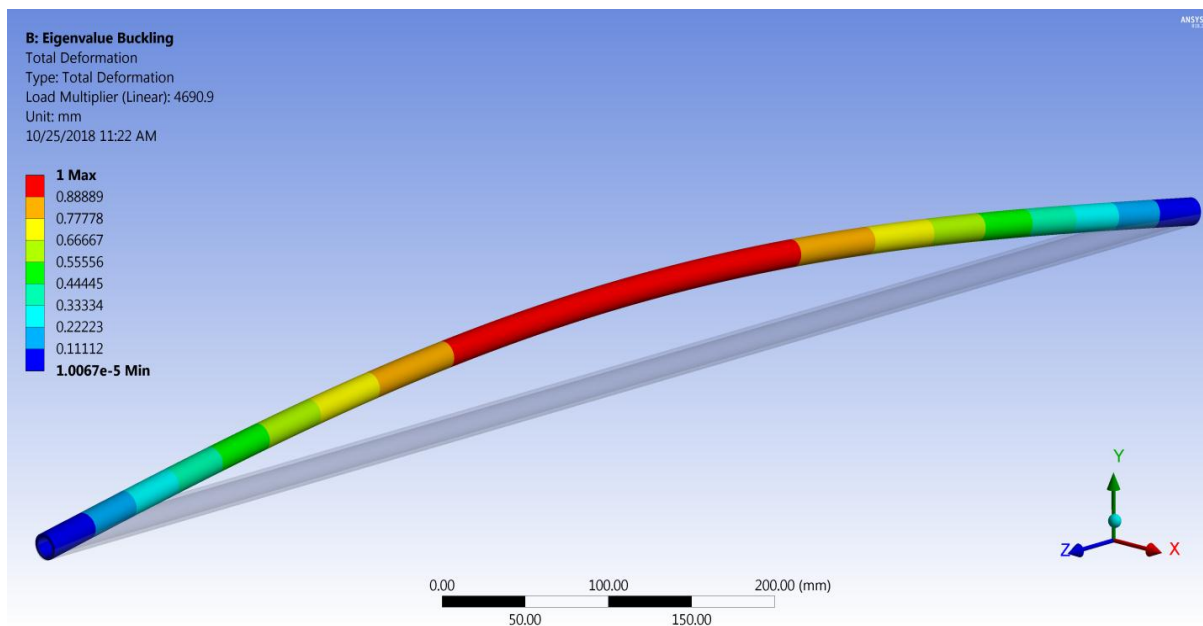


Figure 4.7 Buckling of Pipe Model 1 without Buckle arrestors.

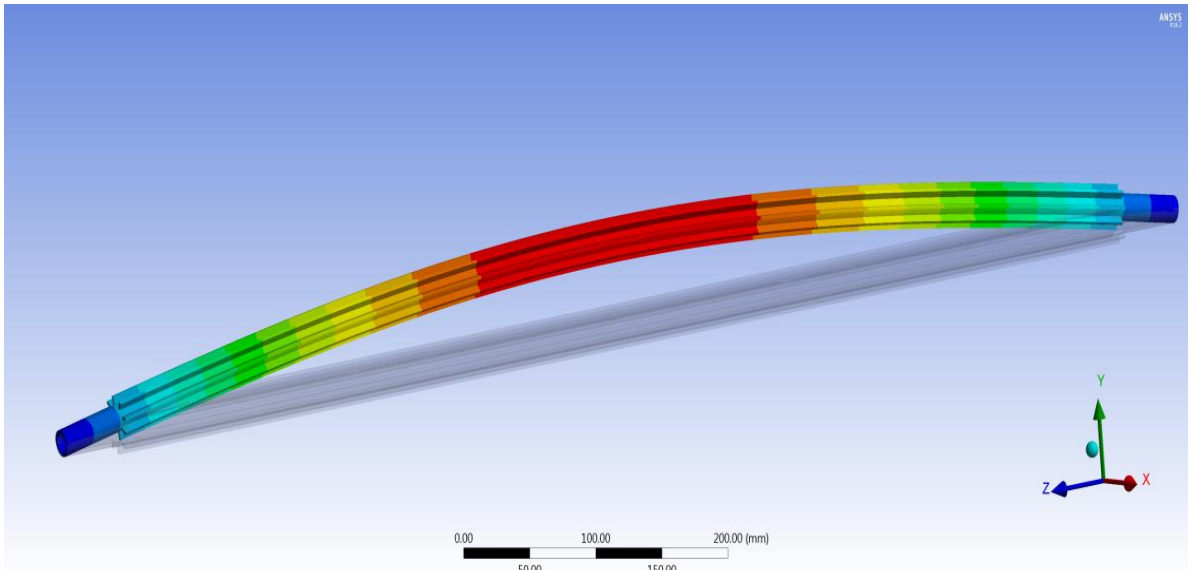


Figure 4.8 Buckling of Pipe Model 2 with Longitudinal Continuous Buckle arrestors.

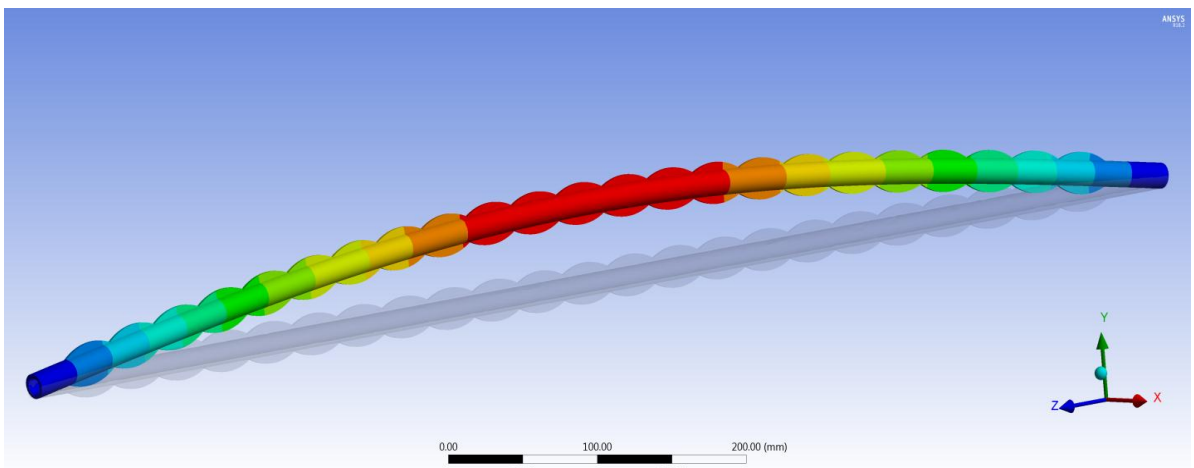


Figure 4.9 Buckling of Pipe Model 3 with Sinusoidal Buckle arrestors.

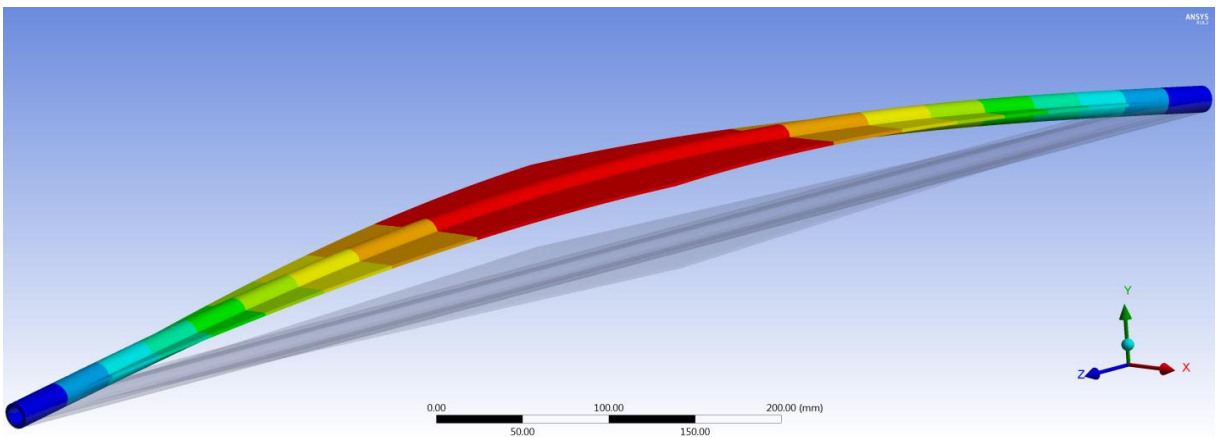


Figure 4.10 Buckling of Pipe Model 4 with Angular Buckle arrestors.

Table 4.3 Summary of buckling analysis results.

No	Models	Critical Buckling Load (kN) (FE Analysis)	% Increase of P_{cr}
1	No Stiffeners	4.690	-
2	Rectangular	13.981	198.1 %
3	Sinusoidal	6.852	46.1 %
4	Angular	4.871	3.86 %

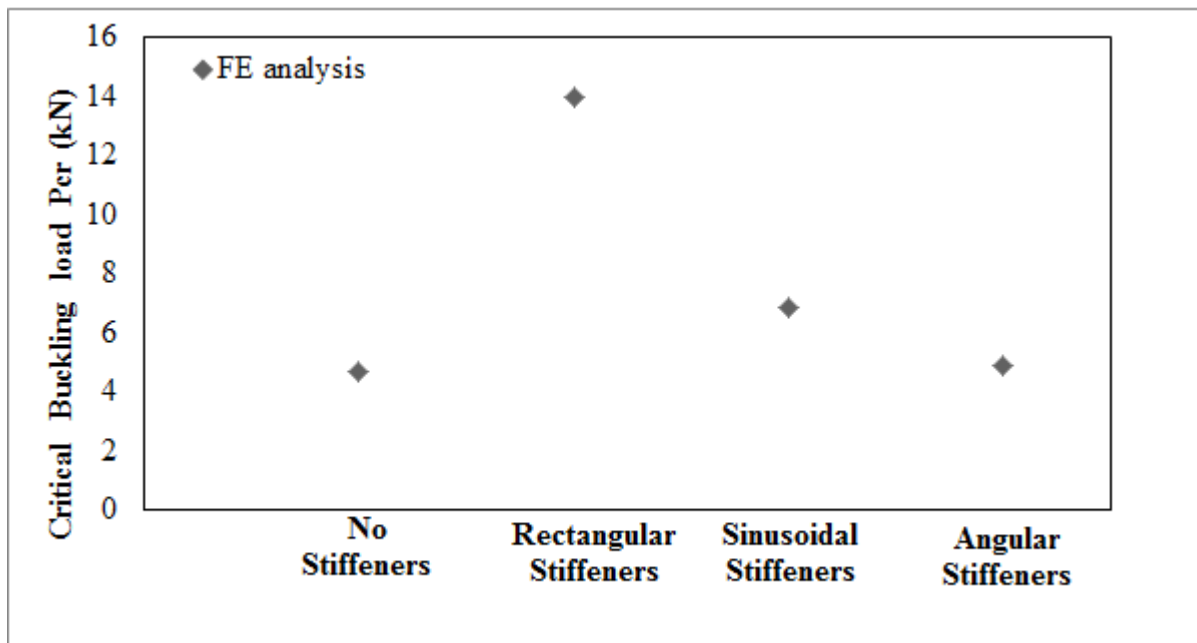


Figure 4.11 Variation of critical buckling load of pipeline model stiffened with different types of buckle arrestors.

4.2 Finite Element Modeling of pipeline stiffened with rectangular pin buckle arrestors with different spacing and locations

4.2.1 Pipeline Material and Properties

The pipeline material considered for finite element analysis is stainless steel, with longitudinal continuous rectangular pin buckle arrestors as shown in Figure 4.12, 4.13, 4.14 and 4.15. Geometric parameters and material properties are given in Table 4.4. Material properties presented here are provided by the manufacturer.

Table 4.4 Geometric parameters and engineering properties of pipe model.

Description	Value
External diameter	16 mm
Internal diameter	13 mm
Length	700 mm
Poisson's ratio	0.3
Young's modulus	197 GPa
Density	7850 kg/m ³

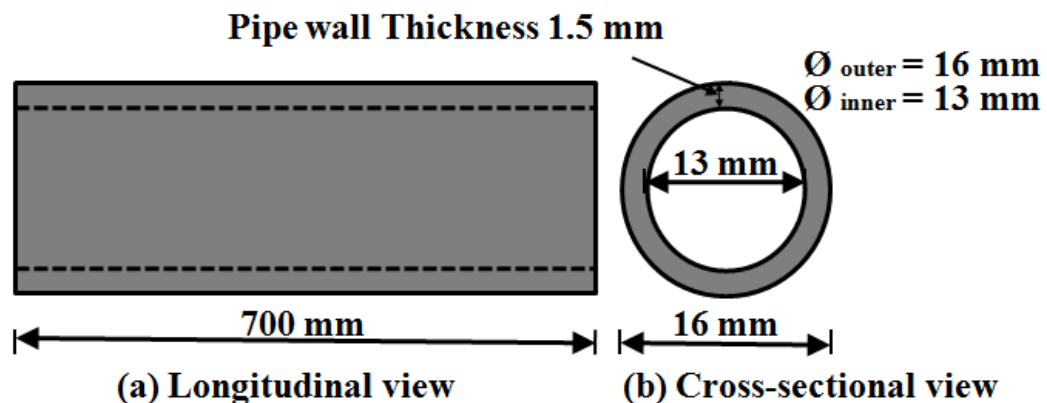


Figure 4.12 Schematic diagram of pipeline model without stiffeners.

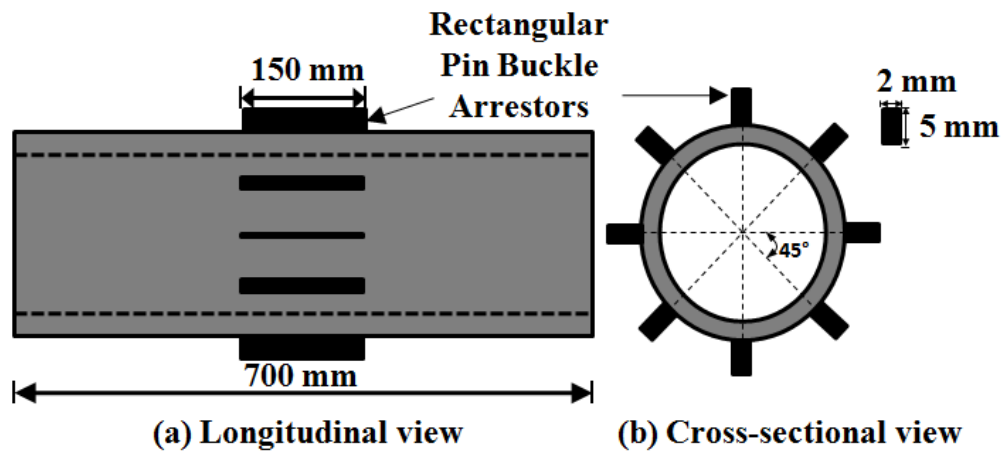


Figure 4.13 Schematic diagram of pipeline model stiffened with centrally placed stiffeners.

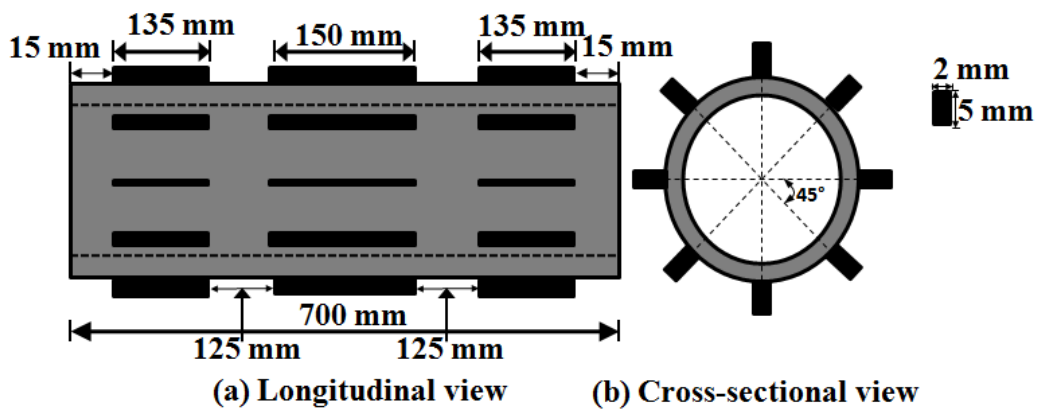


Figure 4.14 Schematic diagram of pipeline model stiffened with centrally placed stiffener and two stiffeners at ends.

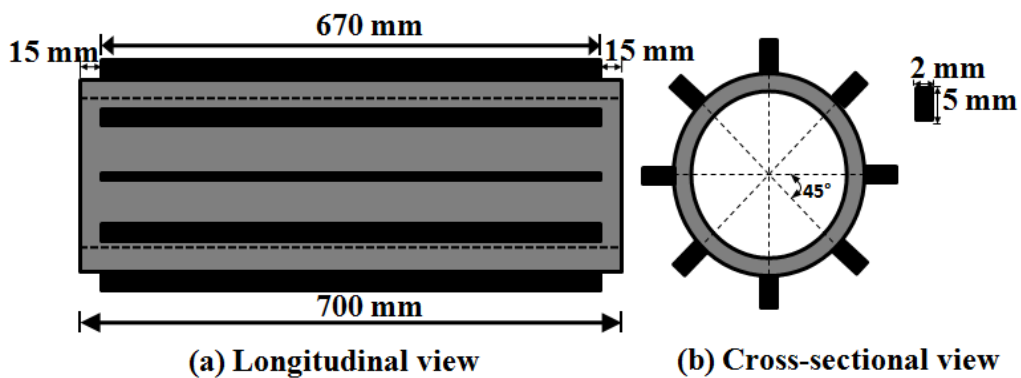


Figure 4.15 Schematic diagram of pipeline model stiffened with longitudinal continuous stiffeners.

4.2.2 Pipe geometry

The pipe models which are considered for finite element modeling consist of steel pipes of 800 mm length, 16 mm outer diameter, 13 mm inner diameter, 1.5 mm thickness and eight rectangular pin buckle arrestors of width 2 mm and height 5 mm integrated on the circumference of pipes. However, the change in length of buckle arrestors in the range of 150 mm, 450 mm and 700 mm for proposed models. Geometries of all the pipe models are drawn using computer-aided design software AutoCAD. Geometrical details of buckle arrestors and change in length of buckle arrestors for each model are given in Table 4.5 and shown in Figure 4.16, 4.17, 4.18 and 4.19.

Table 4.5 Geometrical details of rectangular pin buckle arrestors.

Pipe models	Dimensions of buckle arrestors (in mm)			No. of elements
	Length	Width	Height	
Model 1	Without Stiffeners			16695
Model 2	150	2	5	98611
Model 3	420	2	5	113007
Model 4	670	2	5	136424

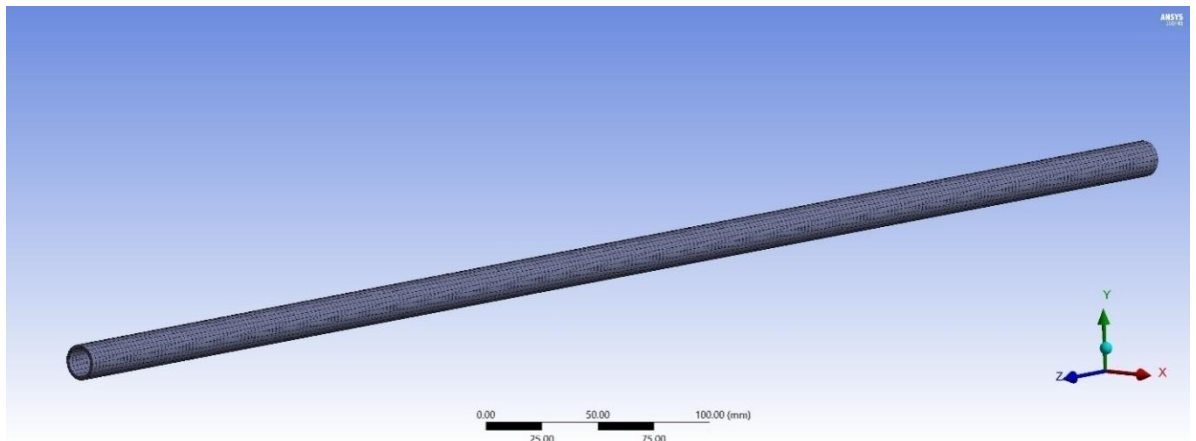


Figure 4.16 Finite element model of pipeline without stiffener.

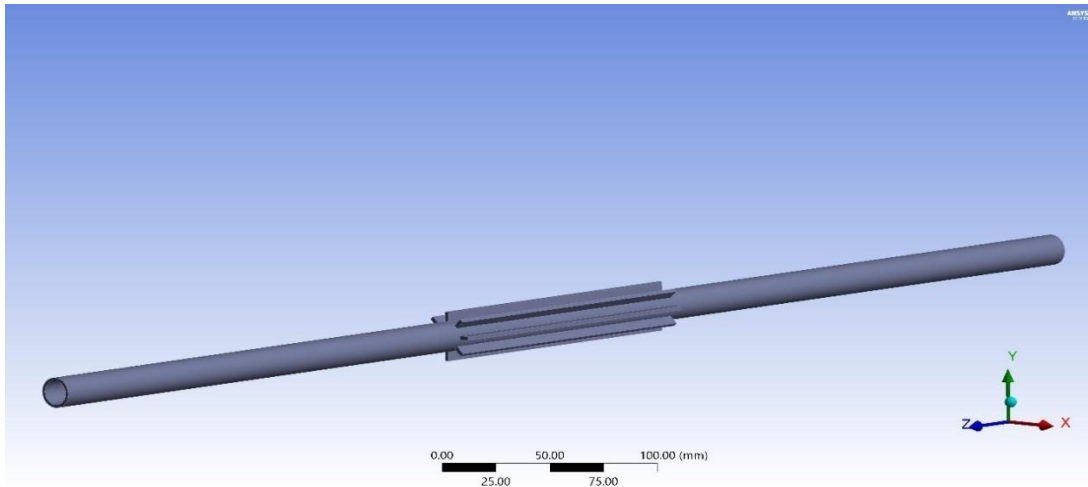


Figure 4.17 Finite element model of pipeline with centrally placed stiffener of length 150 mm.

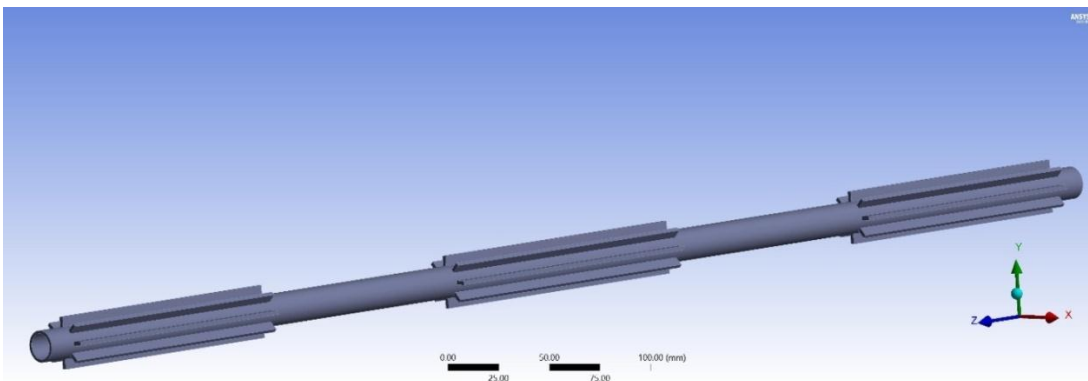


Figure 4.18 Finite element model of pipeline with centrally placed stiffener of length 150 mm and two stiffener of length 135 mm each placed at ends.

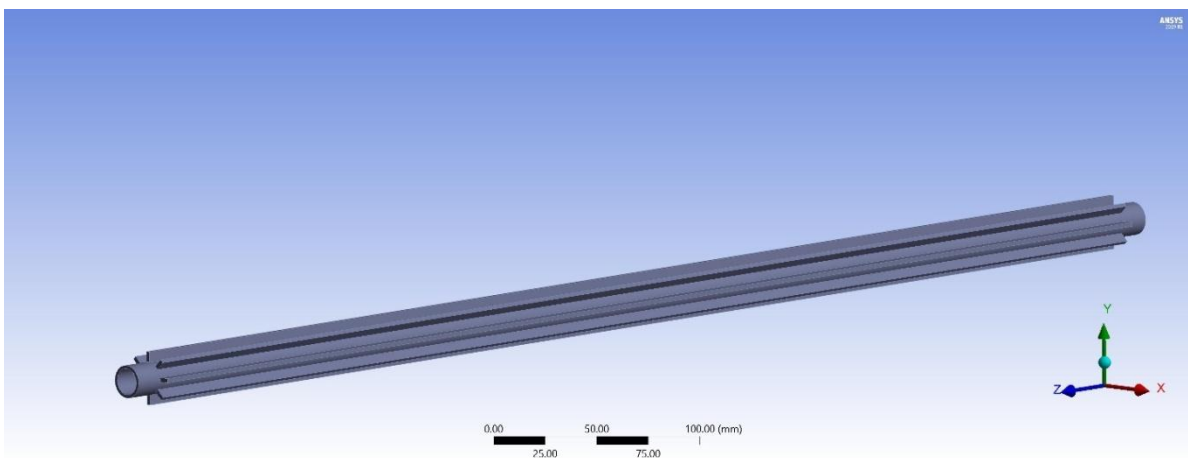


Figure 4.19 Finite element model of pipeline with longitudinal continuous stiffener of length 670 mm.

4.2.3 Meshing Parameter, Boundary Conditions and Loading

Pipeline models were analyzed employing eigenvalue buckling analysis; finite element models were developed in ANSYS Workbench. For modeling and meshing offshore pipelines, SOLID186 elements were considered to study deformation along X, Y and Z axes (u, v and w). SOLID186 element comprises 8 nodes along outer surface of the pipe model, 8 nodes along inner surface of the pipe model and 4 nodes in mid-thickness of a pipe. Meshing was performed using automatic method and program controlled parameters. Span angle centre and smoothing parameter was set to be medium. Element size for pipeline meshing is 1.5 mm. Element size was decided based on the mesh convergence study (Figure 4.21). Total no of elements for finite element analysis of each model listed in Table 4.5.

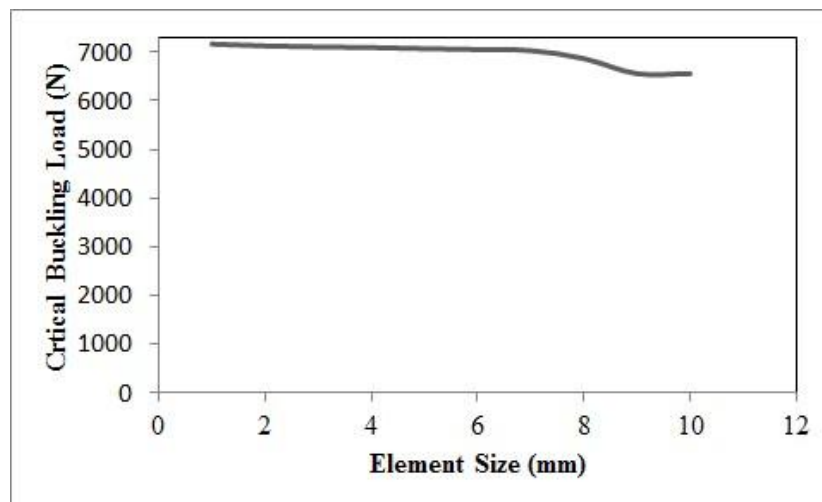


Figure 4.20 Convergence study of finite element mesh (plain pipeline model).

The boundary conditions considered for Finite Element Analysis at the one end are $u=0$, $v=0$, $w=0$, $\theta_x \neq 0$, $\theta_y \neq 0$, $\theta_z \neq 0$. The boundary conditions considered for Finite Element Analysis at loading end are $u=0$, $v=0$, $w \neq 0$, $\theta_x \neq 0$, $\theta_y=0$, $\theta_z=0$. An axial compressive load of 1N applied over the circumference face (loading end) of a pipeline. An Eigenvalue buckling analysis was used in the simulation to study a buckling due to the axial compressive load. Figure 4.21 shows pipeline model meshing in ANSYS.

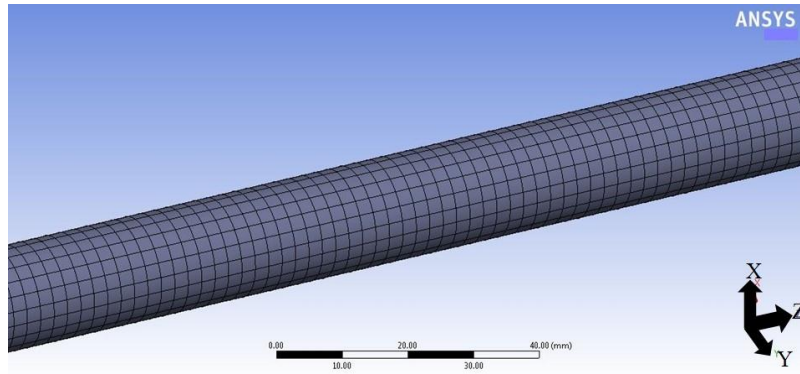


Figure 4.21 Solid element mesh of the plain pipeline.

For understanding boundary conditions, the schematic representation of 2-D pipeline model shown in Figure 4.22.

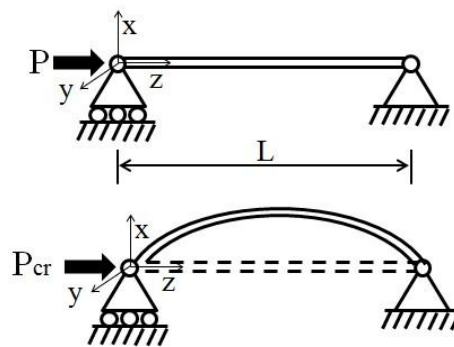


Figure 4.22 Boundary conditions of proposed models ($P_{cr} > P$).

4.2.4 Finite Element Analysis Results

The values of buckling load obtained from eigenvalue buckling analysis of different buckle arrestor models are compared with that of pipe model without buckle arrestor, and the results of experiments are compared with Finite Element models. The value of buckling load for the pipe section without buckle arrestor is 7.167 kN. For the second pipe model with buckle arrestor 150 mm long, the value of the critical buckling load is 9.937 kN which gives 38.65% higher buckling load than that of the pipe model without buckle arrestor. Hence, it is clear that by providing buckle arrestor, buckling resistance can be increased. However, this kind of buckle arrestor configuration can't be used effectively due to less increment in buckling load. In model 3, the length of buckle arrestors provided is 420 mm to identify increase in buckling load contributed

by increasing length of buckle arrestors. The value of the critical buckling load of model 3 is 11.050 kN which increases buckling load by 54.18 % higher when compared to that of the pipe model without buckle arrestor. In model 4, the length of buckle arrestors provided is 670 mm. The value of the critical buckling load of model 4 is 25.026 kN which increases buckling load by 249.18% higher when compared to that of the pipe model without buckle arrestor.

The values of buckling load and percentage increase for all the models shown in Table 4.6. From Table 4.6, it was observed that reinforcing pipeline with buckle arrestor increases the stiffness of the pipeline and contributes to increase in buckling load. Buckling of pipe models is shown in Figure 4.23 to Figure 4.26. Longitudinal continuous stiffener model provides an increase in buckling load of 249.18% when compared to the pipeline with buckle arrestor. From Model 1 (Figure 4.23) to Model 4 (Figure 4.26), provided with longitudinal continuous buckle arrestors contribute to increasing the buckling load of the pipelines and improves stability of the pipelines. The critical buckling load value for the model 4, stiffened with continuous buckle arrestors is 25.026 kN has given the highest increase (249.18%) of buckling load among all the models considered.

Table 4.6 Summary of buckling analysis results.

Pipe section models	Critical buckling load P_{cr} (kN)	% Increase of P_{cr}
Model 1	7.167	-
Model 2	9.937	38.65 %
Model 3	11.050	54.18 %
Model 4	25.026	249.18 %

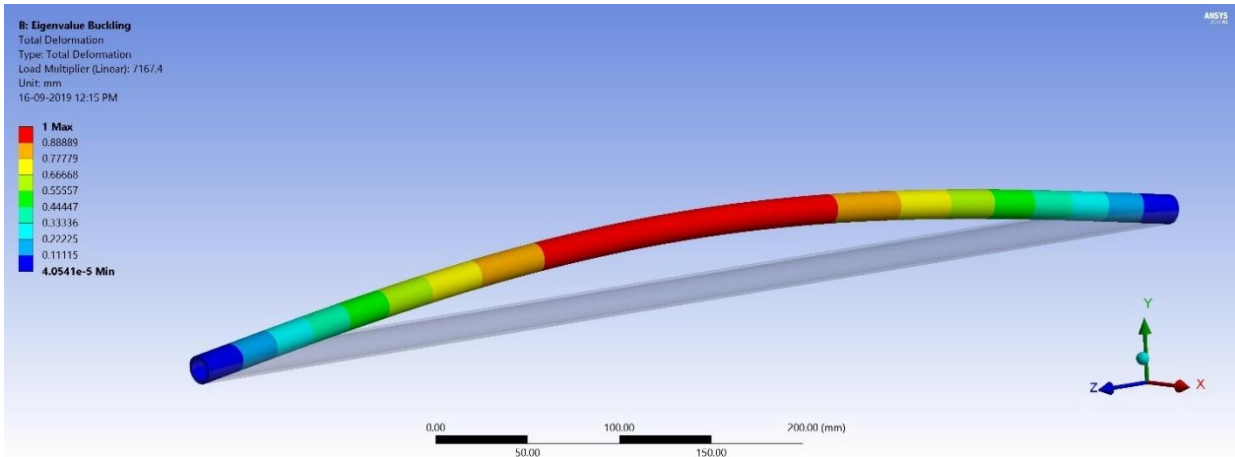


Figure 4.23 Buckling of Pipe Model without stiffener.

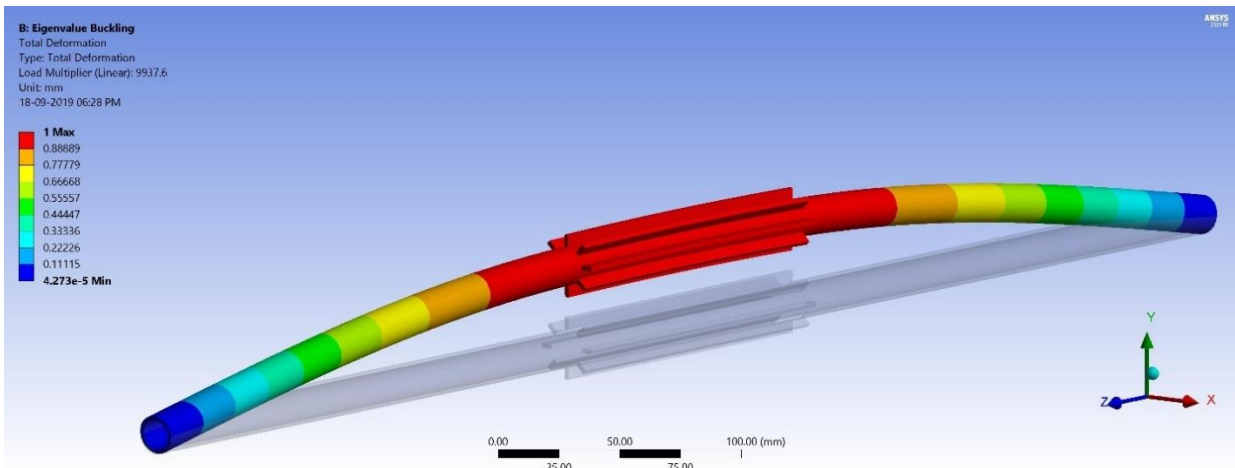


Figure 4.24 Buckling of Pipe model with stiffener of 150 mm length.

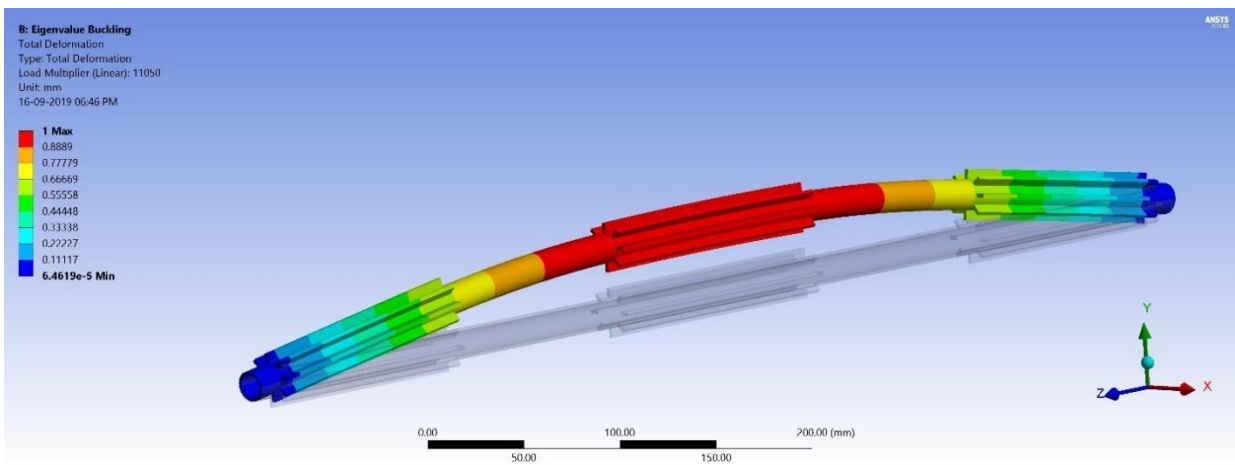


Figure 4.25 Buckling of Pipe model with 150 mm long centrally located stiffener and 135 mm long stiffeners at both ends.

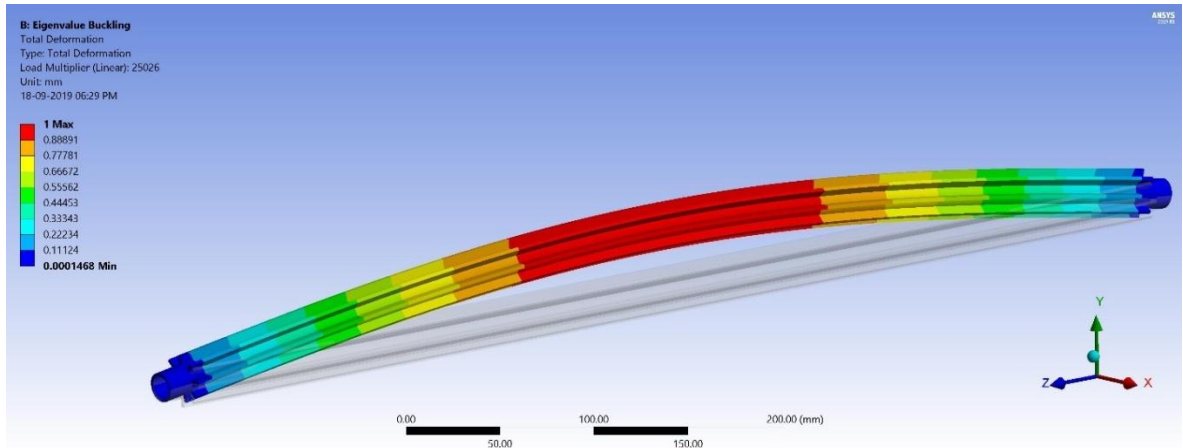


Figure 4.26 Buckling of Pipe model with stiffener of 670 mm length.

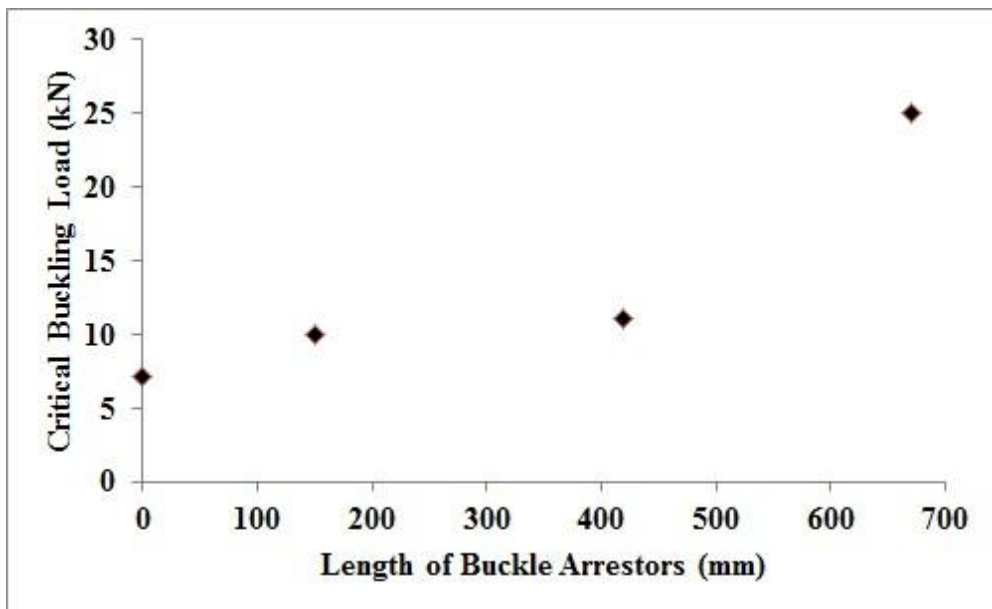


Figure 4.27 Variation of critical buckling load of pipeline model stiffened with and without buckle arrestors of varying length and location.

Rectangular pin buckle arrestor of smaller length (150 mm) was not contributing significantly to resist the forces causing buckling as the pins were placed at middle of the pipeline this is observed in Figure 4.27, where critical buckling load shows a slight increase. Buckle arrestors of length (420 mm) located at center (150 mm) of the pipeline and at both ends of pipeline (135 mm each) display a marginal increase of critical buckling load as shown in Figure 4.27. Longitudinal continuous rectangular

buckle arrestors of length (670 mm) were placed in the middle of the pipeline uniformly and displayed a significant increase in critical buckling load shown in Figure 4.27. Longitudinal continuous rectangular buckle arrestors, provided at 45° along the circumference, strengthen the pipeline uniformly along x-axis, y-axis and at intermediate locations contributing significantly to the critical buckling load (P_{cr}) and as the pipeline has a tendency to buckle along the direction of least moment of inertia.

CHAPTER 5

EXPERIMENTAL RESULTS THEIR VALIDATION AND VERIFICATION

5.1 Experimental results for pipeline stiffened with various buckle arrestors configurations

The values of buckling load obtained from the experiments conducted on pipe model stiffened with 920 mm longitudinal continuous stiffeners, sinusoidal stiffeners (880 mm) and angular stiffeners (900 mm) were compared with that of a pipeline model without stiffeners (Table 5.1). From Table 5.1, it has been observed that for a pipeline with longitudinal continuous stiffeners there is an increase of 155.02 %, for sinusoidal stiffeners there is an increase of 56.63 % and for angular stiffeners there is an increase of 0.8 % in critical buckling load when compared with a pipeline without buckle arrestors. As the length of buckle arrestor increases the buckling load carrying capacity of a pipeline also increases. Figure 5.1 shows experimentally determined critical buckling load of a pipeline without stiffeners, pipeline with longitudinal continuous stiffeners, pipeline with sinusoidal stiffeners and pipeline with angular stiffeners. Figure 5.2 shows variation in buckling load of buckled pipeline models used for experiments.

Table 5.1 Summary of buckling Experimental results of buckle arrestors with three different configurations.

No	Models	Critical Buckling Load (kN) (Experiment)	% Increase of P_{cr}
1	No Stiffeners	4.980	-
2	Longitudinal continuous stiffeners	12.700	155.02 %
3	Sinusoidal Stiffeners	7.800	56.63 %
4	Angular Stiffeners	5.020	0.8 %

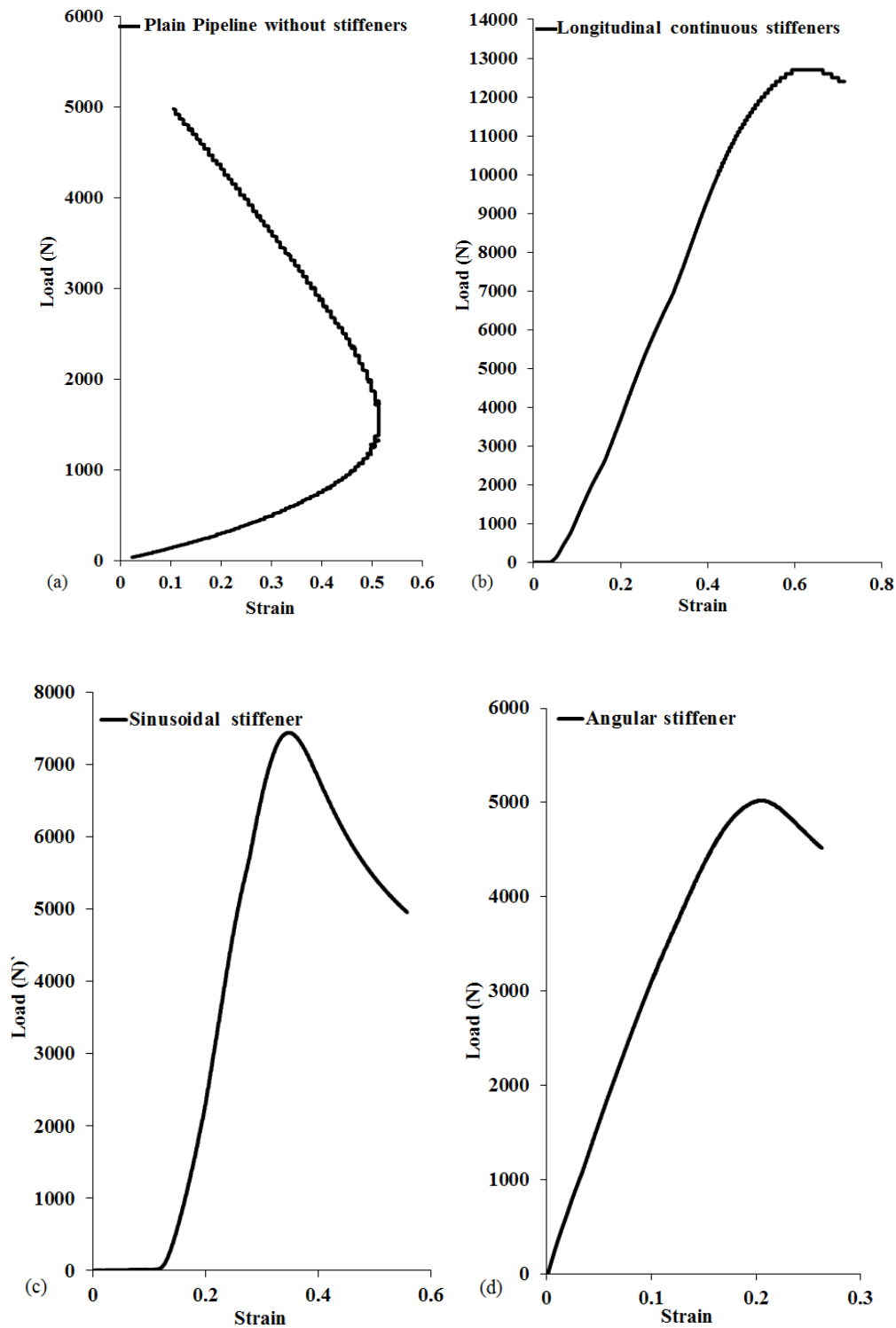


Figure 5.1 Graph shows experimentally determined critical buckling load of (a) pipeline model without stiffeners, (b) with longitudinal continuous stiffeners, (c) sinusoidal stiffeners and (d) angular stiffeners.

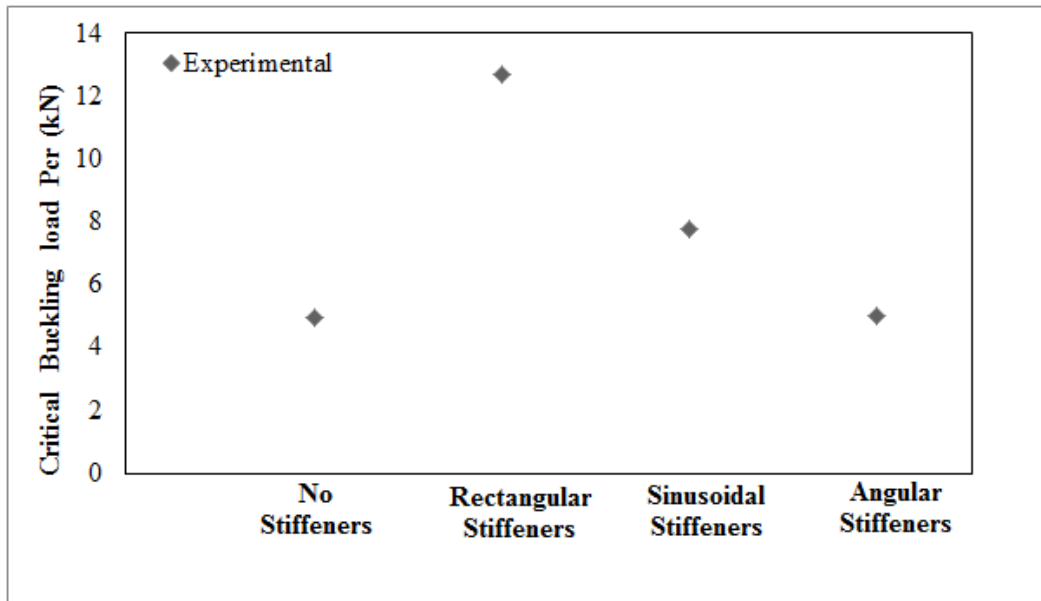


Figure 5.2 Variation of experimentally determined critical buckling load.

5.2 Comparison of the Finite Element analysis Results Using the Experimental Results

In Figure 5.3 we compare, for a pipeline without stiffeners and pipeline with longitudinal continuous stiffeners, sinusoidal stiffeners and angular stiffeners, the experimentally determined and FEA predicted buckling load. Summary of finite element analysis and experimental results has been presented in Table 5.2.

Table 5.2 Summary of finite element analysis and experimental results.

No	Models	Critical Buckling Load P_{cr} (kN)	
		FE Analysis	Experimental Results
.1	Pipeline without Stiffeners	4.690	4.980
2	Longitudinal Continuous Stiffeners	13.981	12.700
3	Sinusoidal Stiffeners	6.852	7.800
4	Angular Stiffeners	4.871	5.020

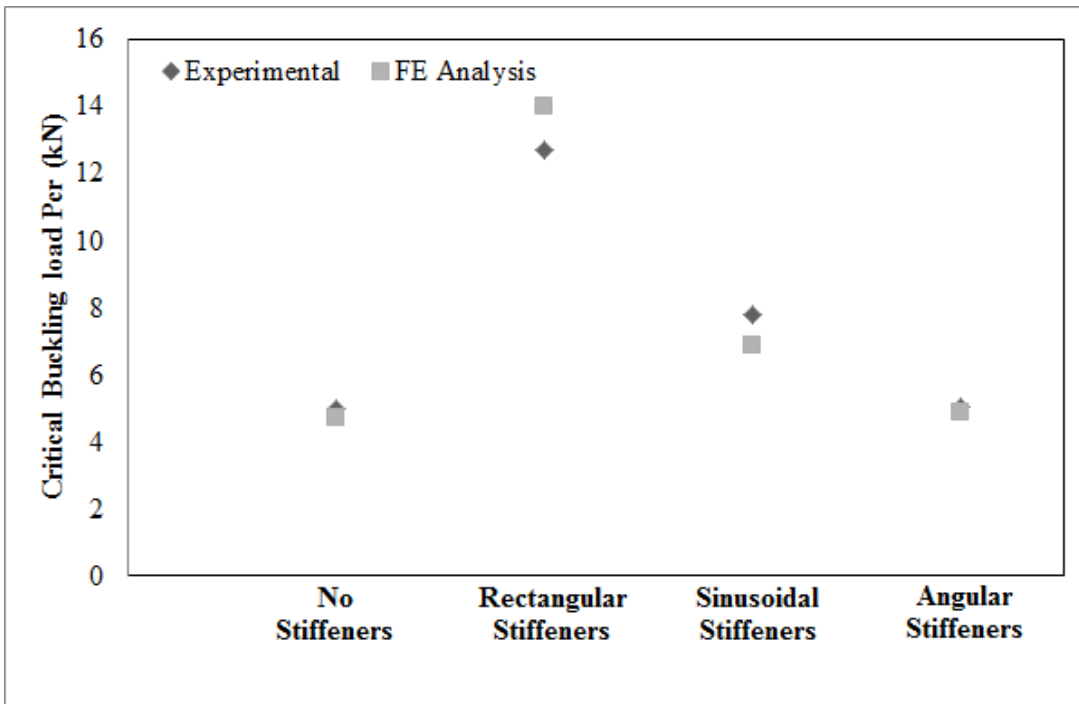


Figure 5.3 Finite element analysis vs experimental results for a pipeline without stiffener and pipeline with different stiffener.

The experimental results presented in Table 5.2 were obtained considering the residual stresses in the pipe models: one without stiffeners and the other with stiffeners. The residual stresses induced during the process of pipe cutting, the welding and groove machining were not considered in the finite element model; this results in experimental results lower than the numerically predicted buckling loads [Luciano O. Manitoban. 2006].

5.3 Experimental results for pipeline stiffened with various buckle arrestors configurations

The values of buckling load obtained from the experiments conducted on pipeline models stiffened with 150 mm long centrally located stiffeners, 150 mm long centrally located stiffeners and 135 mm long stiffeners at both ends and longitudinal continuous rectangular stiffeners 670 mm long was compared with those of a pipeline model without buckle arrestors (Table 5.3). From Table 5.3, it could be observed that

for pipeline model stiffened with 150 mm long centrally located buckle arrestors there is an increase of 43.48 % in critical buckling load, for pipeline model stiffened with 150 mm long centrally located and 135 mm long stiffeners at both ends there is an increase of 52.17 % in critical buckling load and for pipeline model with longitudinal continuous rectangular stiffeners 670 mm long there is an increase of 247.83 % in critical buckling load when compared with that of pipeline model without buckle arrestors. Not only length of buckle arrestors but also their location contributes to critical buckling load carrying capacity of a pipeline.

Table 5.3 Summary of buckling Experiment results with rectangular pin buckle arrestors placed at different locations.

Pipe section models	Critical buckling load P_{cr} (kN)	% Increase of P_{cr}
Pipeline without Stiffeners	6.9	-
Pipeline with central Stiffeners	9.9	43.48 %
Pipeline with central Stiffeners and two stiffeners at the ends	10.5	52.17 %
Pipeline with Longitudinal Continuous Stiffeners	24	247.83 %

Load versus displacement data obtained by conducting buckling experiments is plotted with displacement along x-axis and Load along y-axis. The resulting plot (Figure 5.4, Figure 5.5, Figure 5.6 and Figure 5.7) shows linear graph (in the elastic region) initially which reaches a stabilized value (in the plastic region); tangents (T_1 , T_2) are drawn to the elastic region of graph and plastic region of the graph, the point where the tangents T_1 and T_2 coincide gives critical buckling load (P_{cr}) as per double tangent method. Double Tangent Method [Tuttle M. et al., 1999] was applied to load – displacement graphs of pipeline models stiffened with buckle arrestors and the critical buckling load obtained was matching with the experimental results.

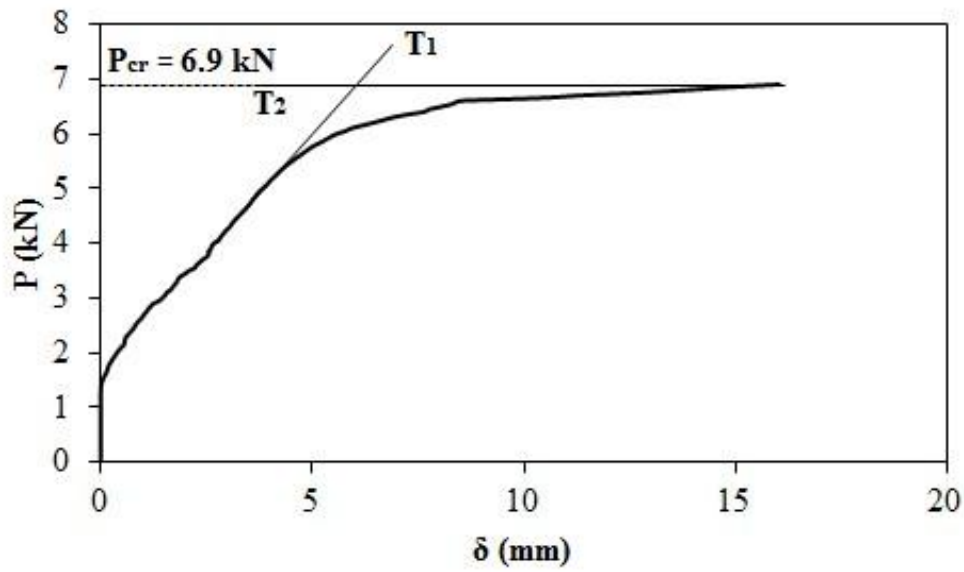


Figure 5.4 Load (Independent variable) versus lateral deflection(dependent variable) at mid length of pipeline without buckle arrestor.

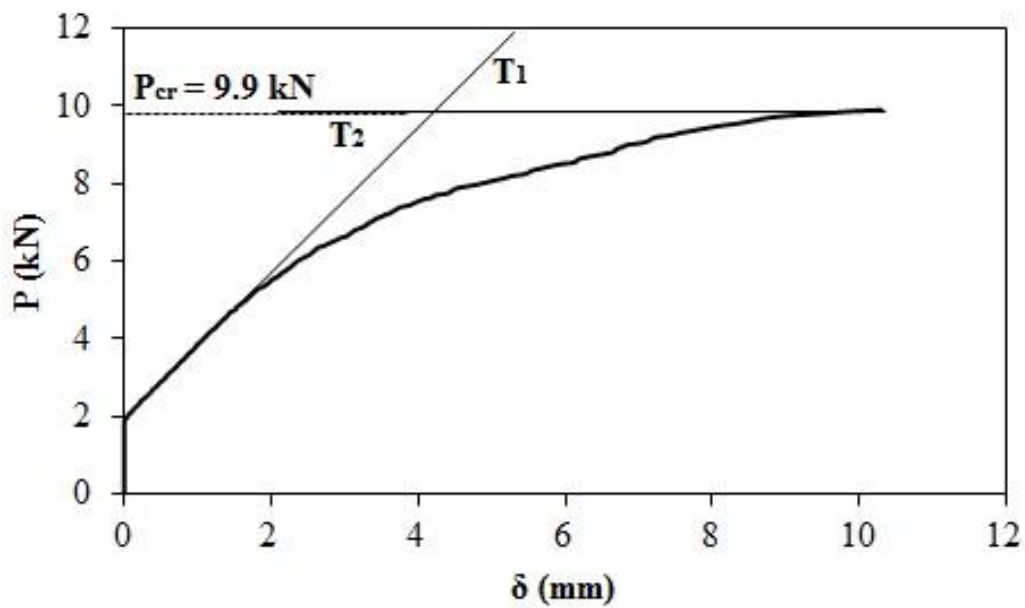


Figure 5.5 Load (Independent variable) versus lateral deflection(dependent variable) at mid length of pipeline stiffened with buckle arrestors 150 mm at middle of the length.

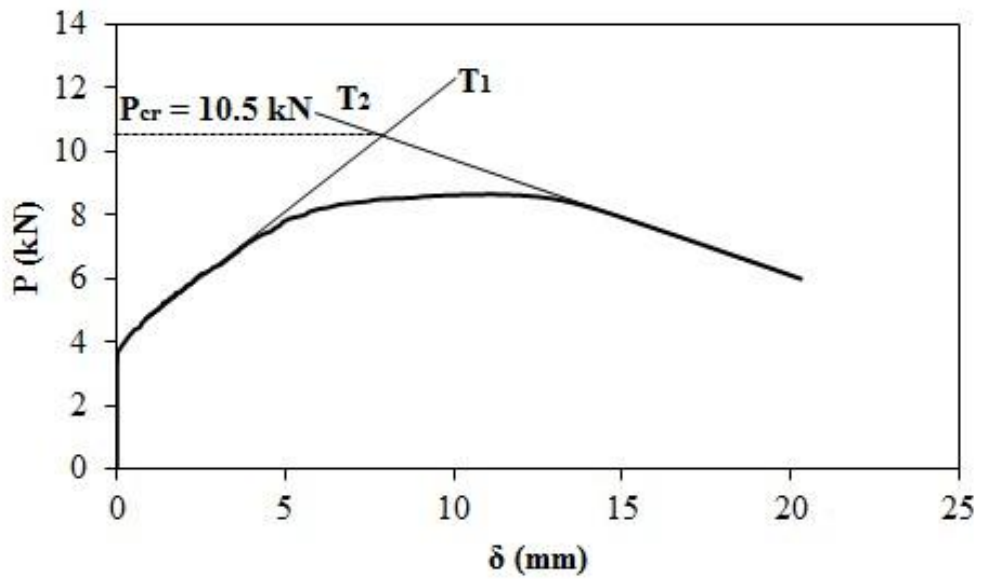


Figure 5.6 Load (Independent variable) versus lateral deflection(dependent variable) at mid length of pipeline stiffened with buckler arrestors 150 mm at middle of the length and two buckler arrestors 135 mm at the ends.

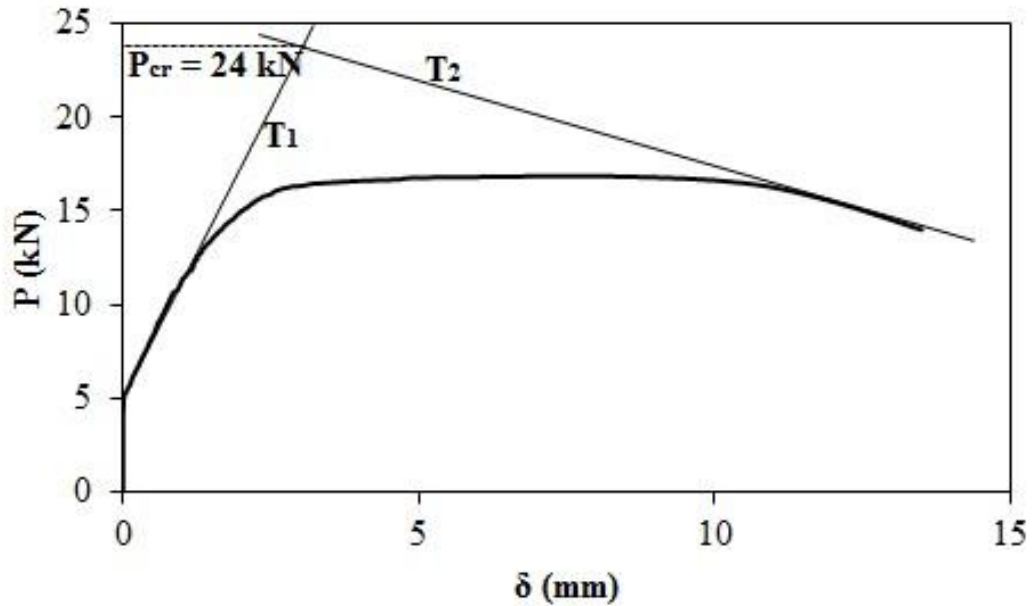


Figure 5.7 Load (Independent variable) versus lateral deflection(dependent variable) at mid length of pipeline stiffened with 670 mm longitudinal continuous buckler arrestors.

5.4 Verification of the Finite Element analysis results by conducting Experiments

In Table 5.4, we present the buckling load of experimental results and Finite Element Analysis results, of pipeline without Stiffeners, pipeline model with central Stiffeners, pipeline model with central Stiffeners and two stiffeners at the ends and longitudinal continuous rectangular Stiffeners. Figure 5.8, shows the buckling pattern obtained before and after conducting experiments.

Table 5.4 Summary of Finite Element (FE) analysis and Experimental results.

No	Models	Critical Buckling Load P_{cr} (kN)	
		FE Analysis	Experimental Results
1	Pipeline without Stiffeners	7.167	6.90
2	Pipeline with central Stiffeners	9.937	9.90
3	Pipeline with central Stiffeners and two stiffeners at the ends	11.050	10.50
4	Pipeline with Longitudinal Continuous Stiffeners	25.026	24.0

The experimental results presented in Table 5.4 were obtained considering the residual stresses in the four pipe models: one without stiffeners and the other with stiffeners. The residual stresses induced during the process of pipe cutting, the welding and groove machining were not considered in the finite element model; this results in numerically predicted buckling loads higher than the experimental results [Luciano O. Manitoban. 2006].

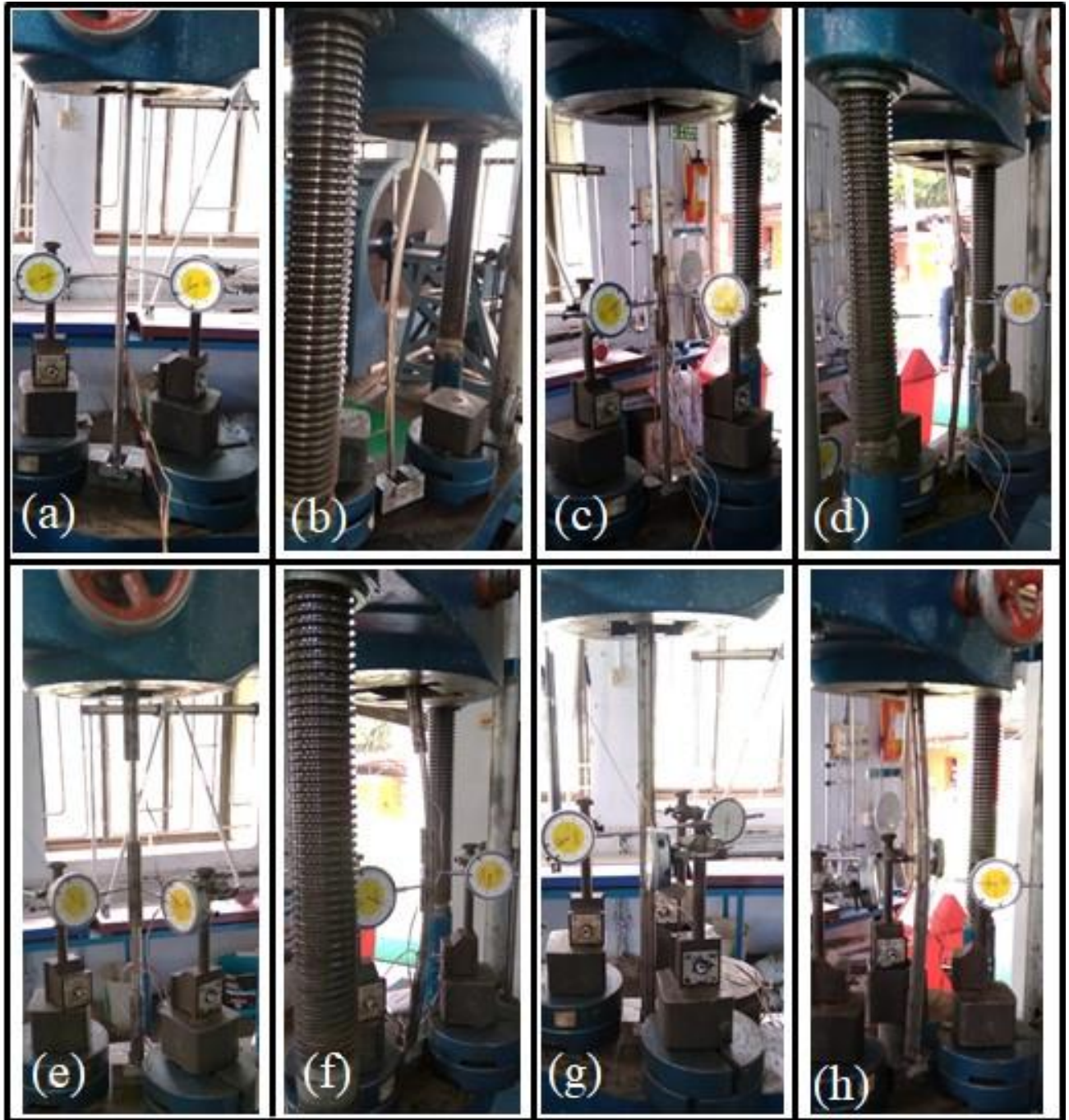


Figure 5.8 Pipeline with different stiffener configurations before and after buckling. (a-b) pipeline without stiffener, (c-d) pipeline with central stiffeners, (e-f) pipeline with central stiffeners and two stiffeners at the ends and (g-h) pipeline with longitudinal continuous stiffeners.

5.5 Three point bending experiments

Three point bending experiments were conducted using Universal Testing Machine (UTM) of capacity 400 kN. Specimens of span length 690 mm were used to conduct three point bending test. The pipe having dimensions of outer diameter 16 mm, thickness 1.5 mm was used for experiments. The pipes with different stiffener configurations were fabricated using stiffeners of cross-section 5 mm x 2 mm. The stiffeners were welded using Tungsten Inert Gas (TIG) welding method. All bending experiments were conducted in load control mode with loading rate of 30 kg/minute. Top surface of pipelines, bottom surface of pipelines and stiffener surface were pasted with strain gauges to measure stresses at selected places. The mid span deflection of pipelines was measured using displacement sensor available in UTM machine and deflection at 1/4th span length of pipe was measured using dial gauge of least count 0.01 mm. The relationship of load and deflection at mid span of pipeline for all the pipeline configurations is given in Figure 5.9. From the experimental observations, the load-deflection relationship followed linear path and then changed to nonlinear form. The threshold of liner relation of load-deflection curve represents the elastic loading limit of the pipeline. The flexural elastic load limits of all the pipeline configurations are given in Table 5.5.

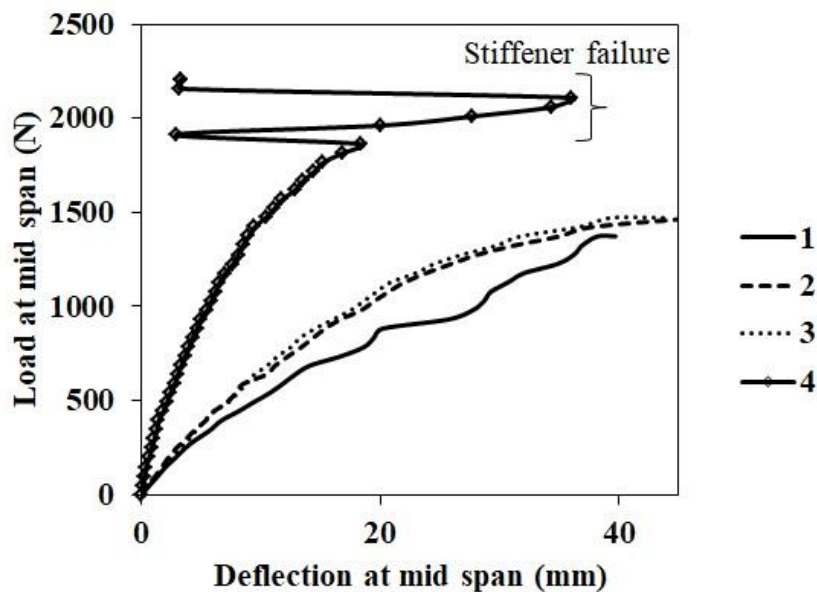


Figure 5.9 Load-deflection curves of pipeline with different stiffeners, 1- pipeline without Stiffeners, 2-pipeline with central stiffener, 3- pipeline with central

Stiffeners and two stiffeners at the ends and 4- pipeline with longitudinal continuous stiffeners.

Table 5.5 Flexural elastic load limit of different pipeline configurations.

Sl. No.	Configuration	Flexural elastic limit (N)
1	Pipeline without stiffeners	300
2	Pipeline with central stiffeners	588
3	Pipeline with central stiffeners and two stiffeners at the ends	883
4	Pipeline with longitudinal continuous stiffeners	1422

From Figure 5.9, the bending load capacity of pipeline increased with increase in stiffener length. The bending load capacity of pipeline with central stiffener and pipeline with central stiffeners & two stiffeners at the ends has not varied significantly. During testing pipeline experiences maximum bending moment at mid span of the pipeline and effect of bending moment decreases when moving towards the supports from mid span of the pipeline. From the curves 2 and 3 in Figure 5.9, the stiffeners at supports have not contributed significantly to bending capacity of pipeline. In curve 4 of Figure 5.9, the disturbance in load deflection curve is due to failure of weld between pipe and stiffener during testing. The failed weld connections between pipeline and stiffeners are given in Figure 5.10 (d). The load transfer from pipeline to stiffeners was confirmed from the reading of strain gauge pasted on surface of stiffeners. The stresses in stiffeners during the experiment are given in Figure 5.10 (a-c). During bending test all the configurations of pipelines showed gradual increase in bending load with increase in mid span deflection and then the load stabilized even with increase in deflection. The stabilized load is considered as ultimate flexural capacity of pipeline as given in Table 5.6. The bending specimens before and after the three-point bending test are given in Figure 5.11.

Table 5.6 The ultimate flexural capacity of different pipeline configurations.

Sl. No.	Configuration	Ultimate flexural load (N)
1	Pipeline without stiffeners	1373
2	Pipeline with central stiffeners	1472
3	Pipeline with central stiffeners and two stiffeners at the ends	1472
4	Pipeline with longitudinal continuous stiffeners	2207

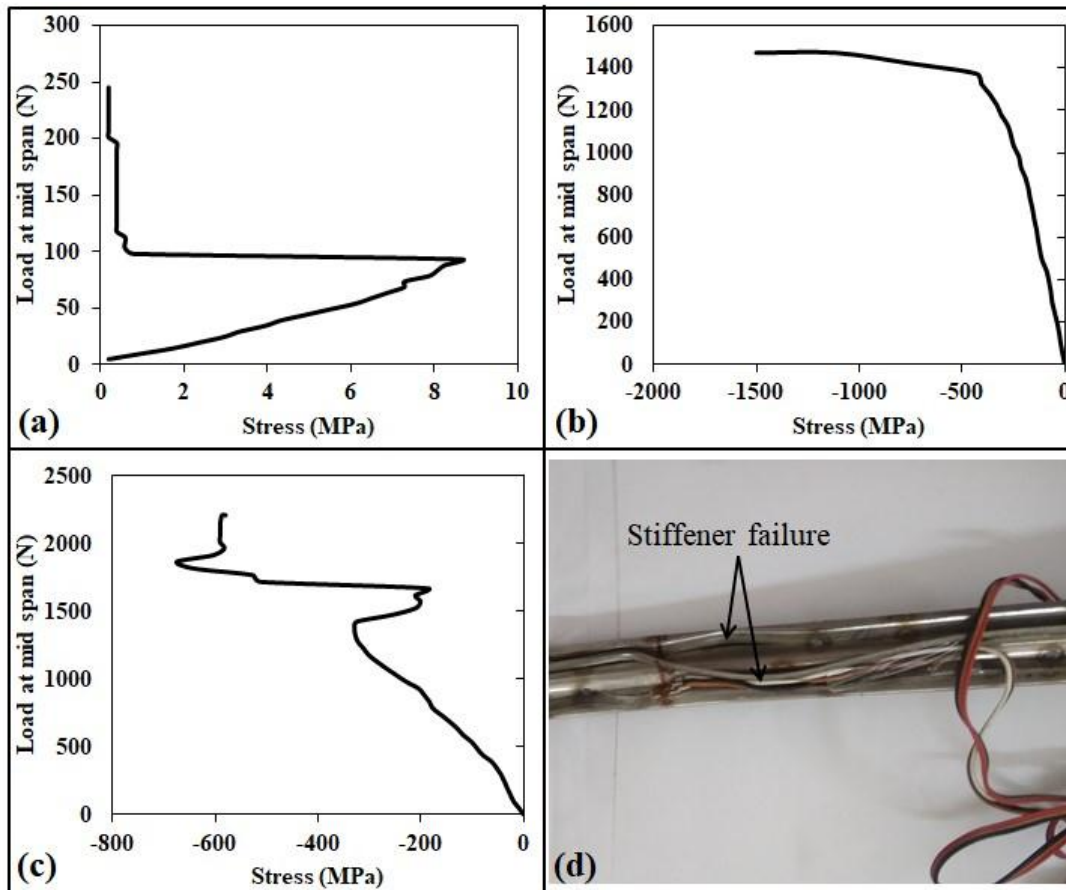


Figure 5.10 Stress in stiffeners from strain gauges pasted on stiffeners of, (a) pipeline with central stiffener, (b) pipeline with central stiffeners and two stiffeners at the ends and (c) pipeline with longitudinal continuous stiffeners (d) Failure of weld connection between pipe and stiffener in pipe with longitudinal continuous stiffeners.

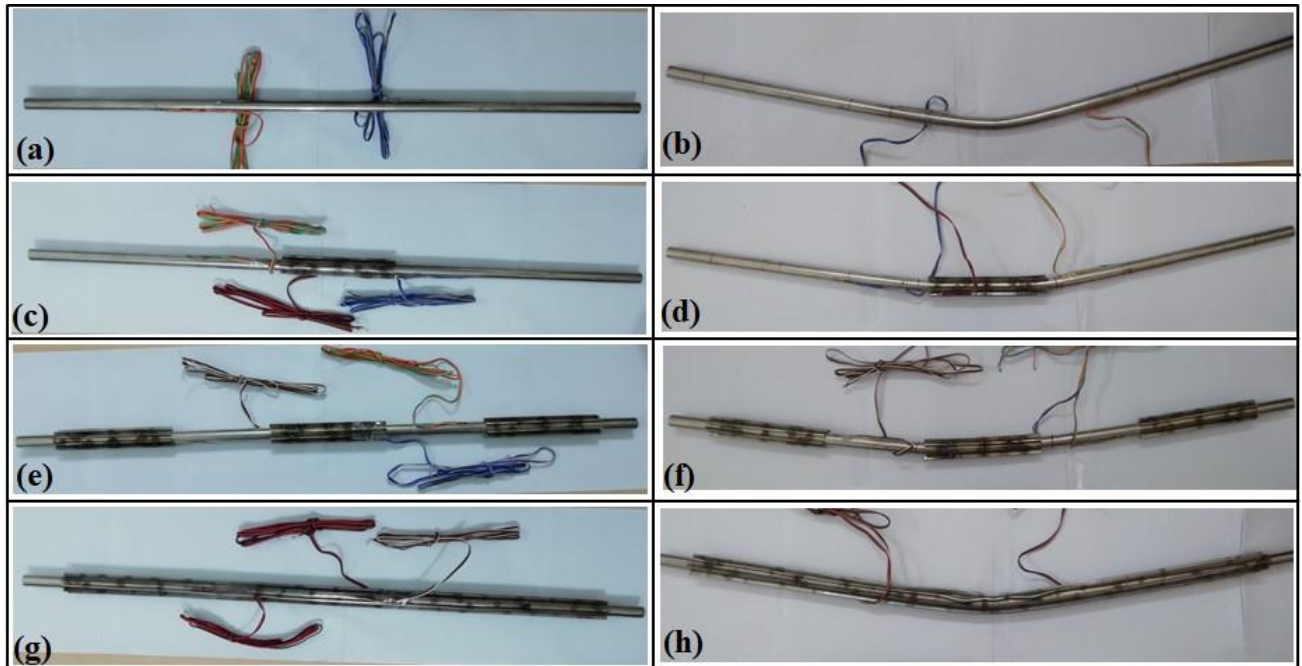


Figure 5.11 Three point bending specimens before and after testing (a-b) pipeline without stiffener, (c-d) pipeline with central stiffener, (e-f) pipeline with central stiffeners and two stiffeners at the ends and (g-h) pipeline with longitudinal continuous stiffener.

The stresses on pipeline were measured using strain gauges pasted on the surface of pipeline. The schematic representation of pipeline without stiffener with locations of strain gauges and support conditions are given in Figure 5.12. The strain at selected positions was measured while conducting the bending experiments and compared with the strain at respective places calculated using Euler's bending theory. From Figure 5.13, the measured strain at selected locations had good agreement with theoretical strains within the elastic limit of material.

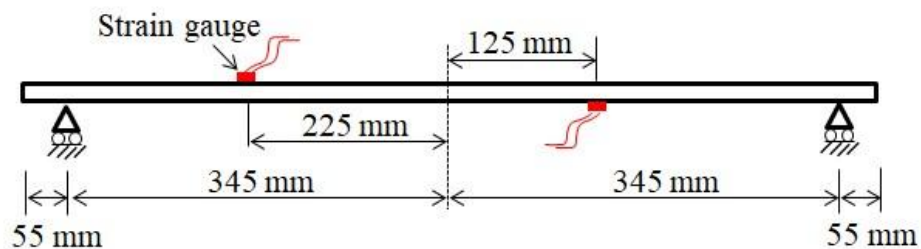


Figure 5.12 Strain gauge pasted locations and support conditions of pipeline without stiffeners.

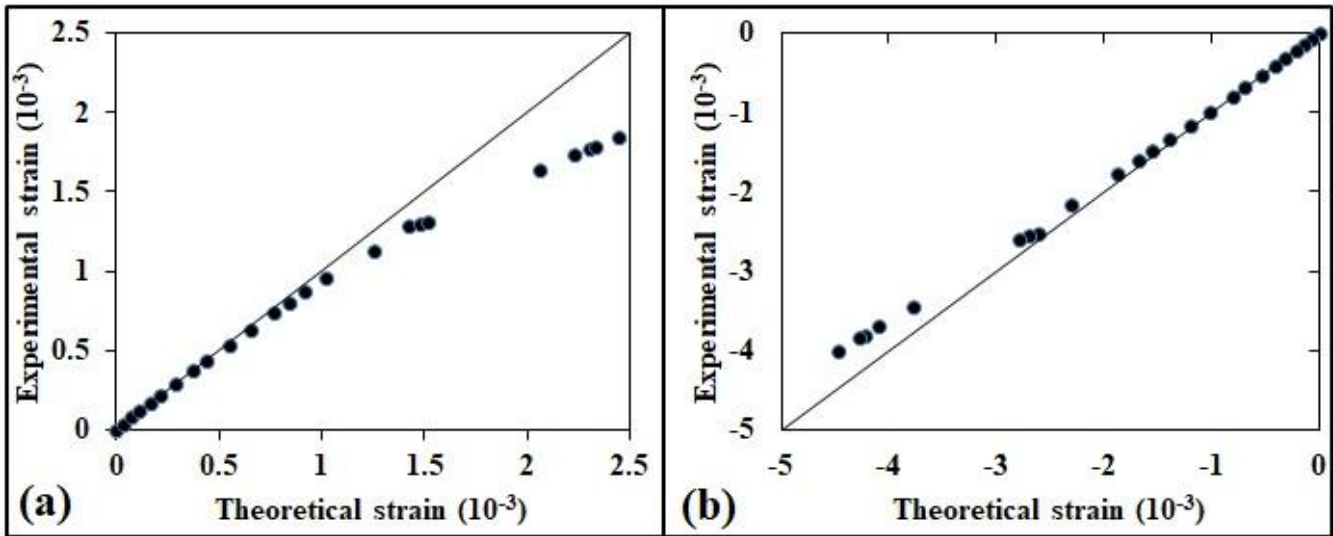


Figure 5.13 Comparison of theoretical and experimental strain at (a) bottom and (b) top strain gauge pasted locations.

CHAPTER 6

CONCLUSIONS

The behavior of rectangular pin buckle arrestors welded to external surface of pipeline models in resisting forces causing buckling and bending were studied. The finite element model was validated by conducting buckling experiments.

1. The finite element analysis performed to identify buckle arrestor configuration and to increase buckling load carrying capacity of pipeline model. Buckling experiments were conducted on pipeline models stiffened with the identified buckle arrestor configurations. For verification and validation of finite element analysis results. Based on the finite element analysis results and experimental results longitudinal continuous buckle arrestors ($P_{cr} = 13.981$ kN) of length 920 mm were identified as optimum buckle arrestor design when compared with sinusoidal buckle arrestors ($P_{cr} = 6.825$ kN) and angular buckle arrestors ($P_{cr} = 4.871$ kN) configurations.
2. Finite element analysis and experiments were conducted to study contribution of length of buckle arrestors and optimum location of buckle arrestors in increasing the axial load carried by the pipe models and thereby, improving the strength of the offshore pipeline.
3. Finite element analysis and the experimental results, showed that pipeline stiffened with centrally placed buckle arrestors ($P_{cr} = 9.937$ kN) of length 150 mm and longitudinal continuous buckle arrestors ($P_{cr} = 25.026$ kN) of length 670 mm showed better results than that of a pipeline stiffened with discontinuous buckle arrestors ($P_{cr} = 11.050$ kN) of length 420 mm.
4. The buckling capacity of pipeline can be improved up to 50% and 250% using rectangular pin stiffeners at mid span of the pipeline and longitudinal continuous stiffeners respectively.
5. Finite element analysis and results of buckling experiments have shown similar trends; hence, finite element models can be used as a dependable method of assessing performance of buckle arrestors for steel pipes. Finite

element analysis of pipe models gave satisfactory results and helped in optimizing the buckle arrestor design.

6. Flexural characteristics of the pipeline with different stiffener configurations were observed by conducting three point bending experiments. The flexural load capacity of pipeline increased with increase in length of the stiffener.
7. The effect of stiffeners nearer to the supports does not contribute to significant improvement of bending capacity of pipeline. The bending capacity of pipeline can be improved significantly using continuous longitudinal stiffeners.

6.1 Limitations of the study

- Residual stresses induced in the pipeline specimen during cutting, welding of buckle arrestors was not considered.
- Use of SS304 grade stainless steel is suitable for offshore pipelines. But, API prescribes use of X-65 grade steels which are not available.
- Brittle stress coatings and paints could not be used due to their unavailability.
- Uniform cross section of pipeline specimen was ensured by measuring dimensions of the pipeline as per prescribed norms. Material discontinuities, if any, could not be measured.

6.2 Scope for future work

- The present study can be conducted with different grades of steel.
- Advanced methods of welding such as metal inert gas welding could be used for fabrication of specimen.
- Use of Composite Materials and Functionally Graded Materials (FGMs) must be explored.
- Use of hyperbaric chamber for conducting experiments to test the offshore pipeline for the higher pressures existing at greater depths of sea water of different salinities.

REFERENCES

- Aguirre, F., Kyriakides, S. and Yun, H. D. (2004). “Bending of steel tubes with Luders bands.” *International Journal of Plasticity*, 20, 1199 – 1225.
- Ahmed Elshafey et al. (2010). “Nonlinear buckling of pipes subjected to external or internal pressure.” *International J. of Recent Trends in Engineering and Technology*, 3, 11 – 15.
- Bardi, F.C. and Kyriakides, S. (2006a). “Plastic buckling of circular tubes under axial compression—part I: Experiments.” *International Journal of Mechanical Sciences*, 48, 830 – 841.
- Bardi, F.C., Kyriakides, S. and Yun, H. D. (2006b). “Plastic buckling of circular tubes under axial compression—part II: Analysis.” *International Journal of Mechanical Sciences*, 48, 842 – 854.
- Burak Can Cerik (2015). “Ultimate strength of locally damaged steel stiffened cylinders under axial compression.” *Thin-Walled Structures*, 95, 138 – 151.
- Bushnell, David (1981). “Computer buckling analysis of shells under.” DTIC
- Celestino Valle-Molina et al. (2014). “Reliability functions for buried submarine pipelines in clay subjected to upheaval buckling.” *Applied Ocean Research*, 48, 308 – 321.
- Corona, E. et al. (2006). “Yield anisotropy effects on buckling of circular tubes under bending.” *International Journal of Solids and Structures*, 43, 7099 – 7118.
- D. M. Haughton and A. Orr (1995). “On the Eversion of Incompressible Elastic Cylinders.” *Inr J. Non-Linear Mechanics*, 30 (2), 81 – 95.

- DeGeer, D.,and Nessim,M.(2008).“Arctic Pipeline Design Considerations.” *ASME 2008 27th International Conference on Offshore Mechanics and Arctic Engineering*, OMAE2008-57802, 3, 583 – 590.
- Erlenc Oslo and Stelios Kyriakides, (2003). “Internal ring buckle arrestors for pipe-in-pipe systems.” *International Journal of Non-Linear Mechanics*, 38, 267 – 284.
- Farhat, C. et al. (2013). “Dynamic implosion of underwater cylindrical shells: Experiments and Computations.” *International Journal of Solids and Structures*, 50, 2943 – 2961.
- Federico Guarracino (2018). “Influence of Stiffeners and Buckling Arrestors on the Behaviour of Offshore Pipelines under Bending.” *International Journal of Petroleum Technology*, 5, 12 – 18.
- Fu, Y.B. and Lin, Y.P. (2002). “A WKB Analysis of the Buckling of an Everted Neo-Hookean Cylindrical Tube.” *Mathematics and Mechanics of Solids*, 7, 483 – 501.
- Hassan Karampour and Faris Albermani (2013). “Buckle interaction in deep subsea pipelines. ” Proceedings of the ASME 2013 32nd International Conference on Ocean, *Offshore and Arctic Engineering OMAE2013*.
- Hassan Karampour, Faris Albermani and Julien Gross (2013). “On lateral and upheaval buckling of subsea pipelines.” *Engineering Structures*, 52, 317 – 330.
- Hassan Karampour and Faris Albermani (2014). “Experimental and numerical investigations of buckle interaction in subsea pipelines.” *Engineering Structures*, 66, 81 - 88.

- Heedo Yun and Stelios Kyriakides (1985). “Model for beam-mode buckling of buried pipelines.” *Journal of Engineering Mechanics*, 111(2), 235 – 253.
- Heedo Yun and Stelios Kyriakides (1990). “On the beam and shell modes of buckling of buried pipelines.” *Soil Dynamics and Earthquake Engineering*, 9, 179 – 193.
- Hibbitt, H.D, Karlsson, B.I., Sorenson, P, (2000), ABAQUS theoretical manual. Version 4.5.
- Inge Lotsberg (2008). “Stress concentration factors at welds in pipelines and tanks subjected to internal pressure and axial force.” *Marine Structures*, 21, 138 – 159.
- James G. A. Croll (1997). “A simplified model of upheaval thermal buckling of subsea pipelines.” *Thin-Walled Structures*, 29, 59 – 78.
- Jian-xing Yu et al. (2014). “Ring–truss theory on offshore pipelines buckle propagation.” *Thin-Walled Structures*, 85, 313 – 323.
- Jian-xing Yu et.al, (2017). “The cross-over mechanisms of integral buckle arrestors for offshore pipelines.” *Applied Ocean Research*, 67, 236 – 247.
- Jianbei Zhu, Mario M. Attard and David C. Kellerman (2015). “In-plane nonlinear localised lateral buckling of straight pipelines.” *Engineering Structures*, 103, 37 – 52.
- Ju, G.T. and Kyriakides, S. (1988). “Thermal buckling of offshore pipelines.” *Journal of offshore mechanics and arctic engineering*, 110, 365 – 364.

- Julian F. Hallai and Stelios Kyriakides. (2011a). “On the effect of Lüders bands on the bending of steel tubes. Part I: Experiments.” *International Journal of Solids and Structures*, 48, 3275 – 3284.
- Julian F. Hallai and Stelios Kyriakides. (2011b). “On the effect of Lüders bands on the bending of steel tubes. Part II: Analysis.” *International Journal of Solids and Structures*, 48, 3285 – 3298.
- Kalliontzis, C. et al. (1997). “Nonlinear static stress analysis of submarine high pressure pipelines.” *Computers and Structures*, 63, 397 – 411.
- Kerr, A. D. (2013). “On the stability of railroad track in the vertical plane.” *Rail International*, 132 – 142.
- Khalilpasha, H. and Albermani, F. (2013) “Hyperbaric chamber test of subsea pipelines.” *Thin-Walled Structures*, 71, 1 – 6.
- Kyriakides, S. et al. (2012). “Wrinkling of Circular Tubes Under Axial Compression: Effect of Anisotropy.” *Journal of Applied Mechanics*, 72, 301 – 305.
- Kyriakides, S. and Edmundo Corona(2007). “Mechanics of offshore pipelines”. 1st Edition Volume 1 Buckling and Collapse, *Elsevier Science*.448 pages.
- Lee, L. H. and Kyriakides, S, (2004). “On the arresting efficiency of slip-on buckle arrestors for offshore pipelines.”*International Journal of Mechanical Sciences*, 46, 1035 – 1055.
- L. H. Lee, S. Kyriakides and T. A. Netto (2008). “Integral buckle arrestors for offshore pipelines: Enhanced design criteria.” *International Journal of Mechanical Sciences*, 50(6), 1058 – 1064.

- Lin, T. J. et al., (2012). “Verification of Numerical Modelling in Buried Pipelines under Large Fault Movements by Small-Scale Experiments.” *World Conference on Earthquake Engineering*.
- Luciano O Manitoban. (2006).“Finite Element Modelling and Experimental Validation of Buckle Arrestors for Deep water Pipelines.” *Mecánica Computacional*. Vol XXV,;687–704.
- Maltby, T. C. and Calladine, C. R. (1995). “An Investigation into upheaval buckling of buried pipelines – Experimental Apparatus and some observations.” *International Journal of Mechanical Sciences*, 37, 943 – 963.
- Martins, J.P., Simoes da Silva, L. and Reis, A. (2013). “Eigenvalue analysis of cylindrically curved panels under compressive stresses – Extension of rules from EN 1993-1-5.” *Thin-Walled Structures*, 68, 183 – 194.
- Megson, T. H. G. (1972) “Aircraft Structures for Engineering Students.” 4th Edition, *Butterworth-Heinemann*,910 pages.
- Michael R. Card and Robert M. Jones. (1966). “Experimental and theoretical results for buckling of eccentrically stiffened cylinders.” *NASA Technical Note*.
- Ming Cai Xu and Guedes Soares, C. (2013). “Comparisons of calculations with experiments on the ultimate strength of wide stiffened panels.” *Marine Structures*, 31, 82 – 101.
- N.Silvestre (2007). “Generalised beam theory to analyse the buckling behaviour of circular cylindrical shells and tubes.” *Thin-Walled Structures*,45(2), 185 – 198.

- Nazary Moghadam, S., et al. (2012). “Simulation of overall and local buckling behaviour of cylindrical tubular members using fuzzy inference system.” *Advances in Engineering Software*, 45, 349 – 359.
- Neil Taylor and Aik Ben Gen (1986). “Submarine pipeline buckling-imperfection studies.” *Thin-Walled Structures*, 4(4), 295 – 323.
- Netto, T. A. and Estefen, S. F., (1996). “Buckle Arrestors for Deepwater Pipelines.” *Marine Structures*, 9, 873 – 883.
- Netto, T.A. and Kyriakides, S. (2000a). “Dynamic performance of integral buckle arrestors for Offshore pipelines. Part I: Experiments.” *International Journal of Mechanical Sciences*, 42, 1405 – 1423.
- Netto, T.A. and Kyriakides, S. (2000b). “Dynamic performance of integral buckle arrestors for offshore pipelines. Part II: Analysis.” *International Journal of Mechanical Sciences*, 42, 1425 – 1452.
- Nourpanah, N. and Taheri, F. (2012). “A Comprehensive Parametric Finite Element Study on the Development of Strain Concentration in Concrete Coated Offshore Pipelines.” *Journal of Pressure Vessel Technology*, 134.
- Palmer, A.C., Baldry, J.A.S.,(1974) “Lateral Buckling of Axially Constrained Pipelines.” *Journal of Petroleum Technology*, 1283-1284.
- Peroti, S. et al. (2013). “Numerical Analysis of Ring-Stiffener Effect on Ultimate Buckling Strength of Pipeline.” *Middle-East Journal of Scientific Research*, 13, 579 – 584.

- Power, T. L. and Kyriakides, S. (1996). “Circumferential stiffeners as buckle arrestors in long panels.” *International Journal of Solids Structures*, 33, 1837 – 1851.
- R.Shahandeh and H.Showkati (2016). “Influence of ring-stiffeners on buckling behavior of pipelines under hydrostatic pressure.” *Journal of Constructional Steel Research*, 121, 237 – 252.
- Rita G.Toscano, et al, (2008). “Collapse arrestors for deepwater pipelines. Cross-over mechanisms.” *Computers & Structures*, 86, 728 – 743.
- Roger E. Hobbs (1984). “In-service buckling of heated pipelines.” *Journal of Transportation Engineering*, 110, 175 – 189.
- Rofooei, Fayaz R., et al, (2012). “Full-Scale Laboratory Testing of Buried pipelines subjected to permanent ground displacement caused by reverse faulting.” *World Conference on Earthquake Engineering*, 2012.
- Run Liu, et al. (2015). “Laboratory tests and thermal buckling analysis for pipes buried in Bohai soft clay.” *Marine Structures*, 43, 44 – 60.
- Run Liu, et al. (2014). “Numerical studies on global buckling of subsea pipelines.” *Ocean Engineering*, 78, 62 – 72.
- Richard Wiebe, Lawrence Virgin, Ilinca Stanciulescu and S. Spotswood (2011).“On Snap-Through Buckling.” *American Institute of Aeronautics and Astronautics*, 2011 – 2083.
- S. Kyriakides, C. D. Babcock (1982). “The Spiral Arrestor”—A New Buckle Arrestor Design for Offshore Pipelines.” *J. Energy Resour. Technol.* 104(1), 73 – 77.

- Schupp, J. et al. (2006). “Pipeline unburial behaviour in loose sand.” *Proceedings of International Conference on Offshore Mechanics and Arctic Engineering*.
- Shuaijun Li, Bryan W. Karney and Gongmin Liu (2015). “FSI research in pipeline systems – A review of the literature.” *Journal of Fluids and Structures*, 57, 277 – 297.
- ShunfengGong, et al. (2012). “Buckle propagation of offshore pipelines under external pressure.” *Marine Structures*, 29(1), 115 – 130.
- Shunfeng Gong et al., (2019). “On the arresting performance of welded-ring buckle arrestor for subsea pipelines.” *Ships and Offshore Structures*, ISSN: 1744-5302.
- Stelios Kyriakides, et al. (1998). “On the design of integral buckle arrestors for offshore pipelines.” *Applied Ocean Research*, 20, 95 – 104.
- Tuttle M., Singhatanadgid, P. and Hinds, G. (1999). “Buckling of Composite Panels Subjected to Biaxial Loading.” *Experimental Mechanics*, 39 (3), 191 – 201.
- Xin Feng, et al. (2015). “Experimental investigations on detecting lateral buckling for subsea pipelines with distributed fiber optic sensors.” *Smart Structures and Systems*, 15, 245 – 258.
- Yidu Bu et.al, (2020). “Flexural buckling behaviour and design of offshore lined pipes under compression.” *Ocean Engineering*, 214, 107829.

- Zhillong Zhu and D. W. Murray (1996). “Pipeline beam models using stiffness property deformation relations.” *Journal of Transportation Engineering*, 122, 164 – 172.
- BS8010:2004 (PD8010-1:2004) The code of practice for pipelines *Part 2: Subsea pipelines*.

PUBLICATIONS BASED ON PRESENT RESEARCH WORK

International Journals

1. **Ramachandra Rao N.** and Vadivuchezhian Kaliveeran, (2020) “Finite element modeling and experimental validation of rectangular pin buckle arrestors for offshore pipelines”, *Mechanics Based Design of Structures and Machines*, <https://doi.org/10.1080/15397734.2020.1725562>. (Taylor and Francis)
2. **Ramachandra Rao N.** and Vadivuchezhian Kaliveeran, (2019) “Effective buckle arrestors for offshore pipelines”, *Materials Today: Proceedings*, Volume 27, Part 3, Pages 2282-2285. <https://doi.org/10.1016/j.matpr.2019.09.113>. (Elsevier).
3. **Ramachandra Rao N. and** Vadivuchezhian Kaliveeran, (2019) “Analysis and design of inclined buckle arrestors for offshore pipeline”, *Materials Today: Proceedings*, Volume 27, Part 3, Pages 2277-2281. <https://doi.org/10.1016/j.matpr.2019.09.112>. (Elsevier).
4. **Ramachandra Rao N.** and Vadivuchezhian Kaliveeran, (2019) “Finite element modeling and experimental validation of rectangular pin buckle arrestors for offshore pipelines”, *Materials Today: Proceedings*, Volume 27, Part 3, Pages 2424-2428. <https://doi.org/10.1016/j.matpr.2019.09.207>. (Elsevier)

International Conferences

1. **N. Ramachandra Rao**, Vadivuchezhian Kaliveeran and Amey Abraham, (2017) “Buckling analysis of offshore pipelines using 3-D finite element analysis”, *International Conference on Recent Advances In Material Chemistry (ICRAMC 2017)*, SRM University, Kattankulathur, India, February 15-17, 2017.
2. **N. Ramachandra Rao**, Vadivuchezhian Kaliveeran and Anem Surya, (2018) “Buckling analysis of offshore pipeline with rectangular pin buckle arrestors”, 7th *International Engineering Symposium - IES 2018*, Kumamoto University, Japan, March 7-9, 2018.

CURRICULUM VITAE



Name: N. RAMACHANDRA RAO

Permanent Address:

3-36/1 Plot No-15, Gouthami Nagar, Saheb Nagar Road, Vanasthalipuram,
Hayathnagar, K. V. Rangareddy, Andhra Pradesh, PIN: 500070.

Contact No.: +91-8147915198

Email ID: ram.nagam@gmail.com

Education:

Diploma in Advance Computing (1999-2000)

Discipline: Software Engineering

College : National Resource center of C-DAC in Advanced Computing Training,
Pune.

Master of Technology (1993-1996)

Discipline: Water Resources

College : Jawaharlal Nehru Technological University, Hyderabad

Bachelor of Engineering (1989-92)

Discipline: Civil Engineering

College : Chaitanya Bharathi Institute of Technology, Hyderabad.

Diploma (1985-88)

Discipline: Civil Engineering

College : Government Polytechnic, Masab Tank, Hyderabad.